The Dissertation Committee for Michael Reuben Elizondo Certifies that this is the approved version of the following dissertation:

Roles for Zebrafish *trpm7* in Growth, Skeletogenesis, Kidney Function and Physiological Ion Homeostasis

Committee:

_____
David M. Parichy, Supervisor

_____
John B. Wallingford

_____
Janice Fischer

_____
Marty Shankland

_____
Tanya Paull

Roles for Zebrafish *trpm7* in Growth, Skeletogenesis, Kidney Function and Physiological Ion Homeostasis

by

Michael Reuben Elizondo, B.S.

Dissertation

Presented to the Faculty of the Graduate School of

The University of Texas at Austin

in Partial Fulfillment

of the Requirements

for the Degree of

Doctor of Philosophy

The University of Texas at Austin

December 2009

Acknowledgements

This work was funded by grants from the National Institutes of Health and by a Ruth L. Kirschstein NRSA Minority Predoctoral Fellowship from the National Institute of Diabetes and Digestive and Kidney Diseases. Chapter 2 was previously published in *Current Biology*.

I thank my parents for their unending love and support, and their encouragement in all my endeavors. I am grateful for my advisor, David Parichy, and his patience and insightfulness in allowing me both the room to work and the occasional prodding and nudging when the way seemed less clear. His drive and commitment helped me find my own. I would also like to thank John Wallingford for his perspective, and my other committee members, Janice Fischer, Tanya Paull, and Marty Shankland, for their continued support.

My fellow graduate students, Ian Quigley and Ray Engezser were a continual source of support, camaraderie, and inspiration. Without their presence I don't where I would have been. I would like to thank my former labmates in Austin, Jessica Turner and June Keay, for making the lab a fun place to be, and Erin MacDonald for her invaluable knowledge of fish skeletons. I would also like to thank my labmates in Seattle, Larissa Patterson, Tiffany Gordon, Helena Christiansen, Margaret Mills, and Erine Budhi for all the discussions we shared in the lab, over lunch, and at ballgames, and for their constant aid in experiments and ever-evolving protocols. They all helped ease my transition to life in Seattle.

Roles for Zebrafish *trpm7* in Growth, Skeletogenesis, Kidney Function and Physiological Ion Homeostasis

Michael Reuben Elizondo, Ph.D.

The University of Texas at Austin, 2009

Supervisor: David M. Parichy

Development of the adult form requires coordinated growth and patterning of multiple traits in response to local gene activity as well as global endocrine and physiological effectors. In recent years the zebrafish has been utilized as a favorable animal model as a step towards dissecting and better understanding these postembryonic developmental processes. One of the more powerful methods utilized in zebrafish has been the identification of new gene functions through the use of mutant screens. The *nutria* mutant was recovered from one such screen to identify postembryonic defects in pigment pattern, growth and metamorphosis. These mutants exhibited a pigment cell defect, touch unresponsiveness and severe growth retardation. Here I will discuss my work towards dissecting the underlying developmental processes governing the phenotypic changes in *nutria* mutants. I characterize gross alterations in skeletal development in *nutria* mutants that lead to accelerated endochondral ossification but delayed intramembranous ossification. I show that the *nutria* phenotype results from

mutations in *trpm7*, which encodes a transient receptor potential (TRP) family member that functions as both a cation channel and a kinase. I find *trpm7* expression in the fish-specific, ion homeostasis-regulating gland known as the corpuscles of Stannius (CS), and in the mesonephric kidney. I show that mutants also develop kidney stones. Together these results suggest a role for trpm7 activity in regulation of physiological ion homeostasis. Next I confirm that role by identifying late-embryonic and early larval defects in the CS and the kidney, two organs that regulate physiological ion homeostasis. I demonstrate the early larval detection of kidney stones in *trpm7* mutants and show that their appearance is presaged by decreased levels of total calcium and magnesium. Furthermore I establish a link between trpm7 function in the CS and stanniocalcin1 (stc1), a potent molecular regulator of calcium homeostasis. Finally, using transgenic overexpression and morpholino-oligonucleotide knockdown, I demonstrate that stc1 modulates calcium and magnesium levels in *trpm7* mutant and wild-type backgrounds. Together these analyses establish postembryonic roles for trpm7 function in growth, skeletogenesis, kidney function, and physiological ion homeostasis.

Table of Contents

List of Tables

List of Figures

Chapter 1: Background

Introduction

Much of what makes an organism is circumscribed by its embryonic development. Germ layers are defined, cell lineages are determined and tissue differentiation occurs. More than a century of effort has gone into dissecting and discerning the mechanisms governing these processes. While much of an organism's development is determined during embryonic stages, still more is established during postembryonic stages. Many organ systems continue to develop and mature, or only become fully functional at postembryonic stages. Furthermore, once many key developmental processes have been established their maintenance and regulation becomes a vital priority. These processes can often be less well defined than those at early embryonic stages.

As a step towards dissecting and better understanding postembryonic development, the zebrafish has been developed into a favorable animal model for studying these processes. Mutant screens were performed to identify postembryonic defects in pigment pattern, metamorphosis, and other related processes. From a mutant screen to identify postembryonic defects in pigment pattern, growth, and metamorphosis we identified the mutant *nutria*. These mutants exhibited a pigment cell defect, touch unresponsiveness and severe growth retardation. In the follow chapters I present my work towards understanding the developmental processes at work in zebrafish *nutria* mutants.

In Chapter 2, I describe the identification of *trpm7* as the gene corresponding to *nutria*. TRPM7 is known to be a primary regulator of cellular magnesium homeostasis in mammalian systems (Schmitz, Perraud et al. 2003). However work in this chapter will show that in zebrafish dysfunctional *trpm7* can have broader impacts. I characterize postembryonic defects present in zebrafish *trpm7* mutants that greatly impact growth, skeletogenesis and kidney function. I demonstrate how mutants exhibit a severe growth retardation that does not manifest until larval stages. Furthermore, I show that at larval stages these mutants also display significant disruption in the sequence and timing of ossification between endochondral and intramembranous bones, with premature ossification of endochondral bones and delayed ossification of intramembranous bones. Finally I identify kidney stone formation within the mesonephric tubules of the larval kidney in mutants. This, together with strong *trpm7* expression detectable in the larval kidney and corpuscles of Stannius, organs responsible for ion homeostasis, suggests a role for *trpm7* in the physiological regulation of postembryonic growth and skeletogenesis.

In Chapter 3, I further explore a potential role for *trpm7* in governing physiological cation homeostasis. I determine that the function of both the kidney and the corpuscles of Stannius (CS), two organs impacting physiological ion homeostasis, is altered in *trpm7* mutants. I demonstrate the presence of kidney stones in mutant larvae shortly after hatching and misregulation of a key calcium regulating hormone, *stanniocalcin1* (*stc1*), in the CS prior to hatching. I find that decreased total calcium and magnesium levels in mutants follows upregulation of *stc1* but precedes kidney stone

formation. Furthermore, using transgenic overexpression and morpholino-oligonucleotide knockdown, I demonstrate that stc1 modulates calcium and magnesium levels in *trpm7* mutant and wild-type backgrounds. Together these analyses demonstrate distinct roles for trpm7 in regulating cation homeostasis through kidney function and via *stc1* expression within the CS.

In the Appendices, I discuss other experiments aimed at a broader understanding of zebrafish trpm7 function. These include establishing zebrafish lines with conditional trpm7 function, either through identification of temperature sensitive (TS) mutant alleles, or through the establishment of a transgenic line capable of inducing overexpression of a dominant-negative form of *trpm7* (DN-trpm7) (Appendix I). Additionally, I describe experiments to identify differences in water composition between fish facilities at the University of Texas and the University of Washington, and how they impact observed phenotypes (Appendix II). Other work discussed includes in vivo detection of kidney stone formation in heterozygous *trpm7* mutants (Appendix III), potential changes in phosphate levels in *trpm7* mutants (Appendix IV), and how the potential effects of *stc1* overexpression at larval stages may provide an explanation for later stage defects in *trpm7* mutants (Appendix V).

To provide a better context for the rationales behind the following experiments in later chapters I briefly review the pertinent topics of bone and kidney development, physiological ion homeostasis, and the functions of the broader family of TRP channels, of which TRPM7 is a member. Much of this reviews the processes as they occur in mammalian systems as a reference point, then discusses how they differ in fish. Since

ultimately the purpose of these studies is to use zebrafish as a broader model for vertebrate postembryonic development, the review is meant to help put the research into this broader context.

Bone Development

One of the defining processes of post-embryonic vertebrate development is the formation and maintenance of bone. This is the process by which a vertebrate organism develops and maintains its skeletal architecture and is governed by a wide range of factors controlling patterning, timing, formation, maintenance and resorption of bone. Often these factors play additional roles in growth, renal function, mineral homeostasis, and metabolism (McCarthy and Centrella 2001; Zhang, Xuan et al. 2002; Olney 2003; Schipani and Provot 2003; D'Souza-Li 2006; Kronenberg 2006; Wu, Yoshiko et al. 2006; Doyle and Jan de Beur 2008; Egbuna and Brown 2008; Quarles 2008; Datta and Abou-Samra 2009; Samadfam, Richard et al. 2009; Theman and Collins 2009; Tsagalis, Psimenou et al. 2009). There is a complex interplay between these factors in maintaining a balance in the regulation of these processes, and disruption of this balance can have severe consequences not only in development or maintenance of bone, but also in the regulation of other developmental processes such as growth or renal function (Schipani, Kruse et al. 1995; Karaplis, He et al. 1998; Kuizon and Salusky 1999; Gonzalez and Martin 2001; Kuizon and Salusky 2002; Bajaj and Saag 2003; D'Souza-Li 2006; Egbuna and Brown 2008; Sipos, Pietschmann et al. 2009). For example, genetic defects related to parathyroid hormone signaling can not only lead to hypo- or hypercalcemia (Schipani,

Kruse et al. 1995; Karaplis, He et al. 1998; D'Souza-Li 2006; Egbuna and Brown 2008; Theman and Collins 2009), but also impact growth and induce precocious maturation of bone (Schipani, Kruse et al. 1995; Karaplis, He et al. 1998).

Aside from genetic defects, non-genetic factors can also influence the skeleton, and lead to diseases such as osteoporosis or renal osteodystrophy (Gonzalez and Martin 2001; Bajaj and Saag 2003; Sipos, Pietschmann et al. 2009). In osteoporosis, hormonal imbalances lead to increased bone resorption and result in delicate or brittle bones. In renal osteodystrophy, kidney dysfunction or kidney failure leads to decreased serum calcium levels and reduced bone mineralization; the result of which include bone deformations and bone fractures. These non-genetic factors may include calcium deficiency, vitamin D deficiency, the loss of estrogen associated with menopause, or kidney failure (Fujita 2000; Cosman 2005; Gal-Moscovici and Sprague 2007; Bischoff-Ferrari and Staehelin 2008; Wolff, Jones et al. 2008; Doumouchtsis, Perrea et al. 2009; Williams 2009). Understanding the mechanisms and factors governing bone development is vital to designing treatments that will combat these defects.

Bone development occurs in one of two ways: endochondral bone formation or intramembraneous bone formation (de Crombrugghe, Lefebvre et al. 2001; Kronenberg 2003; Provot and Schipani 2005; Cohen 2006). Endochondral bone is formed through a cartilage intermediate while intramembraneous bone is formed without a cartilage intermediate (de Crombrugghe, Lefebvre et al. 2001; Kronenberg 2003; Provot and Schipani 2005; Cohen 2006). Furthermore, once bone is formed, it is maintained, renewed and resorbed through the process of bone remodeling (de Crombrugghe,

Lefebvre et al. 2001; Kronenberg 2003; Provot and Schipani 2005; Cohen 2006). The mediators of bone formation and bone remodeling are chondrocytes (cartilage-forming cells), osteoblasts (bone-forming cells) and osteoclasts (bone-resorbing cells) (de Crombrugghe, Lefebvre et al. 2001; Kronenberg 2003; Provot and Schipani 2005; Cohen 2006).

In endochondral bone development, chondrocytes differentiate from condensations of mesenchymal precursors and lay down a cartilage matrix on which subsequent bone matrix will be added. The differentiation of the chondrocytes is primarily controlled by Sox9 (Bell, Leung et al. 1997; Bi, Deng et al. 1999), though Sox5 and Sox6 also work synergistically to promote early stages of chondrocyte differentiation (de Crombrugghe, Lefebvre et al. 2001; Kronenberg 2003; Provot and Schipani 2005; Cohen 2006). Chondrocytes lay down a cartilage matrix comprised primarily of collagen II, though cartilage matrix is also comprised of proteoglycans such as aggrecan (de Crombrugghe, Lefebvre et al. 2001; Kronenberg 2003; Provot and Schipani 2005; Cohen 2006; Domowicz, Cortes et al. 2009; Gentili and Cancedda 2009). As chondrocytes mature, Indian hedgehog (Ihh) works through Parathyroid hormone-related protein (PTHrP) signaling to promote chondrocyte proliferation and bring them to the threshold of hypertrophy, but then prevents them from crossing that threshold (Chung, Lanske et al. 1998; de Crombrugghe, Lefebvre et al. 2001; Kronenberg 2003; Amizuka, Davidson et al. 2004; Li, Dong et al. 2004; Provot and Schipani 2005; Cohen 2006; Guo, Chung et al. 2006). Then modulation of Ihh signaling through Fgf/Fgfr3 and Igf1/Igf1r may throw the switch to chondrocyte hypertrophy and subsequent osteoblast differentiation (de

Crombrugghe, Lefebvre et al. 2001; Kronenberg 2003; Marie 2003; Amizuka, Davidson et al. 2004; Provot and Schipani 2005; Cohen 2006).

Osteoblast activity and differentiation is controlled by a sequential series of transcription factors. Runx2 is one of the main transcription factors controlling osteoblasts differentiation and development, and its expression in the mesenchymal cells precedes osteoblast differentiation and is sufficient for mesenchymal differentiation towards the osteoblast lineage (de Crombrugghe, Lefebvre et al. 2001; Franceschi and Xiao 2003; Kronenberg 2003; Li, Dong et al. 2004; Provot and Schipani 2005; Cohen 2006; Guo, Chung et al. 2006). Osterix (Osx) is another osteoblast-specific transcription factor that is a direct downstream target of Runx2 (de Crombrugghe, Lefebvre et al. 2001; Kronenberg 2003; Koga, Matsui et al. 2005; Provot and Schipani 2005; Cohen 2006; Baek, Lee et al. 2009). A number of other signals are thought to work in synergy with either Runx2 or Osx to promote osteoblast-specific gene expression at later stages (Franceschi and Xiao 2003; Koga, Matsui et al. 2005; Baek, Lee et al. 2009). Among the genes differentially regulated by these signals are collagen I, which is the primary structural element of bone matrix, and osteocalcin, a bone mineralization protein found in more mature bone (Franceschi and Xiao 2003; Koga, Matsui et al. 2005; Cohen 2006; Deng, Sharff et al. 2008; Baek, Lee et al. 2009). As the bone matures, it becomes mineralized with calcium and phosphate, and provides storage for excess levels of these minerals.

When the bone matures or is restructured, osteoclasts are responsible for resorbing bone matrix. They secrete matrix metalloproteinases (MMPs) that degrade the

bone and release stored minerals (Delaisse, Andersen et al. 2003; Hou, Troen et al. 2004; Cohen 2006). Receptor activator of NFκB (RANK) and RANK ligand (RANKL) are mediators of osteoclast differentiation, while cathepsin K (CtsK) and MMPs accounts for the majority of the osteoclast activity (Delaisse, Andersen et al. 2003; Hou, Troen et al. 2004; Feng 2005; Cohen 2006; Logar, Komadina et al. 2007; Boyce and Xing 2008). Osteoclast activity is often closely linked with physiological cation levels (Feng 2005; Logar, Komadina et al. 2007; Boyce and Xing 2008). Excess calcium is often stored in bone and when there are drops in calcium levels osteoclast activity can be increased to mobilize calcium stored in bone.

Defects in osteoclasts can lead to osteopetrosis. In osteopetrosis a disruption in a hydrogen ion pump leads dysfunctional osteoclasts and decreased bone resorption. This in turn results in excessive bone formation and bone density (Stark and Savarirayan 2009). In contrast, elevated osteoclast activity contributes to osteoporosis (Bajaj and Saag 2003; Cosman 2005; Logar, Komadina et al. 2007; Sipos, Pietschmann et al. 2009). In osteoporosis, disruption of estrogen levels can lead in increased osteoclast activity, and consequently, increased bone resorption and reduced bone mass. Similarly, the parathyroid gland can respond to low calcium by increasing PTH levels which in turn stimulate osteoclast activity to mobilize calcium.

Bone defects can reflect broader defects beyond the skeleton. Not only can they disrupt the overall architecture and structural stability of an organism, a disruption of the balance of bone remodeling or bone composition can reflect larger problems in the regulation of homeostatic processes. They may indicate changes in ion levels such as

calcium or phosphate and hormonal imbalances such as PTH. Dissecting the mechanisms of underlying bone defects can be of vital importance to understanding and treating broader defects. In the following chapters I will discuss identification of bone defects in *trpm7* mutants and how they led us to identify broader defects in kidney function and cation homeostasis.

Kidney Development

The mammalian kidney is a complex organ responsible for removal of nitrogenous waste, blood filtration, and regulation of osmolarity, fluid balance and pH. It greatly impacts physiological ion homeostasis by controlling the levels of reabsorption or excretion of physiological ions like calcium, magnesium and phosphate. The kidney is composed of numerous functional units known as nephrons, with more than ~800,000 nephrons existing in a human kidney (Bankir, Bouby et al. 1989; Reilly and Ellison 2000; Di Sole 2008; Jabbour and Goldstein 2008; Thomson and Blantz 2008; Wingert and Davidson 2008; Biber, Hernando et al. 2009; Boros, Bindels et al. 2009; Haraldsson and Jeansson 2009; Layton, Layton et al. 2009; Wagner, Devuyst et al. 2009; Wang, Armando et al. 2009). Each nephron regulates metabolite and electrolyte levels and blood pH through distinct subcomponents. The nephron is divided primarily into the glomerulus, a tubule, and a collecting duct (Bankir, Bouby et al. 1989; Reilly and Ellison 2000; Thomson and Blantz 2008; Wingert and Davidson 2008; Haraldsson and Jeansson 2009; Layton, Layton et al. 2009). The glomerulus is responsible for the initial filtration

and concentration of solutes and metabolites from the blood (Bankir, Bouby et al. 1989; Thomson and Blantz 2008; Haraldsson and Jeansson 2009).

This concentrated glomerular filtrate then passes through the tubules where distinct sections of the tubules are responsible for secreting waste and reabsorbing different minerals or metabolites, before the remaining filtrate is excreted as waste (Bankir, Bouby et al. 1989; Kamel, Cheema-Dhadli et al. 2004; Di Sole 2008; Jabbour and Goldstein 2008; Biber, Hernando et al. 2009; Boros, Bindels et al. 2009; Wagner, Devuyst et al. 2009; Wang, Armando et al. 2009). Distinct segments of the tubules are known for secretion of nitrogenous waste and reabsorption of components such as sodium, potassium, glucose, magnesium, calcium, parathyroid hormone, phosphate, and aldosterone (Bankir, Bouby et al. 1989; Kamel, Cheema-Dhadli et al. 2004; Di Sole 2008; Jabbour and Goldstein 2008; Biber, Hernando et al. 2009; Boros, Bindels et al. 2009; Wagner, Devuyst et al. 2009; Wang, Armando et al. 2009). After filtration, secretion and reabsorption in the glomerulus and tubule, the remaining filtrate and waste then passes through the collecting duct to be excreted (Bankir, Bouby et al. 1989; Kamel, Cheema-Dhadli et al. 2004).

Mammalian kidneys are composed of a pronephros and mesonephros at embryonic and fetal stages, but are replaced by the characteristic complexity of the metanephros in later fetal development (Kuure, Vuolteenaho et al. 2000; Wingert and Davidson 2008). In contrast to the mammalian kidney, the teleost and amphibian kidneys each represent a much less complex apparatus (Drummond 2004; Zhou and Vize 2004; Drummond 2005; Wingert and Davidson 2008). In embryonic and early larval stages the

zebrafish kidney is referred to as the pronephros, and comprises only a bilateral pair of nephrons (Drummond 2004; Drummond 2005; Wingert and Davidson 2008). At later larval stages additional nephrons differentiate from the surrounding mesenchyme to form the mesonephros (Drummond 2004; Drummond 2005; Wingert and Davidson 2008). Zebrafish and frog pronephric nephrons appear to be anatomically and functionally similar to a mammalian nephron. They consist of the same fundamental subunits, a glomerulus, a tubule, and a collecting duct (Drummond 2004; Drummond 2005; Wingert and Davidson 2008). Furthermore recent work in zebrafish has shown a large degree in conservation in the segmental gene expression pattern along the tubule which is largely conserved in mammals (Wingert, Selleck et al. 2007; Wingert and Davidson 2008). The zebrafish kidney has at least 8 distinct regions of gene expression, many of which are comparable to patterns of gene expression in discrete segments of mammalian tubules (Wingert, Selleck et al. 2007; Wingert and Davidson 2008). This segmental conservation suggests that the zebrafish nephrons are a promising option for studying processes governing kidney development and function, and how disruption of these processes leads to prevalent renal disorders.

Defects in kidney function can have a severe impact on an organism's development and survival, and are evident in a number of primary and secondary disorders. An estimated 7.4 million adults are affected by chronic kidney disease (National Kidney Foundation 2002) and ~90,000 new cases of end-stage renal disease (ESRD) resulting from diabetes, hypertension and other disorders appear in the U.S. each year (National Kidney Foundation 2002). Treatment of ESRD is estimated to cost more

than $22 billion annually (United States Renal Data System 2003), and treatment of less severe manifestations of renal dysfunction, such as kidney stone formation, is estimated to cost more than $1.8 billion annually (Clark, Thompson et al. 1995; Kuizon and Salusky 1999). Furthermore, renal dysfunction can lead to secondary developmental defects in growth and bone development, as evidenced in children with chronic renal failure (Kuizon and Salusky 1999) and renal osteodystrophy (Gonzalez and Martin 2001; Kuizon and Salusky 2002). Renal dysfunction results in significant biomedical and economic consequences. Improved understanding of the mechanisms and consequences of renal dysfunction can lead to new treatments of related disorders. The zebrafish kidney therefore presents an opportunity to advance understanding of kidney development and function, as well as potentially identifying new methods in treating kidney disorders.

Physiological Ion Homeostasis

As discussed in previous sections, both bone and the kidney impact physiological ion homeostasis. The kidney is the organ responsible for regulating filtration and reabsorption of ions from the blood. Bone acts as a reservoir of ions like calcium and phosphate in its matrix. Physiological ion homeostasis largely represents a complex interplay between bone and kidney in the intricate regulation of ion levels. In mammals a third component, the parathyroid gland, also has a strong influence on ion homeostasis (Akerstrom, Hellman et al. 2005; Zajac and Danks 2008). In teleost fish it is the corpuscles of Stannius (CS) which also impacts ion homeostasis (Krishnamurthy 1976; Lafeber, Flik et al. 1988; Pandey 1994; Greenwood, Flik et al. 2009). These three

components regulate ion homeostasis through a number of tightly controlled endocrine signaling molecules. Many of these molecules can have multiple effects on different components of the parathyroid-bone-kidney axis or the CS-bone-kidney axis. Some of these important regulators include parathyroid hormone (PTH), stanniocalcin (STC), calcitriol, FGF23, cation-sensing receptor (CaSR), and the ions themselves (Lafeber, Flik et al. 1988; Fujita 2000; D'Souza-Li 2006; Gal-Moscovici and Sprague 2007; Bischoff-Ferrari and Staehelin 2008; Doyle and Jan de Beur 2008; Egbuna and Brown 2008; Talmage and Mobley 2008; Wolff, Jones et al. 2008; Greenwood, Flik et al. 2009; Samadfam, Richard et al. 2009; Theman and Collins 2009; Tsagalis, Psimenou et al. 2009). Misregulation of homeostasis can lead to a number of defects, ranging from brittle, poorly mineralized bone (Bajaj and Saag 2003; D'Souza-Li 2006; Egbuna and Brown 2008; Sipos, Pietschmann et al. 2009) or premature bone formation (Schipani, Kruse et al. 1995; Karaplis, He et al. 1998; D'Souza-Li 2006; Egbuna and Brown 2008) to kidney stone formation (Parmar 2004; Stechman, Loh et al. 2007; Moochhala, Sayer et al. 2008; Worcester and Coe 2008), chronic kidney disease (Gonzalez and Martin 2001; Kuizon and Salusky 2002; National Kidney Foundation 2002; Gal-Moscovici and Sprague 2007; Williams 2009), renal failure (Clark, Thompson et al. 1995; Kuizon and Salusky 1999; Gonzalez and Martin 2001; Kuizon and Salusky 2002; Goodman 2006; Rodriguez, Canadillas et al. 2006; Doumouchtsis, Perrea et al. 2009; Williams 2009) and severe growth retardation (Clark, Thompson et al. 1995).

In terrestrial mammals the parathyroid gland, a primary regulator of calcium homeostasis, controls secretion of the anti-hypocalcemic factor PTH. Many of the

disorders associated with imbalances in ion homeostasis often involve dysfunction of the parathyroid gland and exhibit either primary or secondary hypo- or hyperparathyroidism. Within the parathyroid production of PTH is regulated by the cation-sensing receptor (CaSR), with stimulation of PTH occurring in response to detection of decreased blood calcium levels by CaSR. Conversely, when high blood calcium levels are detected, inhibition of PTH production occurs (Akerstrom, Hellman et al. 2005; D'Souza-Li 2006; Egbuna and Brown 2008; Zajac and Danks 2008; Theman and Collins 2009). Hyperparathyroidism is indicative of over-stimulation of PTH production and consequentially often leads to hypercalcemia and bone loss (Fujita 2000; D'Souza-Li 2006; Maeda, Fortes et al. 2006; Egbuna and Brown 2008). Conversely, hypoparathyroidism is indicative of decreased PTH production, leads to hypocalcemia and has associated phenotypes of tetany, seizures, and decreased sensation in extremities (Fujita 2000; Chen and Goodman 2004; D'Souza-Li 2006; Egbuna and Brown 2008).

PTH is both an anti-hypocalcemic and anti-hyperphosphatemic hormone that acts on bone and kidney to effect changes in serum calcium levels (Schipani and Provot 2003; Akerstrom, Hellman et al. 2005; Cohen 2006; Talmage and Mobley 2008; Zajac and Danks 2008; Datta and Abou-Samra 2009). Bone acts as a reservoir for excess calcium and when increased PTH signals to bone, osteoclasts are activated and increased bone resorption is triggered (Akerstrom, Hellman et al. 2005; Cohen 2006; Talmage and Mobley 2008). This bone resorption releases calcium and phosphate stored in the bone matrix. In the kidney PTH contributes to the regulation of divalent cation transport and reabsorption, as well as signaling an increase in phosphate excretion (Akerstrom,

Hellman et al. 2005; Cohen 2006; Doyle and Jan de Beur 2008; Quarles 2008; Talmage and Mobley 2008; Samadfam, Richard et al. 2009; Williams 2009). This increased phosphate excretion lowers serum phosphate levels which in turn increases the calcium to phosphate ratio and leads to more free calcium in the blood (Cohen 2006; Doyle and Jan de Beur 2008; Quarles 2008; Vezzoli, Soldati et al. 2009). PTH also activates a vitamin D hydroxylase in the kidney to promote hydroxylation of 25-hydroxy-vitamin D into its active form (1,25-dihydroxy vitamin D), which is also known as calcitriol (Cohen 2006; Gal-Moscovici and Sprague 2007; Bischoff-Ferrari and Staehelin 2008; Wolff, Jones et al. 2008). Calcitriol then acts on the intestine to increase calcium absorption (Cohen 2006; Gal-Moscovici and Sprague 2007; Bischoff-Ferrari and Staehelin 2008; Wolff, Jones et al. 2008).

In addition to acting as the calcium sensor in the parathyroid to control the set point of physiologic calcium by regulating PTH secretion, CaSR is also located in the kidney and in bone (Brown 2007; Brown and Lian 2008; Vezzoli, Soldati et al. 2009). By regulating PTH secretion in the parathyroid, CaSR indirectly affects divalent cation transport in the kidney. However, CaSR expression in the kidney also leads to a direct role in regulating divalent cation transport (Brown 2007; Vezzoli, Soldati et al. 2009). The role of CaSR in bone is debatable as conflicting reports exist about its presence in osteoblasts or osteoblast-like cells (Pi, Garner et al. 2000; Pi and Quarles 2005; Brown and Lian 2008). However, a CaSR-like receptor does appear to be present in osteoblasts and stimulates proliferation, differentiation and mineralization at high calcium levels (Pi, Garner et al. 2000; Pi and Quarles 2005).

One additional factor that has been characterized recently is FGF23 (Riminucci, Collins et al. 2003; Segawa, Kawakami et al. 2003; Shimada, Hasegawa et al. 2004; Sitara, Razzaque et al. 2004; Doyle and Jan de Beur 2008; Gattineni, Bates et al. 2009; Samadfam, Richard et al. 2009; Tsagalis, Psimenou et al. 2009). Expression of FGF23 has been found in both the bone and kidney, and it is also referred to as phosphatonin (Riminucci, Collins et al. 2003; Segawa, Kawakami et al. 2003; Shimada, Hasegawa et al. 2004; Sitara, Razzaque et al. 2004; Doyle and Jan de Beur 2008; Quarles 2008; Gattineni, Bates et al. 2009; Samadfam, Richard et al. 2009; Tsagalis, Psimenou et al. 2009). As the name implies, FGF23 is an anti-hyperphosphatemic factor which acts on the kidney to control phosphate uptake. FGF23 regulates the expression of the Na/Pi cotransporters in the kidney (Gattineni, Bates et al. 2009; Samadfam, Richard et al. 2009). These transporters control phosphate uptake and reabsorption in the kidney, and are suppressed by circulating levels of FGF23 (Gattineni, Bates et al. 2009; Samadfam, Richard et al. 2009). Though FGF23 expression has been detected at sites within the kidney, its expression is thought to be the most prevalent in osteocytes in bone (Shimada, Hasegawa et al. 2004; Sitara, Razzaque et al. 2004; Doyle and Jan de Beur 2008; Quarles 2008; Samadfam, Richard et al. 2009; Tsagalis, Psimenou et al. 2009). Activating mutations of FGF23 (Segawa, Kawakami et al. 2003) show that high levels of FGF23 lead to hypophosphatemia, whereas ablation of FGF23 causes hyperphosphatemia (Sitara, Razzaque et al. 2004). Furthermore, FGF23 is also known to inhibit production of calcitriol in the kidney, thereby counteracting effects of PTH with respect to phosphate homeostasis and intestinal calcium absorption. It has been hypothesized that the activities

of FGF23 and PTH are antagonistic towards one another and calcitriol is used to maintain a balance (Shimada, Hasegawa et al. 2004), however that remains to be definitively determined.

In terrestrial animals, whose only source of calcium is from diet, PTH acts as anti-hypocalcemic factor to promote storage of calcium in bone and prevent too much loss through urinary excretion. In contrast, fish are surrounded by an abundant external supply of calcium and magnesium and must prevent an overload of these ions to their systems. The corpuscles of Stannius (CS) represent a fish-specific gland primarily responsible for prevention of this overload (Krishnamurthy 1976; Lafeber, Flik et al. 1988; Pandey 1994; Greenwood, Flik et al. 2009). It does this through the secretion of hormones known as stanniocalcins. As opposed to PTH, these factors have both anti-hypercalcemic and anti-hypophosphatemic activity and regulate the transport of calcium across gills and the reabsorption of renal phosphate (Lafeber, Flik et al. 1988; Pandey 1994; Greenwood, Flik et al. 2009). Together this provides a mechanism in which excess circulating calcium can combine with physiologic phosphate to form deposits on bone, and helps limit the uptake of calcium from external media (Lafeber, Flik et al. 1988; Pandey 1994; Greenwood, Flik et al. 2009).

As can be observed with the antagonistic activities of PTH and FGF23 with respect to phosphate regulation, these factors do not act independently of one another. Rather an intricate balance exists between them to maintain set levels of ion homeostasis. Furthermore, for the sake of simplicity the factors discussed here are only a subset of the mechanisms by which ion homeostasis is regulated. Many other components exist which

modify and regulate these signals in a complex interplay between the parathyroid, the kidney and bone to maintain set ion levels.

The TRP family of ion channels

The TRP family members of ion channels have diverse functions and are divided into multiple subfamilies, TRPC (Canonical), TRPV (Vanilloid), TRPP (Polycystin), TRPML (Mucolipin), TRPA (Ankyrin), TRPN (NOMPC), and TRPM (Melastatin) channels (Pedersen, Owsianik et al. 2005; Venkatachalam and Montell 2007). All TRP superfamily members contain six putative transmembrane domains, have varying levels of permeability to cations and exhibit a wide array of cation selectivities (Pedersen, Owsianik et al. 2005; Venkatachalam and Montell 2007). The channels form homo- or heteromultimeric complexes with each other or with close family members. However, possibly the most distinguishing aspects of the TRP superfamily members are the diverse ways these channels can be activated and their responsiveness to disparate signals. TRP channels have been identified with responses to stimulation to touch, sound, light, temperature, and chemicals (Pedersen, Owsianik et al. 2005; Venkatachalam and Montell 2007). TRP channels are also known to have roles in regulation of cations at the organismal and cellular levels and are often vital to cell survival in neuronal and other cell types (Nadler, Hermosura et al. 2001; Walder, Landau et al. 2002; Aarts, Iihara et al. 2003; Monteilh-Zoller, Hermosura et al. 2003; Schmitz, Perraud et al. 2003; Clark, Langeslag et al. 2006; Krapivinsky, Mochida et al. 2006; Su, Agapito et al. 2006; Wei, Sun et al. 2007).

The TRPC subfamily consists of 7 members and represents nonselective Ca^{2+} permeable cation channels which often require PLC for activation (Pedersen, Owsianik et al. 2005; Venkatachalam and Montell 2007). These channels are often broadly expressed but have diverse functions. One family member, TRPC2 has been identified to respond in a pheromone response in mice, where male knockouts fail to show characteristic aggression towards other invading male mice (Liman, Corey et al. 1999; Leypold, Yu et al. 2002; Stowers, Holy et al. 2002). Another member, TRPC6, has been identified as the cause of a kidney disorder, focal and segmental glomerulosclerosis (FSGS) (Reiser, Polu et al. 2005; Winn, Conlon et al. 2005). Here a breach in the capillary/kidney permeability barrier occurs and causes progression towards end stage renal disease. Failure of TRPC6 to interact with nephron and podocin in the foot processes of glomeruli has been proposed as the likely cause of this disease (Reiser, Polu et al. 2005; Winn, Conlon et al. 2005).

The TRPV subfamily contains 6 members, some of which are thermosensitive and also responsive compounds such as capsaicin (spicy foods), piperine (black pepper), and allicin (garlic) (Caterina, Schumacher et al. 1997; Voets, Prenen et al. 2001; Yue, Peng et al. 2001; Hoenderop, van Leeuwen et al. 2003; Muraki, Iwata et al. 2003; Nilius 2003; Macpherson, Geierstanger et al. 2005; McNamara, Randall et al. 2005). The TRPV family members have moderate Ca^{2+} permeability, but only TRPV5-6 are highly selective for Ca^{2+} with their activity tightly regulated by intracellular calcium concentration (Voets, Prenen et al. 2001; Yue, Peng et al. 2001; Nilius 2003). TRPV5 is expressed in the kidney and knockout leads to increased Ca^{2+} absorption due to an inability to reabsorb

calcium (Hoenderop, van Leeuwen et al. 2003). Other TRPV members are activated by cell swelling, cell shearing or hypotonicity (Muraki, Iwata et al. 2003; Nilius, Watanabe et al. 2003; Nilius, Vriens et al. 2004; Liu, Bandyopadhyay et al. 2006). They function in mechanosensing and osmosensing (Liedtke and Friedman 2003).

The TRPP subfamily is best characterized by TRPP1 and TRPP2, mutations in which lead to polycystic kidney disease (PKD) and autosomal dominant polycystic kidney disease (ADPKD), respectively (Mochizuki, Wu et al. 1996; Peral, San Millan et al. 1996; Sutters and Germino 2003). They are localized to primary cilia where they are thought to make cilia capable of sensing fluid flow, osmolarity, and mechanical stretch, by responding to these stimuli with Ca^{2+} elevation (Pennekamp, Karcher et al. 2002; McGrath, Somlo et al. 2003; Nauli, Alenghat et al. 2003).

The TRPML subfamily, consists of three members, but only the first member, TRPML1 (Mucolipin 1), has been well characterized (Sun, Goldin et al. 2000; Bach 2001; Altarescu, Sun et al. 2002; LaPlante, Falardeau et al. 2002; LaPlante, Ye et al. 2004). Mutations in mucolipin1 are known to cause a lysosomal storage disorder known as Mucolipidosis IV, and this disease leads to severe neurodegeneration (Sun, Goldin et al. 2000; Bach 2001; Altarescu, Sun et al. 2002; LaPlante, Falardeau et al. 2002; LaPlante, Ye et al. 2004). Mucolipin 1, which is localized to lysosomal membranes and permeable to monovalent cations is thought to act as a proton channel that regulates lysosomal pH (Sun, Goldin et al. 2000; Bach 2001; Altarescu, Sun et al. 2002; LaPlante, Falardeau et al. 2002; LaPlante, Ye et al. 2004).

The TRPA and TRPN family members are less well characterized. TRPA only consists of 1 member, which is localized in the tips of stereocilia (Corey, Garcia-Anoveros et al. 2004). Knockdown of TRPA1 in zebrafish and mouse embryos reduces auditory-evoked potentials, therefore it is hypothesized that TRPA1 may play a role in auditory response (Corey, Garcia-Anoveros et al. 2004). The TRPN subfamily does not have any mammalian homologues, though members exist in flies, worms and zebrafish (Walker, Willingham et al. 2000; Sidi, Friedrich et al. 2003). TRPN1 is expressed in the hair cells of the zebrafish ear and its knockdown also induces sound-evoked potentials (Sidi, Friedrich et al. 2003).

Of most relevance to my work is the TRPM subfamily of cation channels, which is composed of 8 members (Kraft and Harteneck 2005; Pedersen, Owsianik et al. 2005; Venkatachalam and Montell 2007). The founding member, TRPM1 (melastatin1), was initially identified because its expression was inversely correlated with the metastatic potential of melanomic cell lines (Duncan, Deeds et al. 1998; Duncan, Deeds et al. 2001; Miller, Du et al. 2004). TRPM2 is unique among TRP members in that it has an ADP-ribose pyrophosphatase domain linked to its C-terminus. It is a Ca^{2+} permeable cation channel that is activated by ADP-ribose and NAD, and is thought to be a sensor of oxidative stress (Perraud, Fleig et al. 2001; Sano, Inamura et al. 2001; Mori, Wakamori et al. 2002). TRPM3 is a constitutively active Ca^{2+} and Mn^{2+} permeable cation channel with activity enhanced by cell swelling and extracellular hypotonicity (Grimm, Kraft et al. 2003; Lee, Chen et al. 2003). TRPM8 is rare in that it is a cold activated cation channel. It is also responsive to menthol, eucalyptol and icilin and its main function is considered

to be as a thermosensor in sensory neurons (Grimm, Kraft et al. 2003; Lee, Chen et al. 2003). TRPM4 and TRPM5 are calcium-activated monovalent cation selective channels (VCAMs). Their activity is thought to be modulated by changes in membrane potentials (Launay, Fleig et al. 2002; Hofmann, Chubanov et al. 2003; Nilius, Prenen et al. 2003; Prawitt, Monteilh-Zoller et al. 2003). Both TRPM4 and 5 are thermal sensitive, and TRPM5 is an established taste-transduction signal. In TRPM5 knockout mice, their responses to sweet and bitter taste are greatly reduced (Perez, Huang et al. 2002; Zhang, Hoon et al. 2003).

Among the TRP superfamily, and even within the TRPM subfamily, TRPM6 and TRPM7 are unique. They are closely related channels that have alpha-kinase domains linked to their C-terminus that regulate channel activity (Nadler, Hermosura et al. 2001; Runnels, Yue et al. 2001; Chubanov, Mederos y Schnitzler et al. 2005; Schlingmann, Waldegger et al. 2007). Both TRPM6 and TRPM7 are preferentially permeable to a number of divalent cations, including Mg^{2+} and Ca^{2+} (Nadler, Hermosura et al. 2001; Monteilh-Zoller, Hermosura et al. 2003; Schmitz, Perraud et al. 2003; Voets, Nilius et al. 2004; Li, Jiang et al. 2006; Topala, Groenestege et al. 2007). Their high degree of permeability to Mg^{2+} highlights the importance of the channels in Mg^{2+} homeostasis. For functional channels to form, TRPM6 must form multimeric complexes and is generally thought to multimerize obligately with TRPM7 (Chubanov, Waldegger et al. 2004; Schmitz, Dorovkov et al. 2005). Other studies suggest homomeric TRPM6 complexes may be active as well (Fujiwara and Minor 2008). By contrast, TRPM7 can function as either a heteromeric or homomeric channel (Runnels, Yue et al. 2001; Monteilh-Zoller,

Hermosura et al. 2003; Schmitz, Dorovkov et al. 2005; Li, Jiang et al. 2006; Fujiwara and Minor 2008).

TRPM6 channels are found primarily in organs at sites that regulate magnesium absorption, such as the intestinal brush border and the renal distal convoluted tubule (DCT) (Voets, Nilius et al. 2004; Fonfria, Murdock et al. 2006; Groenestege, Hoenderop et al. 2006; Kunert-Keil, Bisping et al. 2006). In humans, mutant forms of TRPM6 are linked to hypomagnesemia with secondary hypocalcemia (HSH or HOMG) (Schlingmann, Weber et al. 2002; Walder, Landau et al. 2002). In HSH, a decrease in renal and intestinal reabsorption of magnesium is observed, resulting in a drop in physiological magnesium levels. This leads to inhibition of the cation-sensing receptor (CaSR) in the parathyroid gland which in turn results in decreased parathyroid hormone production and a secondary drop in calcium levels (Vetter and Lohse 2002; Iwasaki, Asai et al. 2007; Alexander, Hoenderop et al. 2008). Thus, TRPM6 is the primary regulator of whole-organism magnesium homeostasis. However the likely necessity of heteromultimerizing with TRPM7 suggests that TRPM7 may be of equal importance to the process.

TRPM7 channels are expressed ubiquitously and regulate cellular magnesium homeostasis (Aarts, Iihara et al. 2003; Wei, Sun et al. 2007). The importance of TRPM7 to cellular magnesium homeostasis was established using DT40 cells lacking TRPM7 (Schmitz, Perraud et al. 2003). These cells were growth-arrested and had depleted Mg^{2+} levels, however with supplementation of extracellular magnesium, the growth arrest and lethality were rescued. In addition to its role in regulating cellular magnesium influx,

other studies have demonstrated the importance of the Ca^{2+} permeability of TRPM7. One group has showed that TRPM7-mediated Ca^{2+} currents are activated by reactive oxygen/nitrogen species (ROS) lead to death of anoxic neurons (Aarts, Iihara et al. 2003). Others identified the importance of TPRM7-mediated Ca^{2+} influx in the proliferation of human retinoblastoma cells (Hanano, Hara et al. 2004). Additionally, other groups have identified the importance of a localized TRPM7-mediated influx of Ca^{2+} associated with changes in cell adhesion, cell spreading and actomyosin contractility (Clark, Langeslag et al. 2006; Su, Agapito et al. 2006).

While many roles have been established for TRPM7 channel activity, other roles have been established for the kinase domain. This domain is known to be the primary regulator of channel activity through auto-phosphorylation at multiple sites and its activity is dependent on intracellular Mg^{2+} and Mg-nucleotide concentrations (Ryazanova, Dorovkov et al. 2004; Takezawa, Schmitz et al. 2004; Demeuse, Penner et al. 2006). However, in addition to this auto-regulation, the kinase domain has other targets within the cell (Dorovkov and Ryazanov 2004; Clark, Langeslag et al. 2006). One of the initial identifications of TRPM7 was through the interaction of the kinase with PLCβ1 (Runnels, Yue et al. 2001; Dorovkov and Ryazanov 2004; Clark, Langeslag et al. 2006). Other identified targets include myosin IIA heavy chain and annexin I (Dorovkov and Ryazanov 2004; Clark, Langeslag et al. 2006).

Most of the investigations into TRPM7 have focused on its impact at the cellular level and the early lethality associated with TRPM7 mutations in mammalian systems has precluded analyses of roles of TRPM7 at the organismal level (Jin, Desai et al. 2008).

The work presented herein focuses on the impact TRPM7 has at the organismal level by making use of zebrafish *trpm7* mutants as an animal model. In the following chapters I will discuss the identification and cloning of *trpm7* mutants, characterize growth and skeletogenic defects, and demonstrate the formation of kidney stones in *trpm7* mutants. Furthermore, I will demonstrate the impact of *trpm7* on pronephric activity and physiologic cation homeostasis. Together this work provides a substantial step towards understanding the impact of TRPM7 at the organismal level.

Chapter 2: Defective Skeletogenesis with Kidney Stone Formation in Dwarf Zebrafish Mutant for *trpm7*

Summary

Development of the adult form requires coordinated growth and patterning of multiple traits in response to local gene activity as well as global endocrine and physiological effectors. An excellent example of such coordination is the skeleton. Skeletal development depends on the differentiation and morphogenesis of multiple cell types to generate elements with distinct forms and functions throughout the body (Karsenty and Wagner 2002; Fisher, Jagadeeswaran et al. 2003; Kronenberg 2003). We show that zebrafish *touchtone/nutria* mutants exhibit severe growth retardation and gross alterations in skeletal development in addition to embryonic-melanophore and touch response defects (Arduini and Henion 2004; Cornell, Yemm et al. 2004). These alterations include accelerated endochondral ossification but delayed intramembranous ossification, as well as skeletal deformities. We show that the *touchtone/nutria* phenotype results from mutations in *trpm7*, which encodes a transient receptor potential (TRP) family member that functions as both a cation channel and kinase. We find *trpm7* expression in the mesonephric kidney and show that mutants develop kidney stones, indicating renal dysfunction. These results identify a requirement for *trpm7* in growth and skeletogenesis and highlight the potential of forward genetic approaches to uncover physiological mechanisms contributing to the development of adult form.

Results and Discussion

Genetic screens for ethyl-*N*-nitrosurea-induced mutations affecting zebrafish postembryonic development uncovered the *nutria*^{j124e2} mutant, named for its small size, odd shape, and tendency to swim near the surface (Figures 2.1A and 2.1B). As embryos and early larvae (2-5 days post fertilization [dpf]), *nutria* are comparable in size to wild-type siblings, but during later development they exhibit a severe growth deficit (Figure 2.1C). Craniofacial and trunk-body proportions are altered, although other external features (e.g. scales, fins, and the complement of adult pigment cells) are not grossly abnormal. To identify the locus causing this dwarf phenotype, we mapped the *nutria* mutation to chromosome 18 in the vicinity of *touchtone* (*tct*) (Arduini and Henion 2004; Cornell, Yemm et al. 2004). Both *tct* and *nutria* mutants exhibit embryonic melanophore deficiencies and touch unresponsiveness prior to hatching. Complementation tests confirmed that *nutria* and *tct* are allelic. Fine mapping of the critical region revealed, among other genes, *trpm7*, which encodes an ortholog of the transient receptor potential (TRP) melastatin-7 dual-function cation channel and kinase (0/2889 recombinants) (Wolf 2004). Although *TRPM7* has not been implicated in growth previously, a member of this family, *TRPM1* (*melastatin*), is expressed in human melanocytic nevi (Duncan, Deeds et al. 1998), and zebrafish melanophores require *tct* cell autonomously (Arduini and Henion 2004; Cornell, Yemm et al. 2004).

Our data show that *trpm7* corresponds to *tct*. Sequencing *trpm7* cDNAs revealed premature stop codons in the severe alleles *tct*^{j124e1} and *tct*^{b508} (Figure 2.S1D and 2.S1E). Moreover, the injection of wild-type embryos with a *trpm7* splice-blocking morpholino

oligonucleotide results in both melanophore deficiencies and touch unresponsiveness and thus phenocopies the mutant (Figure 2.S1A-2.S1C). Finally TRPM7 acts as an inwardly rectifying cation channel with broad specificity but high affinity for Mg^{2+} and Ca^{2+}, suggesting that manipulating divalent-cation availability might rescue embryonic phenotypes of *trpm7* mutants (Monteilh-Zoller, Hermosura et al. 2003; Schmitz, Perraud et al. 2003). Supplemental Mg^{2+} partially rescued melanophore development, whereas supplemental Ca^{2+} partially rescued melanophore development and touch responsiveness (Figures 2.1D-2.1F; Figure 2.S2). Thus, *trpm7* is the gene affected in *tct* mutants.

To clarify the mode(s) of *trpm7* activity, we examined *trpm7* expression in wild-type embryos and larvae. Consistent with previous observations, we detected widespread *trpm7* expression at embryonic stages, including in the central nervous system, pronephros, lens, and other tissues (The Zebrafish Information Network 2005; data not shown). In metamorphic larvae, transcripts were abundant in liver, mesonephric kidney tubules, and corpuscles of Stannius, which are teleost glands that contribute to calcium homeostasis (Krishnamurthy 1976) (Figures 2.2A-2.2C). In contrast to severe alleles, *trpm7*^{j124e2} (*nutria*) individuals are viable, allowing us to assess functional consequences of *trpm7* mutation during postembryonic development. Consistent with kidney expression of *trpm7*, histological examination of *trpm7*^{j124e2} mutant larvae revealed mineralization within mesonephric tubules (Figures 2.2T and 2.2X). These data suggest that altered *trpm7* function in the kidney, in the corpuscles of Stannius, or in both affects whole-organism cation homeostasis and leads to nephrolithiasis.

Because dwarfism syndromes in humans are associated with a range of skeletal defects (Hall 2002) and cation homeostasis affects bone development and maintenance (Dvorak and Riccardi 2004), we asked whether the growth deficit and disproportionality of *trpm7*^{j124e2} mutants is associated with changes in ossification. A comprehensive analysis of 87 bones between 9 and 51 dpf revealed extensive re-alterations in ossification sequence between wild-type and mutant larvae (Figures 2.3 and 2.4). Among numerous examples of sequence reordering is the epural bone of the caudal fin, which is the 78th bone to ossify in the wild-type but only the 32nd to ossify in *trpm7* mutants. Conversely, the maxilla is the 15th bone to ossify in the wild-type but the 40th to ossify in *trpm7* mutants. Thus, *trpm7*$^{+}$ is essential for the normal sequence of ossification.

To better understand ossification changes, we categorized bones according to function and anatomical location as well as cellular origin. The most dramatic differences were between endochondral bones, which develop through mineralization of a cartilage model, and intramembranous bones, which develop directly, without a cartilage model (Cubbage 1996; Karsenty and Wagner 2002; Bird and Mabee 2003). In *trpm7* mutants, endochondral bones (red connectors in Figure 2.4A) appeared on average earlier in the ossification sequence than they did in the wild-type, whereas intramembranous bones (green connectors) appeared on average later. Dissociation of endochondral and intramembranous ossification is exemplified by the caudal complex, in which the endochondral hypurals and epural ossify much earlier in *trpm7* mutants compared to the wild-type, whereas the intramembranous urostyle, centra, and other bones ossify much later in *trpm7* mutants (Figures 2.3A–2.3H). Precocious endochondral ossification is

similarly evident in the suspensorium and the branchial arches of *trpm7* mutants (Figures 2.3I–2.3P), whereas delayed intramembranous ossification is apparent for several bones of the anterior head (Figures 2.3Q–2.3V). The accelerated ossification of endochondral bones and the delayed ossification of intramembranous bones reflect order in the ossification sequence as well as absolute timing. One can most easily visualize these timing differences by plotting how genotype affects the likelihood of bones being ossified at any given age against the statistical significance of these differences (Figures 2.4B and 2.4C). Defects in ossification timing do not simply reflect growth retardation; even severely runted wild-type fish develop skeletal elements of normal shape without premature ossification (Figure 2.S4).

Furthermore, functional-anatomical units in close proximity were found to be differentially affected, even after we controlled for the relative contributions of endochondral and intramembranous bones within these units. For example, otic bones are accelerated, whereas orbital bones are delayed, despite the anatomical proximity of these bones and their similar endochondral and intramembranous compositions (Figure 2.4C; Table 2.S1). Finally, *trpm7* mutants exhibited skeletal dysplasia, including extreme malformation of the Weberian (auditory) apparatus and the ribs, compressed vertebrae (of normal number), and kinks in the posterior vertebral column (Figures 2.3D, 2.3H, 2.3S, and 2.3W).

We have demonstrated that *trpm7* is essential for growth and skeletogenesis during the zebrafish larval-to-adult transition and for melanophore development and touch response during embryogenesis. *trpm7* expression in kidney and corpuscles of

Stannius, as well as the presence of kidney stones in *trpm7* mutants, support a model in which effects on growth and skeletogenesis reflect physiological regulation of cation homeostasis. These effects may be analogous to those of parathyroid hormone/parathyroid hormone receptor type 1 (PTHR1) regulation of calcium homeostasis in mammals, in which changes in PTHR1 signaling or downstream effectors such as Runx2 can lead to premature endochondral ossification (Schipani, Kruse et al. 1995; Karaplis, He et al. 1998; Takeda, Bonnamy et al. 2001; Ueta, Iwamoto et al. 2001). However, this model does not readily explain the delayed intramembranous ossification observed in *trpm7* mutants. Although the precise functions of *trpm7* in promoting normal ossification sequence and timing, as well as melanophore development and touch response, remain to be elucidated, our analyses reveal important roles for *trpm7* in the physiological regulation of postembryonic growth and skeletogenesis.

Experimental Procedures

Fish Stocks and Maintenance

Mutations were induced in wild-type AB, SJD, and wik^{ut} genetic backgrounds by standard methods of ethyl-*N*-nitrosourea mutagenesis. Fish were reared at 28.5˚C and fed rotifers, paramecia, or dry flake food, as appropriate. For growth series of wild-type fish and *nutria* mutants, fish were reared individually from embryonic through adult stages and fed ad libitum to eliminate competition. For staining series, wild-type and mutant

individuals were sorted at 3 dpf and then reared separately at equivalent densities to minimize variation in growth rates within each genotype.

Skeletal Staining and Classification

Fish were fixed in 4% paraformaldehyde in phosphate-buffered saline (PBS) for 48 hr and dehydrated over 2 days to 100% ethanol. They were then stained with Alcian blue for cartilage, digested with trypsin, and stained with Alizarin red for bone according to the standard protocol for fish larvae (Potthoff 1984). Fish were transferred to 100% glycerol over 1 week for analysis and storage. For calcein staining, we fixed larvae with 4% paraformaldehyde in PBS, embedded them in OCT, and collected cryosections on Fisherbrand Superfrost Plus slides. After they were dried and rinsed in PBS, slides were immersed in 0.1% calcein in PBS for 10 min, rinsed extensively in PBS, and coverslipped. The classification of bones by method of ossification and anatomical-functional units followed that used by references (Cubbage 1996; Bird and Mabee 2003; Fleming, Keynes et al. 2004).

Genetic Mapping and Sequencing

Meiotic mapping was performed by standard methods using haploid and diploid mapping panels constructed with AB and wik mapping strains (panel sizes: *trpm7*^{j124e2}, 1400 haploid embryos; *trpm7* ^{b722}, 1000 diploid embryos; *trpm7*^{b508}, 435 haploid embryos; and *trpm7*^{b508}, *trpm7* ^{os1}, and *trpm7* ^{os2}, 54 diploid embryos). For identification of mutant lesions, polymerase-chain-reaction (PCR) products of *trpm7* cDNAs were

sequenced directly and compared with sequences derived from the corresponding mutagenized genetic background.

Morpholino-Based Gene Knockdown

For morpholino-injection experiments, eggs were obtained from natural matings of wild-type fish of the ZDR strain (Scientific Hatcheries, Huntington Beach, California). Morpholino oligonucleotides (GeneTools, Sumerton, Oregon) were diluted to 20 mg/ml in Danieau buffer and then to 0.8 mg/ml in 0.2 M KCl for injection. We designed a morpholino (GTG TGT GAG ATT TAC TCT GCT GTT C) to interfere with splicing (Draper, Morcos et al. 2001) at the junction between exon 12 and intron 12. Embryos were injected at the 2- to 4-cell stage with approximately 5 nl of 0.8 mg/ml *trpm7* morpholino or of the standard negative control morpholino (GeneTools). Sequencing of morpholino-injected embryos confirmed failed splicing of intron 12, and this failure resulted in a frameshift and a premature stop codon (not shown). With all morpholinos, we observed approximately 5% mortality before 12 hpf, presumably from injection wounds. At all stages, embryos injected with standard negative-control morpholino appeared identical to uninjected embryos (not shown). A phenotype of highly reduced melanophore differentiation throughout the embryo (shown in Figure 2.S1) was observed in 80% of injected embryos ($n = 60$), with other embryos showing a less-pronounced phenotype. Limited morpholino perdurance precluded testing for effects of morpholino knockdown on late-developing kidney and ossification phenotypes.

In Situ Hybridization

Whole-mount in situ hybridization, with minor modifications, followed (Quigley, Turner et al. 2004). In brief, larvae were fixed over 2 nights in 4% paraformaldehyde and 1% DMSO in PBS, transferred to methanol, and then rehydrated to PBST (PBS with 0.2% Tween-20). Larvae were treated for 30 min with 20 mg/ml proteinase-K in PBST containing 1% DMSO, postfixed for 20 min in 4% paraformaldehyde in PBST, washed in PBST, and then washed three times in a hybridization solution lacking transfer RNA (tRNA) and heparin. Prehybridizations were performed overnight at 68˚C in a hybridization solution (50% formamide, 5x SSC, 500 mg/ml yeast tRNA, 50 mg/ml heparin, 0.2% Tween-20, and 9.2 mM citric acid). Hybridizations were performed over two nights at 68˚C in a fresh hybridization solution containing antisense digoxygenin-labeled riboprobes fractionated to ~300 nucleotides. Probes derived from 5' and 3' ends of *trpm7* transcripts yielded qualitatively similar results. Larvae were then washed twice in 2x SSCT and three times for 2 hr each in 0.2x SSCT at 68˚C. After graded changes were made to maleic acid buffer (MAB; 100 mM maleic acid [pH 7.5] and 150 mM NaCl), larvae were blocked overnight with Roche blocking reagent in MAB at 4˚C, incubated over 3 nights in a fresh blocking reagent containing 1:5000 anti-digoxygenin alkaline phosphatase-conjugated Fab fragments (Roche), and then washed over 3 additional nights in MAB. Larvae were then transferred to alkaline phosphate buffer (100 mM Tris [pH 9.5], 50 mM MgCl2, 100 mM NaCl, and 0.1% Tween-20), and the color was developed with NBT/BCIP.

Cation Rescue Experiments

tct^{b508} mutant embryos and wild-type siblings were obtained from matings of heterozygous carriers. Chorionated embryos were reared to the 26-somite stage in water and then transferred to embryo medium (Westerfield 2000) (17.9 mM NaCl; "0" in Figure S2) or modified embryo medium (4.2 mM NaCl; "0" in Figure S2) with or without the addition of MgCl2 (100 mM) or CaCl2 (50 mM or 100 mM). We tested touch response by prodding embryos still in their chorions one time with a probe at the midtrunk level; any response to this stimulus was considered a rescue. Melanophore morphologies were examined over the head and trunk; the presence of any well-spread melanophores of normal size was considered a rescue. Both melanophore and touch-response phenotypes were observed between 48 and 60 hpf. Treatments were replicated across multiple families two to seven times with seven to 35 embryos per condition.

Quantitative Analyses of Ossification Sequence and Timing

We reconstructed ossification sequences in wild-type fish and *trpm7* mutants by determining the frequency with which each skeletal element was ossified within all individuals of each genotype and then ordering these frequencies into ranks (Mabee, Olmstead et al. 2000). Elements that failed to ossify within the range of ages examined were ordered arbitrarily (ranks 83–87 in Figure 2.4A in the main text). Differences in rank between wild-type fish and mutants were highly significant between endochondral and intramembranous bones (Wilcoxon test: $Z = 6.03$, d.f. = 1, $\rho < 0.0001$).

To assess the likelihood of bone ossification, we performed separate logistic regression analyses for each bone, developmental mode (endochondral and intramembranous), or functional-anatomical unit with genotype as a main effect and dpf as a covariate. Alternative models, including only genotype or including genotype and other main effects to control for stage and batch variability (e.g., standard length of wild-type siblings), yielded qualitatively similar results. Note that estimates of timing differences between genotypes reflect only the onset of ossification as evidenced by the first indication of Alizarin-red staining; they do not account for differences in rate once ossification has started. Overall, *trpm7* mutants exhibited greatly accelerated ossification rates for endochondral bones and correspondingly delayed ossification rates for intramembranous bones even after ossification had commenced. Analyses shown here thus underestimate the magnitude of rate differences between genotypes. Because of the large numbers of individual tests for logistic regression analyses, we assessed overall significance levels by means of a standard Bonferroni correction ($\alpha = 0.05$, adjusted critical-significance level = 0.000127), which is likely to be overly conservative, as well as a more recent method of assessing false discovery rate (q value) (Storey and Tibshirani 2003). We provide both significance thresholds in Figure 2.4B in the main text. For the smaller number of tests for developmental mode and functional-anatomical units, we provide only Bonferroni-corrected significance threshold (Figure 2.4C in the main text). See Table 2.S1 for a complete listing of effects and significance levels by bone. Statistical analyses were performed with JMP 5.0.1a for Apple Macintosh computers (SAS Institute, Cary NC) and software of (Storey and Tibshirani 2003).

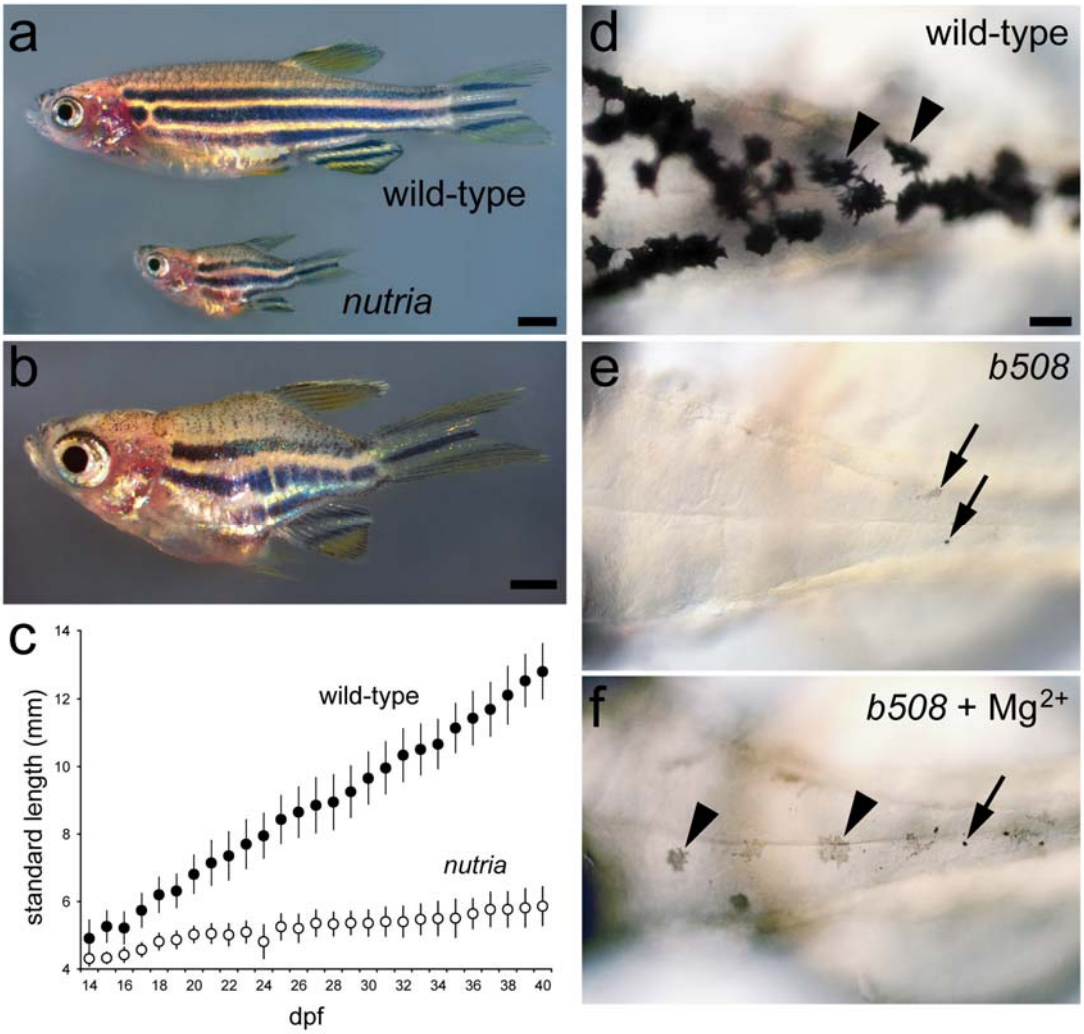

Figure 2.1. **Retarded growth and altered body proportions in *nutria* (*tct*) mutant zebrafish with embryonic melanophore defect rescuable by divalent-cation supplementation.** (A) Wild-type and *nutria* siblings, 50 dpf. (B) Higher-magnification image of a *nutria* mutant. (C) Diminished growth of *nutria* compared to wild-type siblings. Each point shows the mean standard length ± standard deviation for seven to 20 individuals. (D–F) Embryonic melanophore defects are rescuable with supplemental Ca^{2+}. (D) Wildtype embryos exhibit well-melanized and well-spread melanophores (arrowheads). (E) Mutants exhibit few poorly melanized and punctate melanophores or melanophore fragments (arrows); *tct* ^{b508} is shown. (F) In a medium supplemented with Ca^{2+}, mutant melanophores are more numerous, spread, and melanized (arrowheads), although some punctate melanophores remain (arrow). Scale bars represent the following: (A), 2 mm; (B), 1 mm; (D–F), 100 μm.

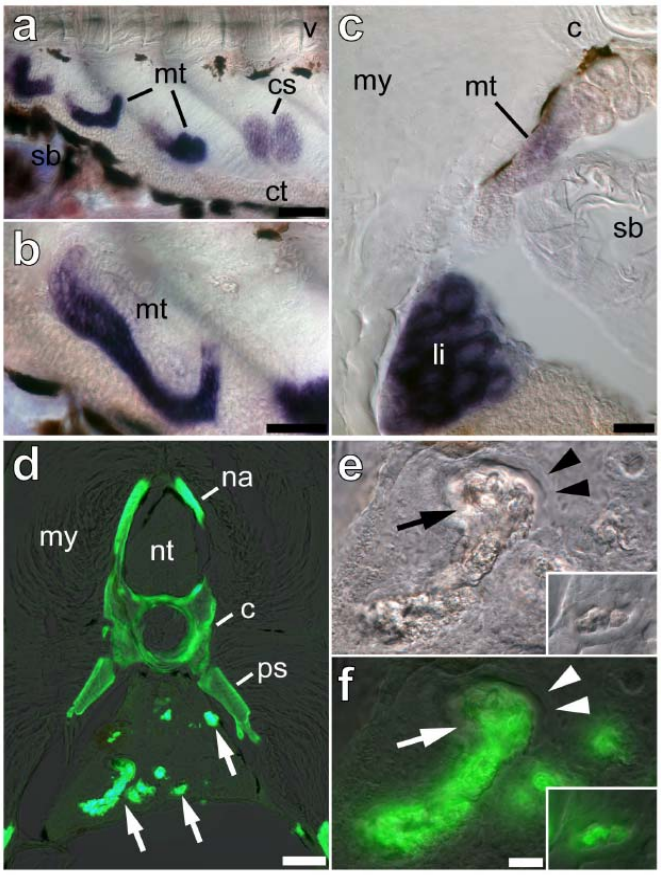

Figure 2.2. *trpm7* expression in wild-type larvae and kidney stone formation in *trpm7* mutants. (A-C) *trpm7* expression in metamorphosing wild-type larvae. (A) At early stages of metamorphosis (14 dpf), *trpm7* mRNA is present in mesonephric tubules (mt) and corpuscles of Stannius (cs). The following abbreviations are used: v, vertebral column; sb, swimbladder; and ct, mesonephric collecting tubule. *trpm7* expression is also detectable in more-anterior regions of the mesonephros (not shown). (B) A higher-magnification *trpm7*$^{+}$ mesonephric tubule is shown. (C) Transverse section of late-metamorphic (24 hpf) larva. *trpm7* transcripts are present in mesonephric tubules and liver (indicated by ("li"). *trpm7* transcripts are not detectable in developing endochondral or intramembranous bones. "my" denotes myotome and "c" denotes centrum. (D-F) *trpm7*^{j124e2} (*nutria*) mutants develop kidney stones. (D) Calcein staining reveals skeletal elements (na, c, ps) and ectopic mineralization (arrows). The following abbreviations are used: na, neural arches; c, centrum; ps, pleural spines; and nt, neural tube. (E) shows left most ectopic mineralization from panel (D). Epithelium (arrowheads), surrounds the mineralized deposit (arrow). the inset shows mineralized deposit within collecting tubule of another larva. (F) shows calcein staining of mineralized deposits shown in panel (E) and the inset.
Scale bars represent the following: (A) µm; (B), 40µm; (C) and (D), 80µm; (E) and (F), 20µm (15µm for insets).

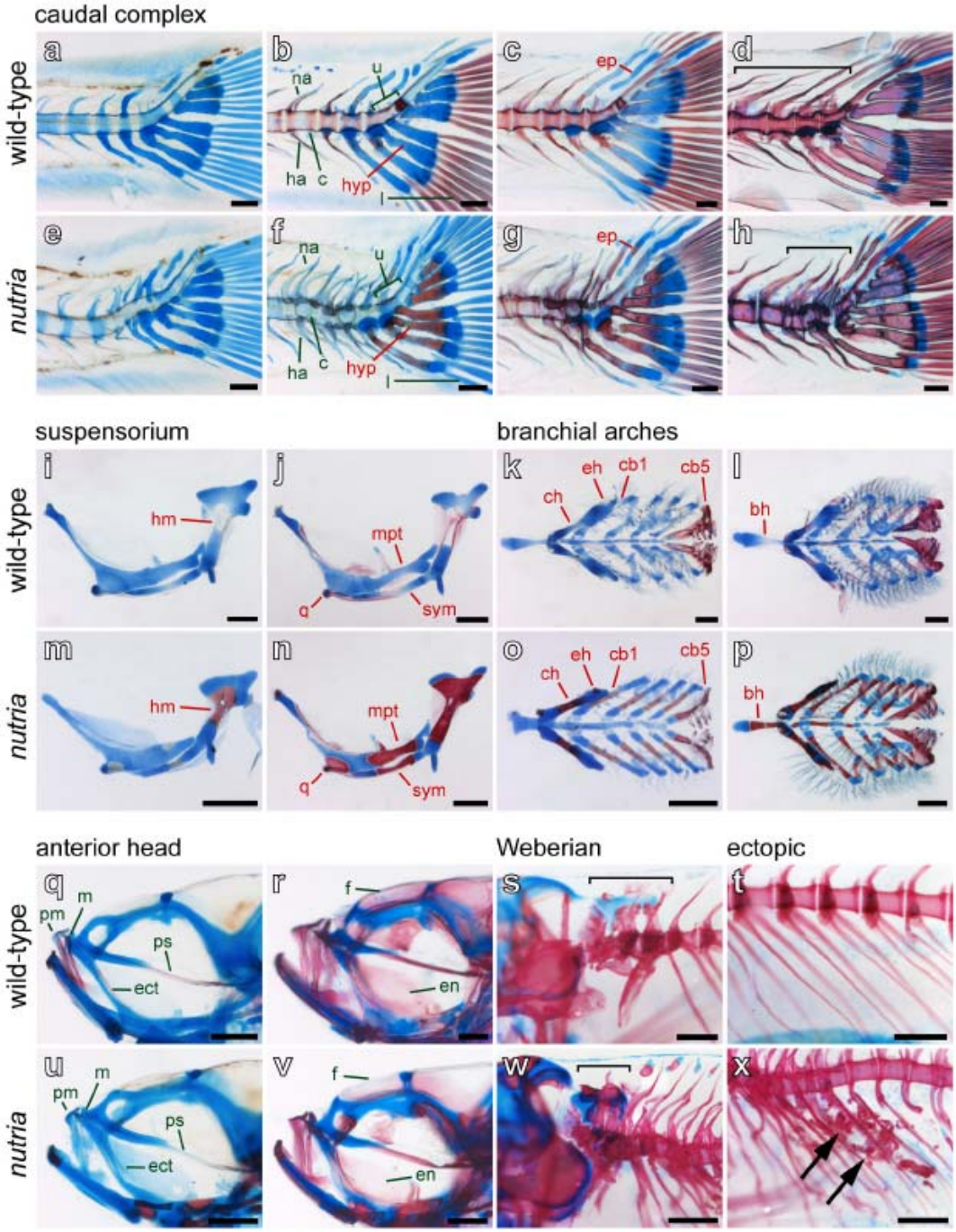

Figure 2.3. *trpm7*^{j124e2} mutants exhibit dramatic differences in skeletal development in comparison to wild-type. Alizarin red stains ossified bone and mineralized tissues. Alcian blue stains cartilage. Endochondral bone labels are red, and intramembranous bone labels are green. (A–H) Differences in ossification timing in the caudal complex between wild-type (A–D) and mutant (E–H) siblings (9–44 dpf, left to right). In mutants, endochodondral bones ossify earlier [panels (B) and (F): hyp. Panels (C) and (G): ep],

whereas intramembranous bones ossify later [panels (B) and (F): na, u, ha, c, l]. Compression of vertebrae and the caudal complex are evident [panels (D) and (H): brackets]. (I–P) The suspensorium (I–N) and branchial arches (K–P) illustrate precocious endochondral ossification in mutants. Advances in ossification are apparent for several endochondral bones at early stages [17 dpf. Panels (I) and (M): hm. Panels (K) and (O): ch, eh, cb1] and later stages [47 dpf. Panels (J) and (N): mpt, q, sym. Panels (L) and (P): bh]. (Q, U, R, V) Bones of the anterior head illustrate delayed intramembranous ossification in mutants. Intramembranous bones are delayed in mutants at early stages [24 dpf. Panels (Q) and (U): pm, m, ps, ect] and later stages [44 dpf. Panels (R) and (V): f, en]. (S, W) Bones of the Weberian apparatus (brackets) are malformed and compressed in mutants. (T, X) Mineralizations within the mesonephros of mutant larvae [arrowheads in panel (X)]. (S) and (T) are at 35 dpf; (W) and (X) are at 30 dpf. The following abbreviations are used: bh, basihyal; c, centra; cb1, ceratobranchial 1; cb5, ceratobranchial 5; ch, ceratohyal; ect, ectopterygoid; eh, epihyal; en, entopterygoid; ep, epural; f, frontal; ha, hemal arches; hm, hyomandibula; hyp, hypurals; l, lepidotrichia; m, maxilla; mpt, metapterygoid; na, neural arches; pm, premaxilla; ps, parasphenoid; q, quadrate; sym, symplectic; and u, urostyle and ural 1 + 2.
Scale bars represent the following: (A–H), 100 μm; (I–X), 250 μm.

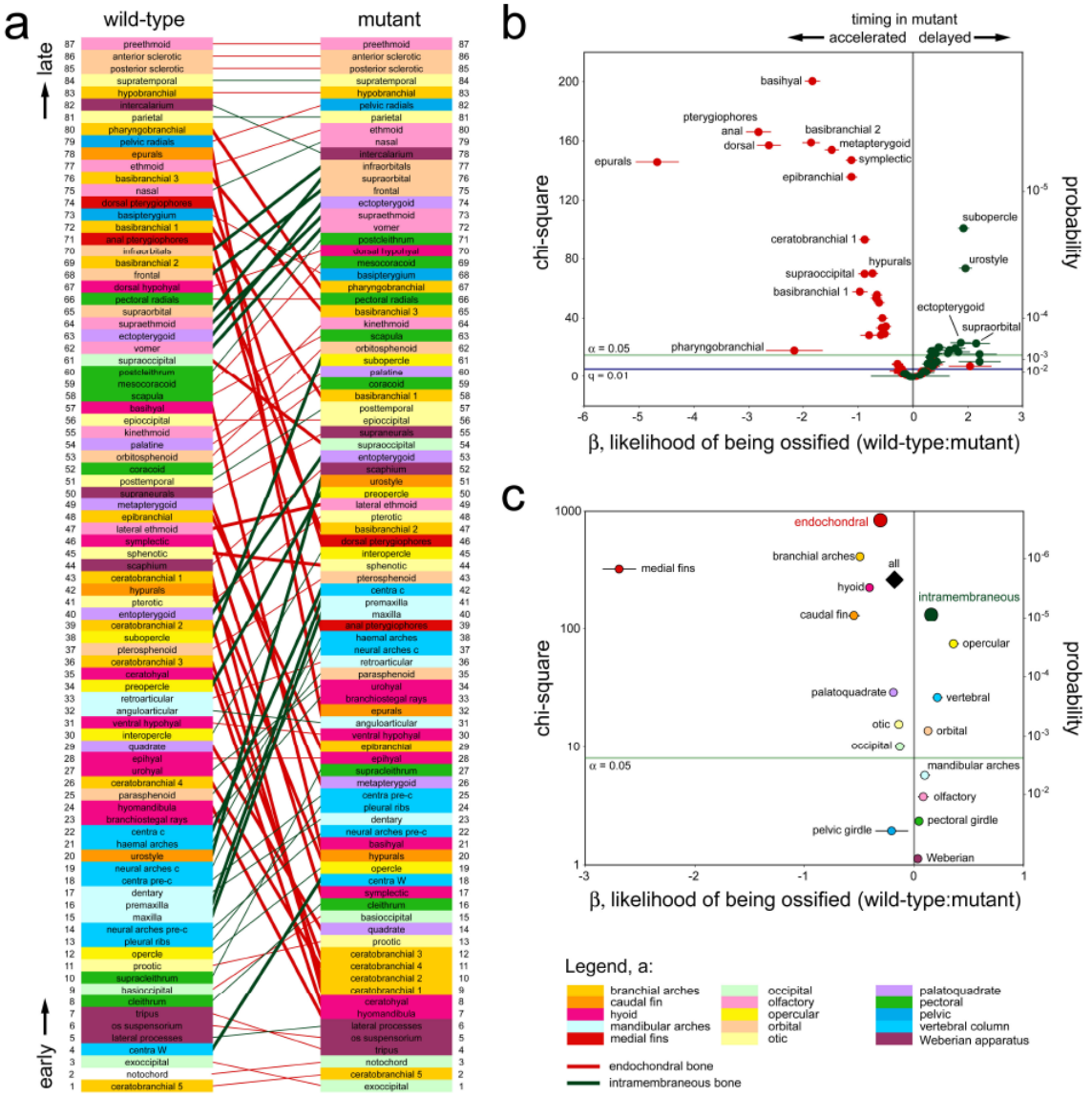

Figure 2.4. Altered sequence and timing of skeletal ossification in *trpm7*^{j124e2} compared to the wild-type. Wild-type larvae (n = 500) and *trpm7* mutant siblings (n = 431) were scored for ossification of 87 bones, yielding 80,997 ossification scores. Schematics of bone locations, functional-anatomical units, and effects for each bone are in the Supplemental Data. (A) In mutants, endochondral bones (red connectors) appear on average earlier in the ossification sequence, whereas intramembranous bones (green connectors) appear on average later in the ossification sequence. Bold connectors show bones in which ossification timing, in addition to sequence, was significantly altered [panel (B)]. (B) In mutants, analyses by developmental mode reveal accelerated ossification for many endochondral bones (red) but delayed ossification for many intramembranous bones (green). The x axis shows the relative likelihood of ossification in the wild-type compared to the mutant: estimates greater than 0 indicate that the bone is

more likely to be ossified in wild-type, and ossification is therefore delayed in the mutant; estimates less than 0 indicate that the bone is less likely to be ossified in wild-type fish, and ossification is therefore accelerated in the mutant. The *y* axis shows statistical significance by chi-square value (left axis) and *p* value (right axis). $\alpha = 0.05$ and $q = 0.01$ are the thresholds of statistical significance after multiple comparisons were controlled for. (C) Analyses by functional-anatomical unit and developmental mode. Functional-anatomical units were differentially affected in the mutants even after their relative endochrondral and intramembranous compositions were controlled for. Averages: of all bones, diamond; of endochondral bones, large red point; of intramembranous bones, large green point.
Error bars in (B) and (C) show one standard error for logistic regression coefficients, β.

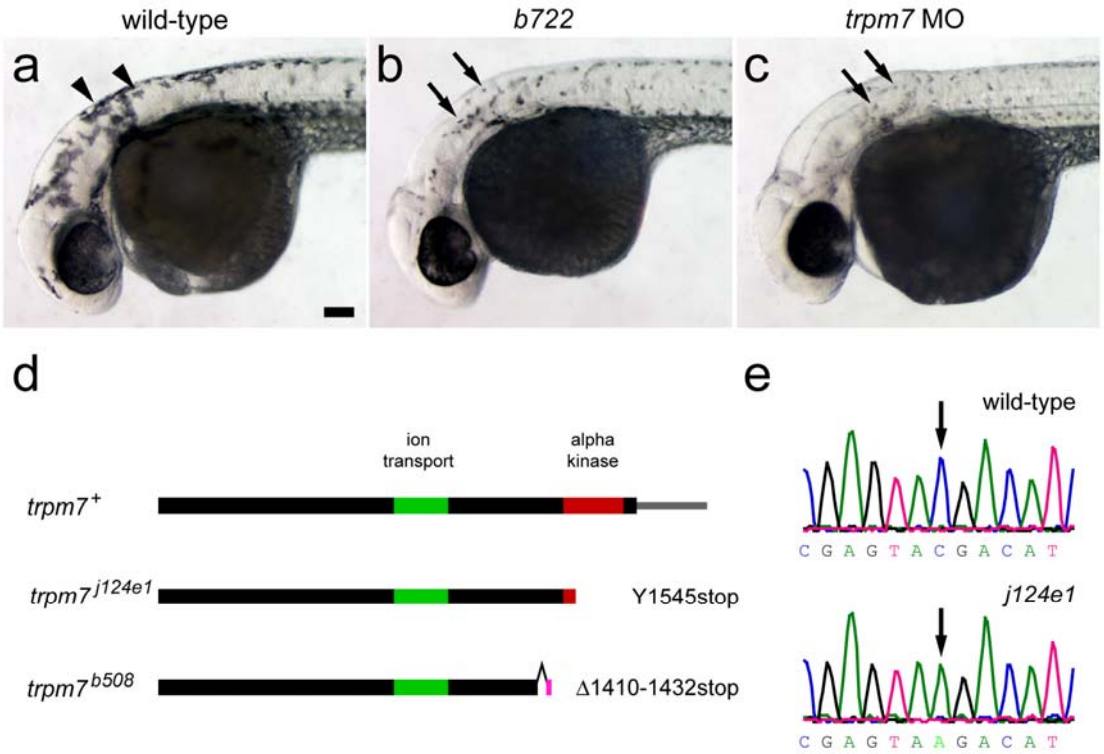

Figure 2.S1. Identification of *trpm7* as the gene mutated in *tct* (*nutria*) mutant zebrafish. (A–C) Morpholino knockdown of *trpm7* phenocopies the *tct* embryonic melanophore defect. (A) In wild-type embryos, well-melanized and well-spread melanophores (arrowheads) cover the dorsum and head at 48 hr. (B) In *tct* embryos, melanophores are fewer, lighter, and punctuate (arrows) (Arduini and Henion 2004; Cornell, Yemm et al. 2004). An allele of moderate severity, tct^{b722}, is shown. (C) Wild-type embryos injected with a splice-blocking morpholino to *trpm7* exhibit fewer, lighter, and punctate melanophores, as in *tct*. (D) Schematic of *trpm7* cDNAs. Seqencing of *trpm7* cDNAs identifies a transcript encoding at least 1773 amino acids (aa), including an ion transport domain (aa 873–1073) and an α kinase domain (aa 1510–1724). tct^{j124e1} shows a C→A transversion resulting in substitution of a premature stop codon for tyrosine at aa 1545, near the start of the α kinase domain. Sequencing of tct^{b508} reveals a 68 nucleotide deletion (aa 1410–1432) comprising a single exon and resulting in a frameshift, 16 novel amino acids, and a premature stop codon. Analyses of genomic DNA reveal a deletion corresponding to one exon in addition to parts of flanking introns. (E) Sequence electropherograms from haploid embryos that are wild-type (upper section) or the strong allele tct^{j124e1} that exhibits a premature stop codon (TAA, lower section). *trpm7* Genbank accession number: AY860421.
Scale bars in (A–C) represent 100 μm.

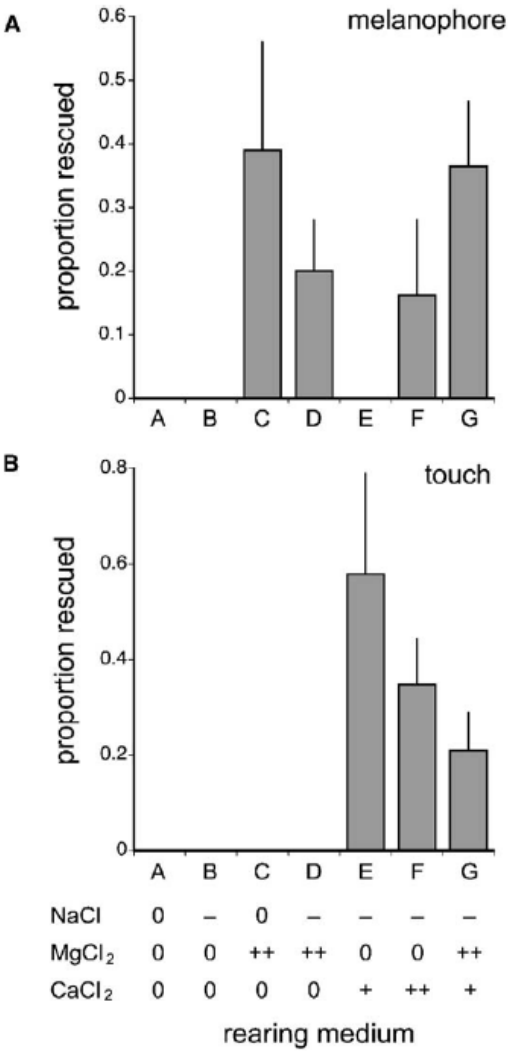

Figure 2.S2. Rescue of *trpm7* embryonic defects with divalent-cation supplementation. Mg^{2+} and Ca^{2+} supplementation differentially rescued melanophore and touch-response phenotypes of *tct* ^{b508} embryos. High concentrations of $CaCl_2$ were toxic at normal NaCl concentrations ("0" in the figure), although embryo viability could be restored at lower NaCl concentrations ("-" in the figure). (A) Mean standard error of the mean (SEM) proportion of *trpm7* ^{b508} embryos exhibiting rescued melanophores (as in Figure 1F in the main text). In the standard embryo medium (solution A) and the reduced-NaCl rearing medium (B), no embryos exhibited rescued melanophores. In the medium with supplementary $MgCl_2$ (100 mM; solutions C and D), many embryos exhibited partial melanophore rescue. Although melanophore rescue was not observed in the medium containing low supplementary $CaCl_2$ (50 mM) without $MgCl_2$ (solution E), partial rescue occurred in media containing high supplementary $CaCl_2$ (100 mM) without $MgCl_2$ supplementation (solution F) or low $CaCl_2$ (50 mM) with high $MgCl_2$ (100 mM; solution G). (B) Mean SEM proportion of *trpm7* ^{b508} embryos exhibiting touch response. In contrast to melanophore rescue, touch response was not rescued by $MgCl_2$ supplementation alone (solutions C and D). Rather, touch response was maximally rescued with low supple-mentary $CaCl_2$ (50 mM) without $MgCl_2$ (solution E), although some rescue also occurred with higher $CaCl_2$ (100 mM) supplementation (solution F) or with low $CaCl_2$ (50 mM) in the presence of $MgCl_2$ (100 mM; solution G). Qualitatively similar responses to $CaCl_2$ and $MgCl_2$ supplementation also were observed with *trpm7* ^{j124e2} (*nutria*), which exhibit a weaker embryonic melanophore phenotype than *trpm7* ^{b508}. The same media did not rescue similar melanophore defects of *sparse* (*kit*) or *colorless* (*sox10*) mutants (Parichy, Rawls et al. 1999; Dutton, Pauliny et al. 2001), demonstrating specificity of the effect for *trpm7* (data not shown). The cellular basis of the touch phenotype is unclear. Because of the timing and recovery of this phenotype, it is unlikely to depend on hair cells of lateral-line neuromasts, recently shown to require TRP family members NompC and TRPA1 (Sidi, Friedrich et al. 2003; Corey, Garcia-Anoveros et al. 2004). Toxicity of high-salt solutions precluded testing for rescue of later, larval ossification phenotypes.

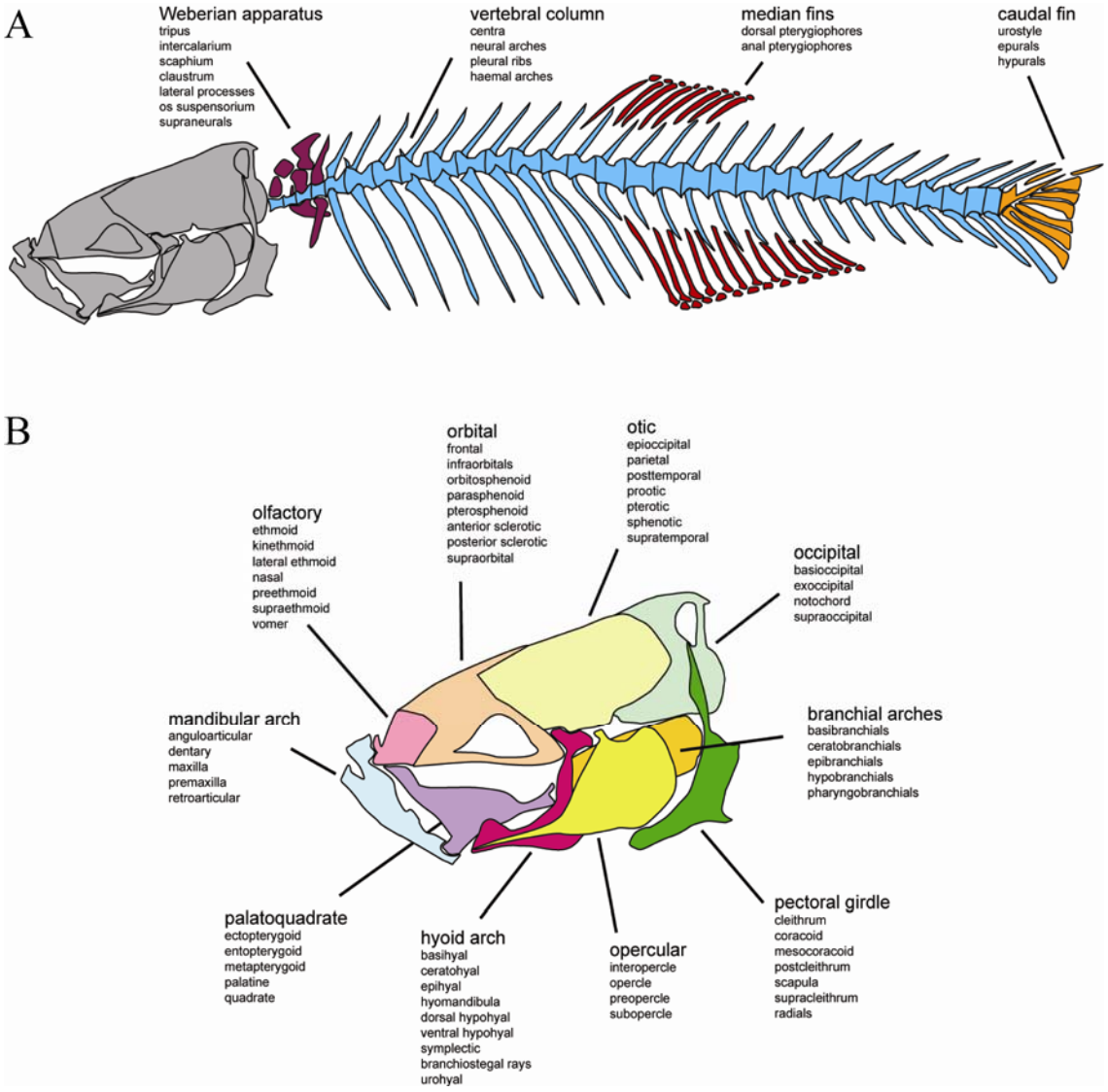

Figure 2.S3. Functional-anatomical units and bone locations examined for ossification sequence and timing. Functional-anatomical units are color coded to match Figures 4A–C in the main text. (A) Units of the postcranial skeleton with bones comprising these units listed in small type. (B) Units and bones of the craniofacial skeleton.

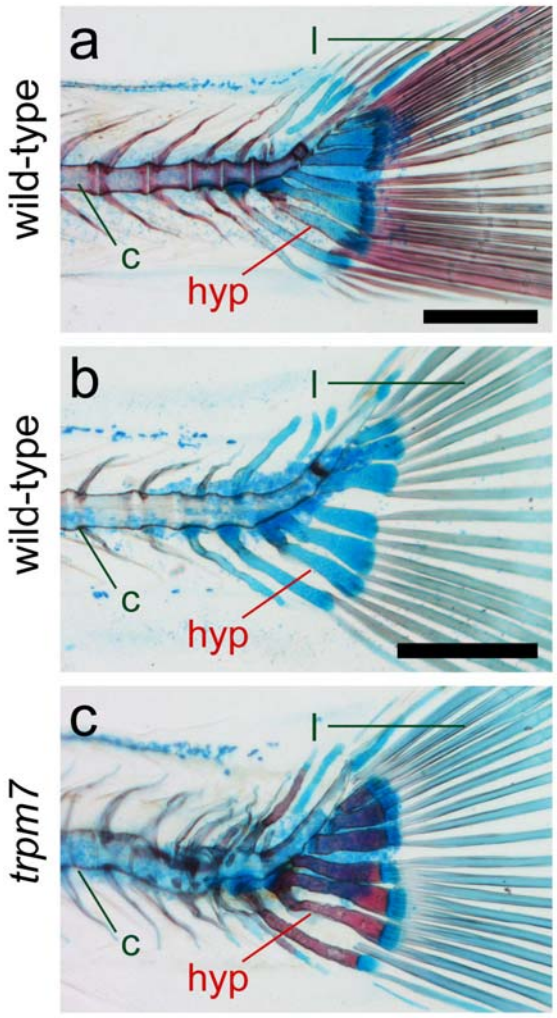

Figure 2.S4. Growth retardation alone does not result in precocious ossification. Three siblings from a cross segregating *trpm7*^{j124e2}. (A) Wild-type fish showing endochondral hypurals (denoted by "hyp") that are not yet ossified, as well as intramembranous vertebral centra (denoted by "c") and fin lepidotrichia (denoted by "l") that are already well ossified. (B) Even severely runted wild-type individuals that are from the same family and are indistinguishable in size from *trpm7* mutants do not show precocious ossification of endochondral hypurals (or other bones); the ossification of intramembranous centra and lepidotrichia is delayed, reflecting an overall retardation of developmental rate in slow-growing fish. (C) *trpm7* mutant has accelerated hypural ossification and delayed centra and lepidotrichial ossification compared to wild-type. In contrast to runted wild-type individuals, delayed ossification of intramembranous bones does not reflect a general developmental retardation because the absolute timing of other events (cartilage formation, chondrocyte and osteoblast appearance, adult pigment pattern formation, gut looping, swim-bladder bifurcation, etc.) does not differ dramatically from wild-type.
Scale bars represent (A), 400 μm and (B and C), 400 μm.

Table S1. Relative Ossification Timing

Endochondral Bones

Bone	Group[a]	Effect ± SEM[b]	χ^2	P[c]	s[d]
anal pterygiophores	medial fins	−2.82 ± 0.219	166.13	0	***
basibranchial 1	branchial arches	−0.97 ± 0.128	57.71	3.0E-14	***
basibranchial 2	branchial arches	−1.86 ± 0.148	159.00	0	***
basibranchial 3	branchial arches	−0.80 ± 0.150	28.42	9.8E-08	***
basihyal	hyoid	−1.84 ± 0.130	200.44	0	***
basioccipital	occipital	−0.02 ± 0.148	0.02	0.9	NS
basipterygium	pelvic girdle	−0.20 ± 0.146	1.94	0.2	NS
ceratobranchial 1	branchial arches	−0.88 ± 0.091	93.59	0	***
ceratobranchial 2	branchial arches	−0.74 ± 0.088	70.04	1.1E-16	***
ceratobranchial 3	branchial arches	−0.62 ± 0.087	50.30	1.3E-12	***
ceratobranchial 4	branchial arches	−0.57 ± 0.099	33.37	7.6E-09	***
ceratobranchial 5	branchial arches	0.40 ± 0.136	8.62	0.003	*
ceratohyal	hyoid	−0.67 ± 0.092	53.45	2.7E-13	***
claustrum	Weberian	0.23 ± 0.112	4.16	0.04	NS
coracoid	pectoral girdle	−0.11 ± 0.097	1.36	0.2	NS
dorsal hypohyal	hyoid	0.17 ± 0.130	1.73	0.2	NS
dorsal pterygiophores	medial fins	−2.63 ± 0.209	157.18	0	***
epibranchial	branchial	−1.12 ± 0.096	135.88	0	***
epihyal	hyoid	−0.28 ± 0.094	8.99	0.003	*
epioccipital	otic	−0.28 ± 0.095	8.60	0.003	*
epurals	caudal fin	−4.67 ± 0.386	145.86	0	***
ethmoid	olfactory	1.04 ± 0.380	7.51	6.1E-03	*
exoccipital	occipital	0.07 ± 0.129	0.28	0.6	NS
haemal arches	vertebral	0.35 ± 0.105	10.86	9.8E-04	*
hyomandibula	hyoid	−0.59 ± 0.110	28.50	9.4E-08	***
hypurals	caudal fin	−0.66 ± 0.088	55.60	8.9E-14	***
kinethmoid	olfactory	0.21 ± 0.103	4.22	0.04	NS
lateral ethmoid	olfactory	−0.56 ± 0.088	39.93	2.6E-10	***
mesocoracoid	pectoral girdle	0.26 ± 0.124	4.49	0.03	NS
metapterygoid	palatoquadrate	−1.48 ± 0.119	154.06	0	***
orbitosphenoid	orbital	0.05 ± 0.103	0.24	0.6	NS
os suspensorium	Weberian	0.06 ± 0.129	0.19	0.7	NS
palatine	palatoquadrate	−0.10 ± 0.092	1.28	0.3	NS
pectoral radials	pectoral girdle	−0.20 ± 0.122	2.64	0.1	NS
pharyngobranchial	branchial arches	−2.17 ± 0.510	18.06	2.1E-05	***
prootic	otic	−0.28 ± 0.137	4.18	0.04	NS
pterosphenoid	orbital	−0.05 ± 0.089	0.31	0.6	NS
pterotic	otic	0.04 ± 0.083	0.28	0.6	NS
quadrate	palatoquadrate	−0.52 ± 0.096	29.39	5.9E-08	***
retroarticular	mandibular	−0.05 ± 0.085	0.28	0.6	NS
scaphium	Weberian	0.17 ± 0.082	4.08	0.04	NS
scapula	pectoral girdle	−0.07 ± 0.105	0.41	0.5	NS
sphenotic	otic	−0.50 ± 0.085	34.26	4.8E-09	***
supraneurals	Weberian	−0.20 ± 0.085	5.57	0.02	*
supraoccipital	occipital	−0.88 ± 0.106	69.74	1.1E-16	***
symplectic	hyoid	−1.12 ± 0.093	147.16	0	***
tripus	Weberian	0.06 ± 0.129	0.24	0.6	NS
ventral hypohyal	hyoid	−0.21 ± 0.090	5.69	0.02	*

Intramembranous Bones

Bone	Group	Effect ± SEM	χ^2	P	s
anguloarticular	mandibular	−0.12 ± 0.087	2.01	0.2	NS
branchiostegal rays	hyoid	0.20 ± 0.101	3.97	0.05	NS
centra W[e]	vertebral	0.64 ± 0.158	16.20	5.7E-05	***
centra c	vertebral	0.42 ± 0.104	15.91	6.6E-05	***
centra pre-c	vertebral	−0.05 ± 0.114	0.17	0.7	NS
cleithrum	pectoral girdle	0.36 ± 0.129	7.60	0.006	*
dentary	mandibular	−0.17 ± 0.115	2.05	0.2	NS
ectopterygoid	palatoquadrate	0.87 ± 0.181	23.31	1.4E-06	***
entopterygoid	palatoquadrate	0.34 ± 0.080	17.66	2.6E-05	***
frontal	orbital	0.83 ± 0.201	17.07	3.6E-05	***
infraorbitals	orbital	1.23 ± 0.308	15.62	7.7E-05	***
interopercle	opercular	0.27 ± 0.088	9.10	0.003	*
lateral processes	Weberian	0.13 ± 0.130	0.96	0.3	NS

(continued)

Table S1. Continued

Intramembranous Bones

Bone	Group	Effect ± SEM	χ^2	*P*	s
maxilla	mandibular	0.48 ± 0.107	20.10	7.4E-06	***
nasal	olfactory	1.22 ± 0.374	10.57	0.001	*
neural arches c	vertebral	0.36 ± 0.108	11.24	8.0E-04	*
neural arches pre-c	vertebral	−0.12 ± 0.123	0.95	0.3	NS
notochord	occipital	0.25 ± 0.137	3.25	0.07	NS
opercle	opercular	−0.07 ± 0.122	0.31	0.6	NS
parasphenoid	orbital	0.18 ± 0.102	3.02	8.2E-02	NS
parietal	otic	−0.05 ± 0.709	0.01	0.9	NS
pleural ribs	vertebral	−0.01 ± 0.129	0.01	1	NS
postcleithrum	pectoral girdle	0.44 ± 0.135	10.49	0.001	*
posttemporal	otic	−0.14 ± 0.093	2.24	0.1	NS
premaxilla	mandibular	0.47 ± 0.104	20.15	7.2E-06	***
preopercle	opercular	0.31 ± 0.085	13.62	2.2E-04	**
subopercle	opercular	0.92 ± 0.092	101.24	0	***
supracleithrum	pectoral girdle	0.40 ± 0.128	9.90	0.002	*
supraethmoid	olfactory	0.77 ± 0.174	19.56	9.8E-06	***
supraorbital	orbital	1.15 ± 0.241	22.82	1.8E-06	***
urohyal	hyoid	−0.01 ± 0.089	0.01	0.9	NS
urostyle	caudal fin	0.96 ± 0.112	73.46	0	***
vomer	olfactory	0.67 ± 0.155	18.30	1.9E-05	***

[a] Functional-anatomical grouping.

[b] Partial logistic regression coefficient: relative likelihood of bone being ossified in wild-type as compared to mutant (negative values reflect precocious ossification in mutant; positive values reflect delayed ossification in mutant).

[c] Probability that effect differs significantly from 0 (χ^2, 1 d.f.).

[d] Significance of effect after controlling for multiple comparisons (q, significance level controlled by false-discovery-rate method; a, significance level controlled by Bonferroni method; see main article text). NS = not significant. *: $q < 0.01$, $a > 0.05$. **: $q < 0.01$, $a < 0.05$. ***: $q < 0.01$, $a < 0.01$.

[e] The following abbreviations are used: W, Weberian; c, caudal; pre-c, pre-caudal.

Table 2.S1. Relative ossification timing of endochondral and intramembranous bones scored in *trpm7*^{j124e2} mutants and wild-type. Chi-squared and *p*-values of the likelihood of ossification of bones in wild-type relative to mutants plotted in Figure 2.4.

Chapter 3: Molecular Regulation of Physiological Calcium and Magnesium Homeostasis in Zebrafish by trpm7 and stanniocalcin1

Summary

Magnesium is vital to numerous cellular processes and the transient receptor potential melastatin 7 (trpm7) channel kinase is a primary regulator of cellular magnesium homeostasis. Here we show that trpm7 is also an important regulator of physiological cation homeostasis in vivo. Using zebrafish *trpm7* mutants we identified defects in the kidney and Corpuscles of Stannius (CS), two organs that regulate physiological ion homeostasis. We demonstrate the presence of kidney stones in *trpm7* mutant larvae shortly after hatching, and we show their appearance is presaged by decreased levels of total calcium and total magnesium. Furthermore we establish a link between trpm7 function in the CS and stanniocalcin1 (stc1), a potent molecular regulator of calcium homeostasis. Using transgenic overexpression and morpholino-oligonucleotide knockdown we demonstrate that stc1 modulates calcium and magnesium levels in *trpm7* mutant and wild-type backgrounds. Together these analyses demonstrate distinct roles for trpm7 in regulating cation homeostasis through kidney function and via *stc1* expression within the CS.

Introduction

Calcium and magnesium are divalent cations critical for numerous biological processes. Calcium is an important second messenger in signal transduction pathways, acts as an enzymatic cofactor, maintains differences in membrane potentials, and

provides a crucial structural element for bone (Gomes, Leite et al. 2006; Blair, Schlesinger et al. 2007; Neher and Sakaba 2008; Laude and Simpson 2009). Magnesium is vital to the majority of cellular processes as an enzymatic cofactor, a structural component for proteins, RNA, and DNA, and as a modifier of receptor and channel activity (Grubbs and Maguire 1987; Wolf and Cittadini 1999; Alexander, Hoenderop et al. 2008). Whereas extensive progress has been made towards unraveling mechanisms underlying calcium homeostasis, relatively less is known about magnesium homeostasis at either cellular or organismal levels. Nevertheless, important new insights have come from the recent identification and analysis of two closely related genes, *TRPM6* and *TRPM7* that encode transient receptor potential (TRP) family channel kinases (Nadler, Hermosura et al. 2001; Runnels, Yue et al. 2001; Walder, Landau et al. 2002; Monteilh-Zoller, Hermosura et al. 2003; Schmitz, Perraud et al. 2003; Chubanov, Schlingmann et al. 2007; Schlingmann, Waldegger et al. 2007; Schmitz, Deason et al. 2007).

Mammalian Trpm6 and Trpm7 proteins function as divalent cation channels with C-terminal alpha-kinase domains that regulate channel activity (Runnels, Yue et al. 2001; Ryazanova, Dorovkov et al. 2004; Takezawa, Schmitz et al. 2004; Demeuse, Penner et al. 2006; Thebault, Cao et al. 2008). Trpm6 and Trpm7 are preferentially permeable to a number of divalent cations (Nadler, Hermosura et al. 2001; Monteilh-Zoller, Hermosura et al. 2003; Schmitz, Perraud et al. 2003; Voets, Nilius et al. 2004; Li, Jiang et al. 2006; Topala, Groenestege et al. 2007), including both magnesium and calcium. For functional channels to form, Trpm6 must form multimeric complexes and is generally thought to multimerize obligately with Trpm7 (Chubanov, Waldegger et al. 2004; Schmitz, Dorovkov et al. 2005). Other studies suggest homomeric Trpm6 complexes may be active

as well (Runnels, Yue et al. 2001; Monteilh-Zoller, Hermosura et al. 2003; Schmitz, Dorovkov et al. 2005; Li, Jiang et al. 2006; Fujiwara and Minor 2008). By contrast, Trpm7 can function as either a heteromeric or homomeric channel (Runnels, Yue et al. 2001; Monteilh-Zoller, Hermosura et al. 2003; Schmitz, Dorovkov et al. 2005; Li, Jiang et al. 2006; Fujiwara and Minor 2008).

Trpm6 channels are found primarily in organs that regulate physiological ion levels, such as the kidney and intestines (Voets, Nilius et al. 2004; Groenestege, Hoenderop et al. 2006; Kunert-Keil, Bisping et al. 2006). In humans, mutations in *TRPM6* are linked to hypomagnesemia with secondary hypocalcemia (HSH or HOMG) (Schlingmann, Weber et al. 2002; Walder, Landau et al. 2002), suggesting that Trpm6 channels are primarily responsible for whole-organism magnesium homeostasis. In contrast to Trpm6, Trpm7 channels are expressed ubiquitously (Aarts, Iihara et al. 2003; Wei, Sun et al. 2007) and regulate cellular magnesium homeostasis (Nadler, Hermosura et al. 2001; Monteilh-Zoller, Hermosura et al. 2003; Schmitz, Perraud et al. 2003). Mammalian Trpm7 also functions in sensing extracellular calcium and magnesium in neurons (Aarts, Iihara et al. 2003; Krapivinsky, Mochida et al. 2006; Wei, Sun et al. 2007) and in regulating cell adhesion (Clark, Langeslag et al. 2006; Su, Agapito et al. 2006). Furthermore, the possibility exists that Trpm7 may regulate whole-organism cation homeostasis through its interaction with Trpm6.

Numerous studies have shown the importance of Trpm7 for cation homeostasis in vitro, yet the early lethality of Trpm7 mutations in mammalian systems has precluded analyses of Trpm7 roles in whole-organism cation homeostasis (Jin, Desai et al. 2008). By contrast, zebrafish *trpm7* mutants survive into embryonic and post-embryonic stages,

permitting analyses of developmental and physiological functions of trpm7 in vivo (Elizondo, Arduini et al. 2005). Zebrafish *trpm7* is detectable in all adult tissues (MRE and DMP, unpublished data). *trpm7* is widely expressed in embryos and larvae as well, with particularly high transcript abundance in the tubules of the pronephric and mesonephric kidneys, and in the Corpuscles of Stannius (CS), a teleost-specific gland that regulates physiological ion homeostasis (Thisse 2004; Elizondo, Arduini et al. 2005; Wingert, Selleck et al. 2007). As embryos, *trpm7* mutants have defects in the survival of melanized pigment cells, melanophores, and also develop a transient unresponsiveness to touch (Arduini and Henion 2004; Cornell, Yemm et al. 2004; McNeill, Paulsen et al. 2007). As larvae, these mutants exhibit severe defects in growth and skeletogenesis while also developing kidney stones (Elizondo, Arduini et al. 2005). The known functions of mammalian Trpm7 channels suggest the pleiotropic phenotypes evident in zebrafish *trpm7* mutants may be related to altered kidney function and cation homeostasis. The zebrafish *trpm7* mutants therefore present a unique opportunity to study the impact of trpm7 activity on pronephric function and physiologic cation homeostasis.

Here we show that zebrafish *trpm7* mutants exhibit multiple indications of defective cation homeostasis. We find that *trpm7* mutants develop kidney stones as early as 5 days post-fertilization (dpf), while exhibiting reduced levels of whole-embryo total calcium and total magnesium by 3 and 4 dpf, respectively. We further show that the CS-specific gene, *stanniocalcin1* (*stc1*) is a potent downstream mediator of altered cation levels in *trpm7* mutants. Additionally, we can demonstrate that wild-type cation levels in *trpm7* mutants can be restored by decreasing the level of *stc1*. Together, our findings lay

the groundwork for further studies of trpm7 and its roles in cation homeostasis during early zebrafish development.

Materials and Methods

Strains and Rearing Conditions

Fish were reared at an average temperature of 28.5 °C except as noted below with a 14:10 light:dark cycle. Mutants were *trpm7*^{j124e1}, *trpm7*^{j124e2}, and *trpm7*^{b508}, with most experiments using the latter allele unless otherwise noted. All mutant stocks and transgenic lines were maintained in the AB genetic background.

Detection of Kidney Stones

We used a 0.5% (w/v) solution of Alizarin Red (Sigma Aldrich, St. Louis MO) diluted in nanopure H2O and adjusted to pH 7.5 with sodium bicarbonate. For staining, we incubated embryos or larvae in Petri dishes in a final concentration of 0.04% Alizarin Red diluted in 10% Hank's Solution (Westerfield 2000). After overnight incubation fish were briefly washed in 10% Hank's before anesthetizing with MS222 and imaging under epifluorescence illumination using a Texas Red filter set. To assess kidney stone migration, individual fish were imaged immediately following a brief rinse and then allowed to recover in 10% Hank's for 12 hrs, when they were imaged for a second time.

Total Calcium and Magnesium Assays

For each sample tested, 25 embryos or larvae were pooled, anesthetized with MS222, rinsed briefly in nanopure H2O and collected in a 1.5 ml microcentrifuge tube. Fish were then dried at 65°C for 30-45 min, at which time 125 µl of 1 M HCl was added to each tube and acid-denatured overnight at 95°C with occasional tapping or brief centrifugation to collect solution at the bottom of the tube. Tubes were then centrifuged at maximum speed for 15 min and supernatant was collected. To assess total calcium and magnesium content from the supernatant, we used QuantiChrom Calcium and Magnesium Assays (BioAssay Systems, Hayward CA, DICA-500, DIMG-250). For magnesium assays, the manufacturer's protocol was used with half-reactions and 5 µl of each sample tested for 2-5 dpf fish. Absorbances were read at 490 nm before and after addition of 10 µl of EDTA to obtain blank readings for individual wells. Statistical analyses were performed using JMP 8.0.1 for Macintosh (SAS Institute, Cary NC).

Total RNA Isolation and cDNA Synthesis

For RNA preparations, 10 embryos were pooled, anesthetized in MS222 and homogenized in 200 µl Trizol (Invitrogen). RNA preps were performed as specified in the manufacturer's protocol, resuspended in 13 µl H2O, and quantitated using a NanoDrop 1000 spectrophotometer (ThermoScientific). Superscript III and RNase Inhibitor (Invitrogen) were used in cDNA synthesis reactions primed with oligo dT primers, as per manufacturer's protocol. cDNAs were diluted with 100 µl TE prior to use.

Quantitative PCR

For quantitative PCR (qPCR), 50 µl reactions were performed in triplicate using 0.5 µl AmplTaq (Applied BioSystems), 5 µl GeneAmp 10x PCR Buffer, 1 µl of 12.5x SYBR Green (Sigma-Aldrich), 1 µl of 10mM dNTPs, 2 µl of 2.5µM forward and reverse primer mix, and 1.5 µl diluted cDNA. For cycling, a Chromo4 real time instrument (MJ Research) was used with the following program: an initial denature step of 94°C for 3 m; followed by 40 cycles of 94°C for 20 s, 56°C for 20 s, 72°C for 20 s; and a final elongation step of 72°C for 5 m. To increase signal intensity, reactions were performed in low profile, unskirted, white 96-well PCR plates (ThermoScientific #AB-0700W). For each primer set, no-template control reactions were performed. Prior to qPCR, multiple primer sets were tested for amplification efficiency, amplification without primer-dimer formation, and optimal annealing temperature using gradient-PCR with annealing temperatures ranging from 54-62°C. Selected primers were determined to have optimal amplification efficiency at 56°C annealing without formation of primer-dimers. Primers sets (forward, reverse, 5' to 3') used for quantiative RT-PCR were: *β-actin*, GCATCACACCTTCTACAACGAG, AGAGTCCATCACGATACCAGTG; *stc1* (endogenous), GCAGGGCAGGAGTATTTATTAGTG, CAGAAAACATCTCAACCACATCCAG; *stc1* (transgenic), TCACCTGTTCGCCAGAAACG, CCAAAAGACGGCAATATGGTGG. Primers used for molecular cloning (attB1F and attB1R sites underlined): *stc1*, GGGGACAAGTTTGTACAAAAAAGCAGGCTACCATGCTCCTGAAAGCGGATTTC, GGGGACCACTTTGTACAAGAAAGCTGGGTTTAAGGACTTCCCACGATGGAGC.

qPCR data was collected using Chromo4 Opticon Monitor 3 Software. For relative expression analysis between trpm7 mutants and wild-type siblings, data were analyzed using REST 2008 software (Pfaffl, Horgan et al. 2002). For absolute expression analysis of transgene induction following heat-shock, data were analyzed using Qgene software (Simon 2003). All data presented are representative of three biological replicates.

Transgenic Expression Constructs

For constructing an *stc1* expression cassette, we used the Tol2kit (Kwan, Fujimoto et al. 2007) and Multisite Gateway reagents (Invitrogen). We amplified full-length *stc1* with primers containing *att*B flanking sequences (Table 3.1), inserted the amplicon into pDONR221 and verified integrity of the open reading frame by sequencing. We used the pDONR-*stc1* clone as the middle entry vector, combined with p5E-*hsp70* 5' entry vector, p3E-IRES-EGFPpA 3' entry vector, and the pDestTol2pA2 destination vector from the Tol2kit. The resulting vector comprised an expression cassette with a heat shock protein *hsp70* promoter controlling expression of the full length *stc1* followed and EGFP linked by internal ribosome entry site (IRES). We co-injected this hsp70:stc1-IRES-EGFP plasmid with Tol2 mRNA transcribed from the pCS2FA-transposase plasmid (Kwan, Fujimoto et al. 2007). Injected embryos were heat-shocked at 38.5°C for 30 m at 24 hpf, then screened for mosaic expression of EGFP at 4 h following heat-shock. GFP-positive embryos were reared to adulthood and screened for germline integration through their progeny. Identified germline carriers were used to

establish stable transgenic lines and the strongest GFP-expressing line was used for experiments. Similar results were observable in other transgenic lines.

Heat Shock Induction

Two methods were used for heat-shock induction experiments. To screen transgenic progeny for GFP, a single heat-shock was performed by placing embryos in 250 ml glass culture dishes (Carolina Biological), then placing dishes in a shaking water bath set to 38.5°C, and heat-shocking embryos for 20 m. For repeated heat-shocking over a period of several days, embryos were placed in clear plastic cups with mesh-covered holes to provide circulating water flow. Cups were then placed in a 10 gal acrylic aquarium with a drain and 28.5°C flowing fish system water. Temperature was controlled using a ProcessTech heater and temperature controller (Aquatic Ecosystems). The heater controller was then plugged into an electrical timer set for a cycle for 30 m on, 5.5 h off.

Antisense Morpholino Oligonucleotide Injections

An *stc1* morpholino (stc1-MO: GAAATCCGCTTTCAGGAGCATGTC) was designed by GeneTools LLC (Philomath, OR) to target the translational start site of the coding sequence. Lyophilized morpholino was resuspended in 300 µl 1x Danieau Buffer. The concentration was determined by diluting 2 µl in 20 µl 0.1N HCl, measuring the absorbance at 265 nm using a NanoDrop spectrophotometer, and calculating the concentration as per specifications on the GeneTools website (www.gene-tools.com). Morpholino was then diluted to 0.2 mM in 1x Danieau Buffer and ~0.6-0.8 nmol (~4.8-6.4 ng) were injected into wildtype embryos at the 1-2 cell stage.

Results

An Early-Larval Defect in Kidney Function

Previous work identified kidney mineralization in late larval *trpm7* mutants (Elizondo, Arduini et al. 2005). However, *trpm7* expression within the pronephros (Thisse 2004; Elizondo, Arduini et al. 2005; Wingert, Selleck et al. 2007) suggests that *trpm7* mutants could exhibit defects in embryonic or early larval defects in kidney function as well. To test this possibility, we examined early larvae for signs of kidney stone formation using the vital dye Alizarin Red (Elizondo, Arduini et al. 2005; Walker and Kimmel 2007).

Using this approach we detected kidney stones in *trpm7* mutants at 5 dpf (Fig. 3.1), but not at 2-4 dpf (data not shown). Homozygous *trpm7* mutants were significantly more likely to exhibit kidney stones as compared to wild-type siblings (*trpm7*/+ and +/+; χ^2=619, P<0.0001; Table 3.1). However, the frequency of kidney stone formation did not differ significantly among *trpm7* mutant alleles that were lethal either at early larval stages (*trpm7*^{j124e1}, *trpm7*^{b508}) or at juvenile stages (*trpm7*^{j124e2}) (χ^2=0.9, P=0.6). Thus, defects in kidney function are neither unique to the previously studied *trpm7*^{j124e2} allele, nor limited to later larval stages. Moreover, the similar frequency of kidney stones across alleles indicates that kidney dysfunction alone is not likely to be a primary cause of lethality in early larval-lethal alleles.

To distinguish between mineralization of the epithelial tissue in the pronephric tubules and mineralized aggregates forming within the lumen, we tested whether kidney

stones moved through the kidney lumen over time. By repeated imaging of individual larvae, we found that kidney stones of 5 dpf mutants migrate through the pronephric tubules, demonstrating that kidney stones formed within the lumen and not in the epithelium (Fig. 3.2). These early larval requirements for *trpm7* in kidney function suggest that disrupted cation homeostasis in *trpm7* mutants begins at late embryonic or early-larval stages.

Reduced Total Calcium and Magnesium in *trpm7* Mutants

In humans, mutations in *TRPM6* lead to hypomagnesemia because of decreased Mg^{2+} reabsorption by the kidney and intestines, which in turn disrupts calcium homeostasis in the parathyroid gland, resulting in hypocalcemia (Schlingmann, Weber et al. 2002; Walder, Landau et al. 2002). Since Trpm6 channels are thought to act in heteromeric complexes with Trpm7 to regulate Mg^{2+} homeostasis (Chubanov, Waldegger et al. 2004; Schmitz, Dorovkov et al. 2005) defects arising from *TRPM7* mutations might be expected to overlap with those exhibited by TRPM6 mutants. We therefore tested if disruptions to cation homeostasis in zebrafish *trpm7* mutants are similar to those associated with mammalian Trpm6 mutation. Because we could not extract sufficient serum from zebrafish embryos, we instead examined physiological cation levels as a proxy, by comparing the total magnesium and total calcium contents of wild-type and mutant embryos between 2–5 dpf.

For total calcium, mutants did not differ significantly from wild-type at 2 dpf, but exhibited significantly reduced levels by 3 dpf and more pronounced reductions at 4–5 dpf (Fig. 3.3A). For total magnesium, we found reduced levels in mutants at 4 dpf and 5

dpf (Fig. 3.3B). While not a direct measurement of serum cation levels, the reduced total cation levels are consistent with hypocalcemia and hypomagnesemia in mutants.

Altered Stanniocalcin-Mediated Regulation of Divalent Cation Homeostasis in *trpm7* Mutants

Terrestrial animals obtain calcium only from their diet and are typically challenged by hypocalcemic conditions. The primary regulators of calcium homeostasis, parathyroid hormone (PTH) and parathyroid hormone related protein (PTHrP), are, therefore, anti-hypocalcemic factors (Rankin, Grill et al. 1997; Akerstrom, Hellman et al. 2005; Talmage and Mobley 2008). In contrast, fish are surrounded by an abundant external supply of calcium and are challenged with preventing hypercalcemia, which they accomplish by controlling ion influx through the gills, kidneys, and intestine. The teleost-specific CS regulates the rates of ion influx at these sites by secreting anti-hypercalcemic stanniocalcins (Lafeber, Flik et al. 1988; Sundell, Bjornsson et al. 1992; Pandey 1994). Zebrafish *stanniocalcin1* (*stc1*) is expressed exclusively by the CS of embryos (Thisse 2004; Wingert, Selleck et al. 2007) (data not shown) and is antihypercalcemic (Tseng, Chou et al. 2009). As *trpm7* is expressed particularly strongly in the CS (Thisse 2004; Elizondo, Arduini et al. 2005), we asked if *trpm7*-dependent changes in calcium might occur via altered *stc1* regulation.

To test this, we assayed *stc1* expression in *trpm7* mutant embryos by quantitative RT-PCR (qPCR). We found significant increases in *stc1* transcript abundance in *trpm7* mutants compared to wild-type beginning at 2 dpf and extending at least through 5 dpf (Fig. 3.4). The increased *stc1* expression in mutants preceded the decrease in total

calcium (Fig. 3.3A), suggesting that upregulated *stc1* and its anti-hypercalcemic activity may be directly responsible for reduced total calcium in *trpm7* mutants.

stc1 Overexpression Reduces both Total Calcium and Total Magnesium Levels

trpm7 mutants exhibited upregulated *stc1* expression followed by decreased total calcium, followed, in turn, by decreased total magnesium. While decreased calcium is explicable by the anti-hypercalcemic activity of stc1, we hypothesized that stc1 also might negatively regulate magnesium levels. To test this idea in a wild-type background, we generated a heat shock-inducible transgenic line to overexpress stc1 (hsp70:stc1-IRES-EGFP). Following 38.5°C heat shock for 30 m, we confirmed transgene-specific expression of *stc1* (*stc1T*) by qPCR (Fig. 3.5).

To mimic the increased *stc1* expression of *trpm7* mutants in a wild-type genetic background, we heat-shocked transgenic and non-transgenic sibling embryos for 30 m at 6 h intervals between 40 hpf and 120 hpf. Following heat-shock, we sorted transgenic embryos for the presence or absence of GFP fluorescence and performed ion assays as described above. We found heat-shocked, *stc1T* embryos exhibited reduced total calcium and total magnesium compared to heat-shocked, non-transgenic siblings (Fig. 3.6). This confirmed the anti-hypercalcemic activity of stc1 and supported the hypothesis that stc1 influences magnesium homeostasis, either directly or indirectly.

The presence of increased *stc1* levels in *trpm7* mutants prior to kidney stone formation also raised the possibility that stc1 overexpression might affect kidney function so as to directly cause kidney stone formation. If so, heat-shocked, *stc1T* embryos might develop stones despite being wild-type for *trpm7*. Contrary to this expectation, however,

staining with Alizarin Red failed to reveal kidney stones (data not shown). This suggests that kidney stone formation in *trpm7* mutants occurs independently of increased stc1 activity or decreases in total cation levels.

Inhibition of stc1 in *trpm7* Mutants Restores Total Calcium and Total Magnesium Levels

Inhibition of zebrafish stc1 activity increased calcium levels (Tseng, Chou et al. 2009). Additionally, our results from overexpressing *stc1* in wild-type embryos suggested that, in *trpm7* mutants, decreased total calcium and total magnesium may result from *stc1* upregulation. We therefore tested whether normal total calcium and total magnesium levels could be restored in a *trpm7* mutant background simply by inhibiting *stc1* translation by morpholino oligonucleotide injection.

Embryos injected with a morpholino targeted to *stc1* (stc1-MO) were morphologically indistinguishable from wild-type [as observed also in (Tseng, Chou et al. 2009)]. Moreover, *trpm7* mutants injected with stc1-MO exhibited total calcium and total magnesium restored to levels comparable to those of uninjected wild-type siblings (Fig. 3.7). As expected, wild-type siblings injected with stc1-MO showed an increase in total calcium relative to uninjected siblings, similar to that found in (Tseng, Chou et al. 2009). However, when comparing injected and uninjected wild-type siblings, we found no significant change in total magnesium (Fig. 3.7B). This result shows that stc1 influences magnesium levels in the absence of trpm7 activity, and that wild-type trpm7 masks this effect. These data indicate that total calcium levels are misregulated in *trpm7*

mutants due to the overexpression of *stc1* and total magnesium levels can be restored in an *stc1*-dependent, but *trpm7*-independent, manner.

Given the restoration of total calcium and total magnesium in *trpm7* mutants by stc1-MO injection, we speculated that such mutants also might fail to develop kidney stones. Contrary to this prediction, we did not detect a significant reduction in kidney stone incidence between stc1-MO injected *trpm7* mutants and uninjected *trpm7* mutant siblings at 5 dpf (Table 3.2). This outcome, along with the lack of kidney stone formation in heat-shocked, *stc1T* embryos, supports the notion that stc1 up-regulation does not affect kidney stone formation in *trpm7* mutants. However, we cannot exclude the possibility of reduced efficacy of the stc1-MO at this later stage of development.

Discussion

We show that *trpm7* functions as a regulator of physiologic cation homeostasis in a *stc1*-dependent manner. Initially we identified early larval kidney stone formation in zebrafish *trpm7* mutants at 5 dpf and demonstrated reduced total calcium and reduced total magnesium at 3 dpf and 4 dpf, respectively. By transgenic overexpression and morpholino-oligonucleotide knockdown, we also found that *stc1* can modulate both calcium and magnesium levels in zebrafish: upregulated *stc1* in a wild-type background decreases total calcium and total magnesium, whereas inhibition of *stc1* translation increases these cations to wild-type levels in *trpm7* mutants. Finally, we were unable to detect any effect of *stc1* on kidney stone formation, consistent with a loss of trpm7 activity in the kidney leading directly to to kidney stone formation in *trpm7*mutants.

This is the first study to demonstrate an association between *trpm7* and physiological cation homeostasis in vivo. The reduced total magnesium and total calcium evident in *trpm7* mutants outwardly appear analogous to the hypomagnesemia and hypocalcemia resulting from *Trpm6* defects in mammals. However, hypomagnesemia precedes hypocalcemia in mammalian *Trpm6* mutants, whereas this sequence is reversed in zebrafish *trpm7* mutants, in which reduced total calcium is evident at 3 dpf whereas reduced total magnesium is not detectable until 4 dpf. This difference between species highlights an important distinction between the underlying mechanisms for these defects. In mammalian, decreased magnesium absorption by the kidney and intestines leads to disruption of the calcium-sensing receptor (CaSR) in the parathyroid gland. This consequently disrupts regulation of calcium homeostasis and results in hypocalcemia (Schlingmann, Weber et al. 2002; Walder, Landau et al. 2002). In zebrafish, our data reveal that decreased total calcium results from misregulation of *stc1* in the CS. This suggests a direct role for trpm7 function in the CS to regulate cation homeostasis, but also highlights the possibility that reduced total magnesium is secondary to reduced total calcium in *trpm7* mutants.

Our identification of stc1 as a mediator downstream of trpm7 in calcium and magnesium homeostasis supports a model in which decreased whole-embryo cation levels are secondary to misregulation of stc1, and do not result directly from decreased trpm7 channel activity in the kidney. The mechanism by which trpm7 regulates *stc1* remains unknown. One possibility is that the kinase domain of trpm7 modulates the activity of CaSR within the CS. Consistent with this idea, a pharmacological activator of CaSR stimulates *stc1* expression in salmon (Radman, McCudden et al. 2002).

Furthermore, CaSR is expressed within the CS, and increased stc1 levels lead to decreased plasma calcium and magnesium in flounder (Greenwood, Flik et al. 2009). These observations are concordant with our finding that increased *stc1* levels in *trpm7* mutants precede decreased total calcium and total magnesium levels.

An intriguing result from our study was the restoration of total magnesium levels in *trpm7* mutants following morpholino-knockdown of *stc1*. This trpm7-independent correction of total magnesium levels implies a still-unknown mechanism for magnesium uptake. A potential mediator of such magnesium uptake in zebrafish would be *Claudin-16*. In mammals, Claudin-16 function in the Loop of Henle is critical for passive, paracellular divalent cation reabsorption (Kausalya, Amasheh et al. 2006), and is distinct from the active, transcellular transport of magnesium by Trpm6/Trpm7 complexes. In zebrafish, we envision that *claudin-16* may be regulated by *stc1* and influences the paracellular transport of both magnesium and calcium in *trpm7* mutants. The paracellular mechanism for claudin-16 transport is distinct from the transcellular mechanism of trpm6/trpm7 channels. Consequently, stc1-regulated claudin-16 activity could function as a trpm7-independent compensatory mechanism. While a zebrafish orthologue of *Claudin-16* has not been identified, the presence of such genes in other fishes (Kollmar, Nakamura et al. 2001; Loh, Christoffels et al. 2004) suggests one may yet be found.

Our study also provides new insights into the development and physiological bases of kidney stone formation in *trpm7* mutants. We found that restoration of total calcium and total magnesium was insufficient to rescue the kidney stone phenotype. This outcome and the strong expression of *trpm7* in the kidney itself, suggest a direct requirement for trpm7 activity in kidney function. Our finding that inhibition of *stc1*

expression failed to repress kidney stone formation also supports this inference, though we cannot exclude the possibility of reduced morpholino efficacy at 5 dpf (Nasevicius and Ekker 2000). We speculate that kidney stone formation in the pronephric tubules may result from a localized decrease in the reabsorption of magnesium, owing to reduced trpm6/trpm7 channel activity, leading to increased precipitation of magnesium or calcium phosphate.

Finally, though we have characterized the early-larval effects of increased stc1 on cation homeostasis in *trpm7* mutants, it is also possible that stc1 is an effector of later stage defects in growth and bone development in these mutants (Elizondo, Arduini et al. 2005). Studies of mammalian stanniocalcins have linked increased expression to disrupted bone development and growth defects (Filvaroff, Guillet et al. 2002; Varghese, Gagliardi et al. 2002; Gagliardi, Kuo et al. 2005; Wu, Yoshiko et al. 2006; Chang, Hook et al. 2008) similar to those found in *trpm7* mutants at later larval stages. The inducible stc1 transgenic zebrafish we have generated for over-expressing *stc1* should be useful for studying these processes.

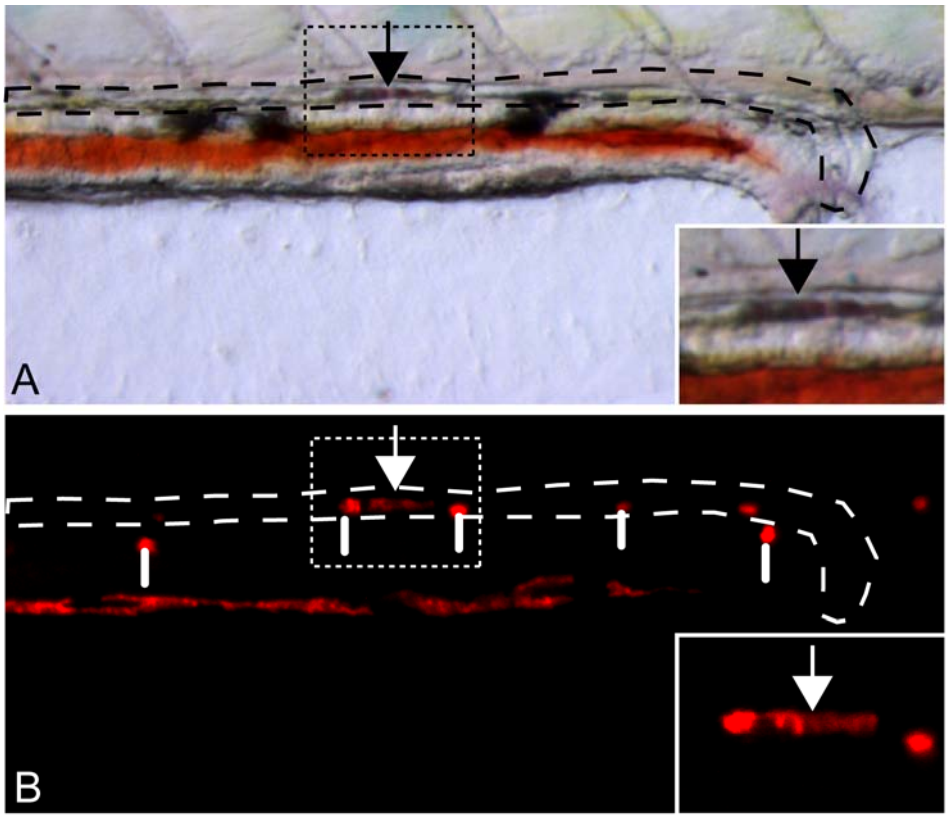

Figure 3.1. Kidney stone formation in early larval *trpm7* mutants. Brightfield (A) and fluorescent (B) views of Alizarin Red-stained kidney stone in the pronephric tubule of a 5 dpf *trpm7* mutant. Dashed lines indicate the dorsal and ventral margins of the pronephric tubule. Arrow indicates Alizarin Red-stained kidney stone visible in both brightfield and fluorescent views. Solid vertical lines indicate reflective pigment cells (iridophores) that are evident in epifluorescent illumination using both the mCherry filter set (shown) and EGFP filter set (not shown). Insets, higher magnification views of boxed areas in main panels.

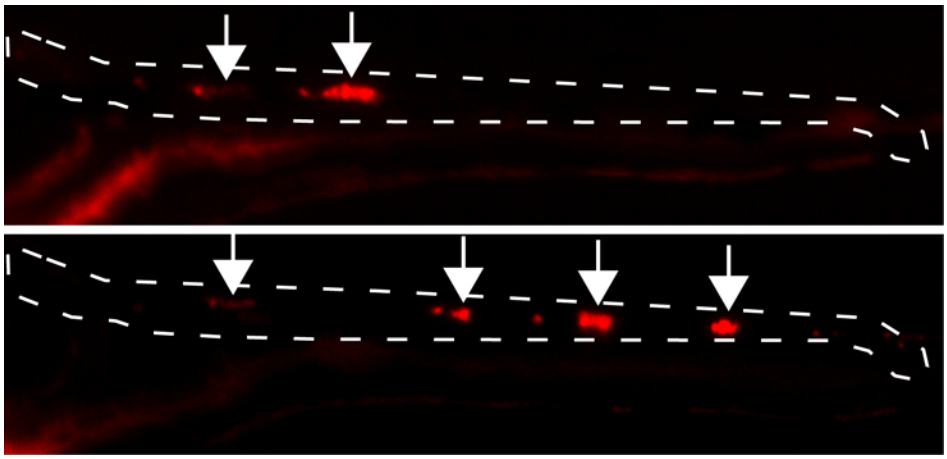

Figure 3.2. Migration of kidney stones in *trpm7* mutants. Alizarin Red-stained *trpm7* mutant kidney stones imaged (A) immediately post-staining and (B) 12 h post-staining. Dotted line indicates pronephric tubule. Arrowheads indicate Alizarin Red-stained kidney stones. The fragmentation and movement of the posterior stone in (A) can be viewed in the 3 posterior stones in (B).

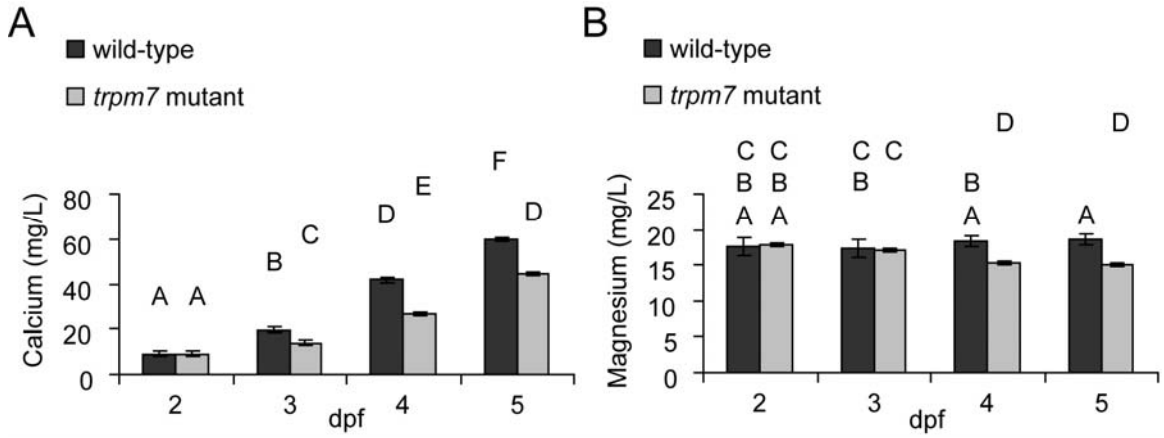

Figure 3.3. Total calcium and magnesium concentrations in *trpm7* mutants. Calcium (A) and magnesium (B) levels are shown as least squares means ± SE after controlling for batch-specific variation (n = 120 mutant and wild-type samples at stages 2–5 dpf). Overall analyses of variance: calcium, $F_{7,112} = 467$, $P<0.0001$; magnesium, $F_{7,112} = 33.8$, $P<0.0001$. Samples with the same letters are not significantly different by Tukey-Kramer HSD Test ($\alpha = 0.05$).

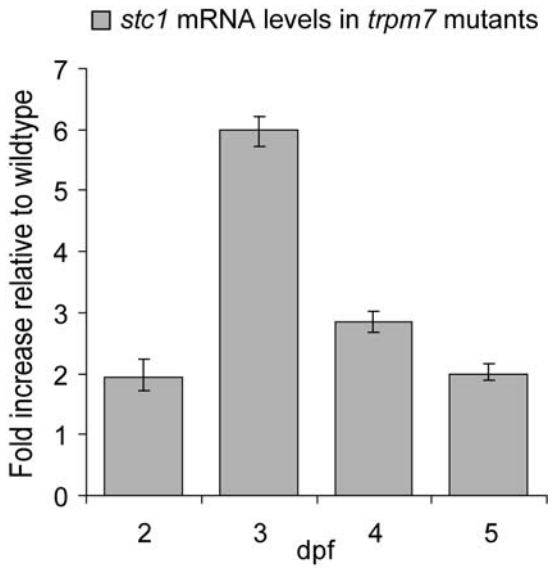

Figure 3.4. Expression of *stc1* in *trpm7* mutants as compared to wild-type by qPCR. *stc1* mRNA is more abundant in *trpm7* mutants at each stage examined. Values were normalized to β-actin and scaled relative to wild-type sibling levels of *stc1*. Error bars represent 95% confidence intervals: all $P<0.05$, using the REST software package.

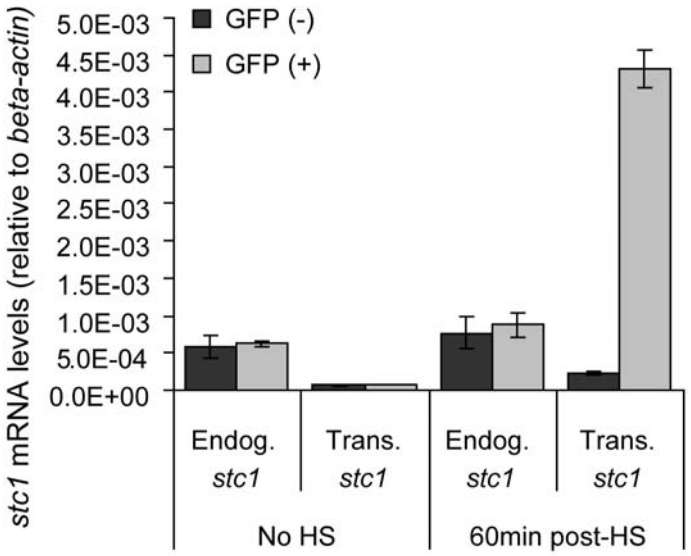

Figure 3.5. Induction of transgenic *stc1* with and without heat-shock (HS) assayed by qPCR. Induction of the transgene is observed in GFP+ embryos 60 min following heat shock of 5 dpf larvae. Absolute expression levels were scaled to β-actin expression. Endogenous *stc1* levels were assayed with primers targeting the 3' UTR while transgenic *stc1* were assayed with primers targeting the 3' coding sequence and the IRES sequence of the transgene. Transgene levels in GFP- larvae and larvae without HS are comparable to those observed with no template qPCR controls (data not shown).

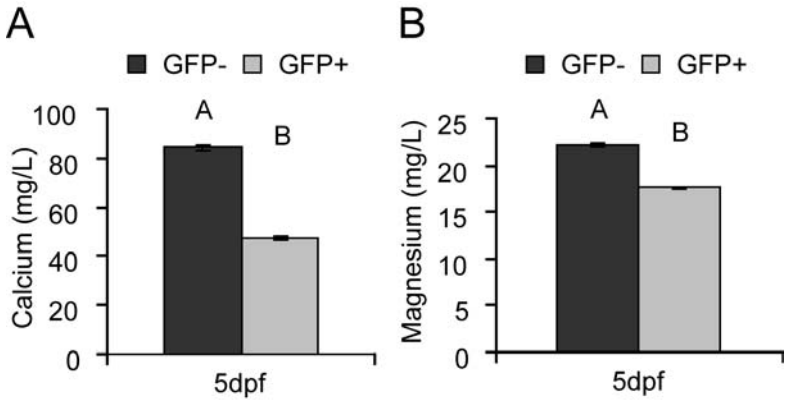

Figure 3.6. Total calcium and magnesium levels in transgenic stc1 larvae. Reduced total calcium (A) and total magnesium (B) levels in heat-shocked transgenic (GFP+) larvae compared to heat-shocked non-transgenic (GFP-) larvae. Calcium and magnesium levels represent least squared means + SE after controlling for variation among batches (n = 16 mutant and wild-type samples at 5 dpf). Overall analyses of variance: calcium, $F_{1,14} = 499$, $P<0.0001$; magnesium, $F_{1,14} = 313$, $P<0.0001$. Samples with the same letters are not significantly different by Tukey-Kramer HSD Test ($\alpha = 0.05$).

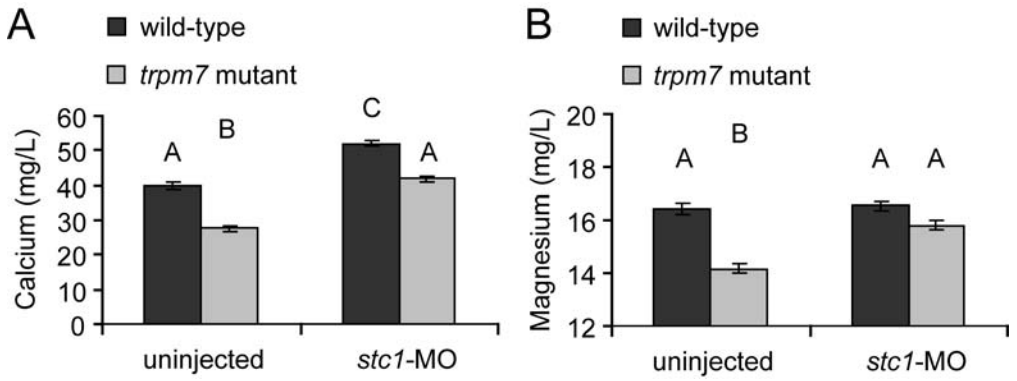

Figure 3.7. Restored cation levels in *stc1* morpholino-injected larvae. *trpm7* mutant larvae injected with stc1-MO exhibit calcium (A) and magnesium (B) levels restored to wild-type levels. Furthermore, wild-type embryos injected with the stc1-MO exhibit significantly increased total calcium (A) as compared with uninjected wild-type siblings, though total magnesium (B) of injected and uninjected wild-type embryos did not differ significantly. Overall analyses of variance: calcium, $F_{3,28} = 29.2$, $P<0.0001$; magnesium, $F_{3,28} = 14.2$; $P<0.0001$. Sample groups with the same letters are not significantly different from each other using a Tukey-Kramer HSD Test; $\alpha=0.050$.

TABLE 3.1. Incidence of kidney stone formation in *trpm7* mutant alleles and wild type siblings at 6 dpf.

	Total	KS+	KS-	%KS+	Likelihood[a]
wt sibling	183	1	182	0.5%	222.937
trpm7-j124e1	60	56	4	93.3%	
wt sibling	146	2	144	1.4%	177.693
trpm7-j124e2	50	47	3	94.0%	
wt sibling	177	0	177	0.0%	221.417
trpm7-b508	57	53	4	93.0%	

[a] χ-squared analysis, all $P < 0.0001$*

TABLE 3.2. Incidence of kidney stone formation in *stc1*-MO injected *trpm7* mutants and wild-type siblings.

	Total	KS +	KS -	%KS +	
wt sibling	127	0	127	0.0%	uninjected
trpm7-b508	41	38	3	92.7%	
wt sibling	104	0	104	0.0%	*stc1*-MO
trpm7-b508	34	32	2	94.1%	

χ-squared analysis

[a] KS x Phenotype, Likelihood = 292; $P < 0.0001$*

[b] KS x Morpholino, Likelihood = 0.0139; $P = 0.9061$

Appendix: Introduction

I have also conducted a number of other experiments that, while somewhat informative towards a broader understanding of zebrafish trpm7 function, are nevertheless incomplete on their own. Briefly I describe work towards establishing zebrafish lines with conditional trpm7 function, both through the identification of temperature sensitive (TS) mutant alleles and establishment of a transgenic line capable of inducible overexpression of a dominant-negative form of *trpm7* (DN-trpm7). Additionally, I discuss experiments conducted to determine distinctions in water composition between fish facilities in Austin and Seattle, and how they impact observable phenotypes. These experiments lay the groundwork for future avenues of research and may contribute to an improved understanding of the mechanisms at play in *trpm7* mutants.

Appendix I: Conditional *trpm7* Activity

As essential to understanding what factors govern developmental changes is determining when these factors are required. Though we have linked *trpm7* to growth, bone development, and kidney function, we know little about the temporal requirements these developmental processes have for trpm7 function. In *trpm7* mutants, while growth and bone defects do not manifest until approximately 14dpf, embryonic melanophore defects and touch insensitivity coupled with early larval kidney stone formation illustrate early requirements for trpm7 function. The distinction between embryonic and larval defects in mutants suggests that distinct temporal requirements for trpm7 function exist. Accordingly, a temporal analysis of trpm7 activity may distinguish between early and late requirements for trpm7 in growth, bone development and kidney function. To test these hypotheses we therefore set out to identify and establish conditional *trpm7* mutant alleles and create an inducible transgenic line capable of overexpressing a dominant-negative *trpm7* (DN-trpm7). In addition to allowing us to study temporal requirements for trpm7 function, this approach may also potentially provide inducible models for studying cation homeostasis, kidney stone formation and bone development.

Identification and Characterization of Temperature Sensitive trpm7 Mutant Alleles

In zebrafish, studies with temperature sensitive (TS) alleles have shown: that kit, a receptor tyrosine kinase, has distinct temporal roles promoting cell migration and cell survival (Rawls and Johnson 2001); that the specific stage of floor plate induction occurs

during gastrulation (Tian, Yam et al. 2003); that reg6 promotes early but not late vascularization in regenerating fins (Huang, Lawson et al. 2003); and that reg6 is just one of many TS alleles identified in a mutant screen for genes affecting fin regeneration (Johnson and Weston 1995). Furthermore TS studies in our lab have allowed identification of a critical period during pigment pattern metamorphosis requiring puma function (Parichy, Turner et al. 2003) and identification of an ongoing requirement for fms activity in maintaining a xanthophore cell-lineage and organizing melanophore stripes (Parichy and Turner 2003). Therefore, TS studies in zebrafish are a proven and powerful approach to assess temporal requirements over a broad range of developmental defects. To identify TS *trpm7* mutant alleles in zebrafish we made use of its thermoplasticity and the ability to obtain large numbers of embryos to perform a non-complementation screen using 24°C and 34°C as permissive and restrictive temperatures.

Non-Complementation Screening

Non-complementation screens are routinely used in zebrafish to identify new alleles of established mutant lines. Briefly, zebrafish males mutagenized with ENU have large numbers of recessive, germline mutations. When these males are crossed to wild-type zebrafish, the individual progeny will each be heterozygous carriers for a number of different mutations. The ability to obtain ~200-400 embryos per clutch allows the production of large numbers of carriers of unique recessive mutations. The majority of these fish are viable and have no observable phenotype. However, if the mutagenized males are crossed into a mutant background, identification of new mutant alleles can be

observed at a low frequency (~1/1000 embryos) through non-complementation of different recessive alleles of the same gene. If the desired mutant phenotype is observable in embryos, large numbers of embryos can be screened in just a few days, and a number of new alleles can be identified within a few weeks. Furthermore, if these embryos are initially reared at a restrictive temperature (34ºC) and a mutant phenotype is observed, the mutant embryo can then be downshifted to permissive temperature (24ºC) to select for TS alleles.

trpm7 mutants display an embryonic melanophore deficiency easily observable at 2dpf. This allows for the rapid identification of new *trpm7* mutant alleles in embryos reared at restrictive temperature. Subsequently, these mutants can be downshifted to permissive temperature to screen for temperature sensitivity. If the new mutant allele is temperature-sensitive, then rearing at permissive temperature will restore *trpm7* gene function and prevent onset of the later-stage phenotypes. Consequently, a viable mutant can be obtained. *trpm7* has a very large coding sequence (~5.3kb), which means there is a higher probability of identifying mutations causing amino acid changes in the coding sequence. Therefore the likelihood that viable TS alleles will be identified is extremely high.

In the non-complementation screen for TS *trpm7* alleles I screened ~81,500 embryos and identified 167 putative new alleles based on melanophore defects, yielding an allelic frequency of 1 mutant allele for every ~488 embryos screened. Of these 167 putative alleles, I recovered 12 founders that grew to adulthood and were sexually fertile and I was able to establish stocks for 9 new alleles.

Characterization of TS alleles

Of the 9 new alleles with established stocks, 5 displayed some measure of temperature sensitivity and variable phenotypic severity with respect to the characteristic embryonic melanophore defect of *trpm7* mutants (Table A.1) and can be compared to previously described non-TS alleles (Table A.2). Of the newly identified TS alleles, the *nutria-110* and *nutria-48* alleles show the most promise with their combination of temperature sensitivity and moderate severity of melanophore defect (Figure A.1). Furthermore, increased severity of melanophore defects is observed with these alleles when placed in combination with the original *nutria* allele (data not shown).

When assessed for growth defects, 3 non-TS alleles showed minor growth retardation, but developed into fertile adults. Furthermore, only 1 TS allele, $trpm7^{n110}$ exhibited any defect in growth, with a minor growth retardation observable when reared at restrictive temperature (Figure A.2). This defect was also only seen when the TS *nutria-110* allele was crossed with the non-TS $trpm7^{j124e2}$ allele and showed variable penetrance. As will be discussed in Appendix II, it is possible that water composition and mineral ion content may influence penetrance of later stage phenotypes; increased severity of TS alleles may be obtainable with different water compositions.

Construction of an Inducible Transgenic Dominant-Negative trpm7 Line

As an alternative and complimentary approach to TS alleles, I developed a transgenic zebrafish line containing a dominant-negative form of zebrafish *trpm7* under the control of the inducible heat-shock protein 70 (HSP70) promoter and with an IRES-

EGFP expression cassette following the DN-trpm7 coding sequence. Using this approach, heat-shock induction of the transgene can inhibit trpm7 activity in a controllable manner and allow for independent testing of temporal requirements for trpm7 activity.

Construction of a Dominant-Negative Zebrafish trpm7 Gene

In research with mammalian *trpm7*, site-directed mutagenesis targeting the coding sequence for a highly conserved region of the channel pore domain yielded a gene with a dominant-negative effect on trpm7 channel activity (Krapivinsky, Mochida et al. 2006). I identified this amino acid sequence as being entirely conserved between mammalian forms of TRPM7 and zebrafish trpm7 (Figure A.3a). I therefore performed site-directed mutagenesis on a full-length zebrafish *trpm7* clone to induce the same amino acid changes as those found in the mammalian DN. After confirming changes by sequencing (Figure A.3b), I used the Tol2 gateway toolkit (Kwan, Fujimoto et al. 2007) to construct an expression vector composed of an HSP70 promoter, the DN-trpm7 coding sequence and an IRES-EGFP cassette.

Establishing and Validating a Transgenic DN-trpm7 Zebrafish Line

After constructing the DN-trpm7 vector, I co-injected the DNA vector with Tol2 mRNA to induce a high degree of incorporation of the expression vector into the genomic DNA. Using this approach I was able to obtain a large number of embryos with mosaic integration of the transgene, and test the efficacy of the DN-trpm7 in recapitulating *trpm7* mutant embryonic phenotypes (Figure A.4a). Embryos at 24 hpf were heat-shocked twice

for 1hr each time, with 3hrs between heat-shocks. After growing injected embryos to adulthood, progeny were screened for the transgene through presence or absence of GFP expression following heat-shock to identify germline carriers. Two germline stocks were established with melanophore (Figure A.4b) and touch unresponsiveness defects following a cycling heat shock at 38.5°C from 20-44hpf, with 30min HS followed by 5.5hrs recovery. Of note is the fact that a single heat-shock was insufficient to obtain any melanophore defects, and only after multiple heat shocks is a phenotype observable. This suggests that a high level of the DN-trpm7 is required to sufficiently repress wild-type trpm7 activity.

Appendix II: The Effects of Water Composition on *trpm7* Mutant Phenotypes

Trpm7 is a divalent cation channel and previous work has shown that high levels of magnesium and calcium in the water can reduce the expressivity of the *trpm7* embryonic mutant phenotypes (Elizondo, Arduini et al. 2005). Similar experiments with high levels of magnesium and calcium proved to be toxic at larval stages. However, when rearing *trpm7*^{j124e2} (*nutria*) mutants in different fish facilities at the University of Texas and the University of Washington, I observed differing expressivity of larval mutant phenotypes, with lesser bone mineralization defects in fish reared at UW. Additionally, characterization of the *trpm7*^{b722} (*dalmation)* mutant allele (Cornell, Yemm et al. 2004) also reveals distinctions between severity of growth defects. When reared at the University of Iowa, these mutants exhibit the severe growth defect characteristic of the *trpm7*^{j124e2} mutant background, however, the *trpm7*^{b722} mutants at UT and UW display little to no growth defects. This phenotypic plasticity across fish facilities suggested the ion content of the different water compositions between the facilities may influence *trpm7* mutant larval phenotypes.

I therefore had the fish water of the facilities at UT, UI, and UW analyzed by AmTest Laboratories for mineral content to determine whether there were changes that were consistent with differences in phenotype severity (Table A.3). I ranked the fish facilities with respect to the phenotypic severity of bone or growth defects in the *nutria* and *dalmation* alleles (Figure A.5). Taking into account the varied expressivity of growth defects for *dalmation* mutants and bone defects for *nutria* mutants, we ranked UI water as

most severe followed by UT with medium severity and UW with low severity. Using this ranking we find that while distinctions existed between sodium levels and potassium levels, only the changes in levels of calcium and magnesium correlate with the range of phenotypic severity. Specifically we find both decreasing levels of calcium and increasing levels of magnesium associated with decreasing phenotypic severity.

The changes in calcium and magnesium levels between the fish facilities occur over a very narrow range of 8.5mg/L to 27mg/L for magnesium and 8.2mg/L to 18mg/L for calcium. This equates to a range of 3.5mM to 11mM for magnesium and 2.5mM to 4mM for calcium, which contrasts with the 100mM and 50mM concentrations for magnesium and calcium used in previous rescue experiments. Therefore it is possible that a narrow range of magnesium and calcium concentrations may influence phenotypic plasticity for *trpm7* mutants at larval stages.

As a test for this, we reconstituted a UT-like water composition with 10mg/L [Ca^{2+}] and 20mg/L [Mg^{2+}] to rear *nutria* mutants at UW, using a 1% Hank's solution (Westerfield 2000) as a foundation, then adding appropriate amounts of $MgSO_4$ and $CaCl_2$. Using this approach we are able to detect bone defects in *nutria* mutants.

While able to reconstitute the bone defects in *trpm7* mutants by altering the levels of calcium and magnesium in the rearing media, it remains uncertain whether one or both of the cation levels is crucial to proper bone development. Similar experiments varying the concentrations of the cations between 10mg/L to 50mg/L proved inconclusive, and it remains possible that there are distinct requirements for these cations in survival, growth, and bone development. For example, decreased calcium levels may reduce the premature

mineralization of bone in mutants, but also may exacerbate hypocalcemia and negatively affect survival. In contrast, while increased magnesium might alleviate hypomagnesemia in mutants and rescue growth defects, it also may exacerbate kidney stone formation and bone defects. There is likely to be a delicate balance between cation levels and distinct effects on growth, bone development and survival in mutants.

Furthermore, other recent findings, (*personal communication* A. Fleig), suggest that other ions, such as potassium and sodium also may influence trpm7 channel activity. As will be discussed in the next section, phosphate levels may also be altered in *trpm7* mutants. Therefore dissecting which cation influences what phenotype may prove more complex than simple changes in calcium or magnesium, but the recent identification of decreased calcium and magnesium levels in early larval mutants should facilitate the design of future experiments.

Appendix III: Kidney Stone Formation in Heterozygous *trpm7* larvae

In Chapter 3 I demonstrated kidney stone formation in homozygous *trpm7* mutants as early as 5dpf. At this stage, mutants manifesting kidney stones are detectable with extended incubation with the vital dye alizarin red. Additionally, when using extended incubation with a similar vital dye, calcein, on aSB:6.1SSL stage larval *trpm7* mutants and siblings, I am able to identify kidney stones in mutants as expected (Figure A.6). However, in some instances when reared in Texas-like water, a subset of wild-type siblings also develop kidney stones (Figure A.6). Genotyping with the tightly linked microsatellite marker, z53176, indicates that 5/5 wild-type siblings manifesting kidney stones are heterozygous for the *trpm7* mutant allele while 3/5 wild-type siblings without kidney stones were also heterozygous. This suggests that *trpm7* mutant carriers have an increased susceptibility to late onset kidney stone formation and indicates that there may be decreased channel activity with in heterozygotes. Future analyses of larval fish heterozygous for the *trpm7* mutant allele may reveal other, more subtle defects.

Appendix IV: Potential Changes in Phosphate Levels in *trpm7* Mutants

In Chapter 3 I discussed the identification of increased levels of *stc1* in *trpm7* mutants. *stc1* is a primary regulator of calcium homeostasis through anti-hypercalcemic activity, however it is also known to regulate phosphate levels through anti-hypophosphatemic activity. In an attempt to ascertain whether there were also changes in the regulation of phosphate in *trpm7* mutants I attempted to evaluate phosphate levels in *trpm7* mutants and to characterize potential changes in an important regulator of phosphate homeostasis, *fibroblast growth factor-23* (*fgf23*).

Using the same samples of total ion preps used to assay calcium and magnesium, I also attempted to evaluate total phosphate levels in *trpm7* mutants with the QuantiChrom Phosphate Assay Kit (Bioassay Systems DIPI-500). I determined that to reach the assay's linear detection range, I needed to dilute samples 1:50. However, in this range there was a high degree of sample to sample variation between replicates, and unlike with magnesium and calcium assays, no individual well blank values could be ascertained through chelation with addition of EDTA. Therefore, I was unable to determine whether any changes in phosphate levels exist for *trpm7* mutants.

An anti-hyperphosphatemic factor (Shimada, Hasegawa et al. 2004), *fgf23* controls uptake of phosphate through regulation of sodium-phosphate transporters in the kidney (Marsell, Krajisnik et al. 2008), is a known molecular marker for kidney stone formation (Rendina, Mossetti et al. 2006), and may influence bone mineralization (Larsson, Marsell et al. 2004). It therefore represents a prime candidate as a molecular

mediator of potential changes in phosphate regulation in *trpm7* mutants. When examining *fgf23* expression in *trpm7* mutants by *in situ* hybridization, I find expression specifically in the CS, and there appears to be a gross increase of expression in *trpm7* mutants when compared to wild-type siblings or *mitfa* mutants (Figure A.7), (which lack melanophores obscuring expression in the CS). When examined by quantitative PCR, increased *fgf23* is also detectable in mutants at 48hpf (Figure A.7). One possible explanation for this increase is a compensatory response to the anti-hypophosphatemic activity of increased *stc1* levels. Additionally, increased *fgf23* may influence bone defects or kidney stone formation in *trpm7* mutants. Therefore I developed an inducible transgenic line for *fgf23* expression following the same approach used for *stc1* discussed in Chapter 3.

I hypothesized that increased *fgf23* expression may lead to kidney stone formation in *trpm7* mutants, however no kidney stones were detectable by Alizarin Red staining in wild-type *HS:fgf23* fish following a 4x/day 30 minute heat shock cycle from 2dpf-5dpf. Furthermore, examination of *fgf23* expression in 3-5dpf *trpm7* mutants from multiple biological replicates showed variable changes in levels of *fgf23* (Figure A.7). With an increase in *fgf23* expression only verifiable at 48hpf and no discernable kidney stone formation after induction of *fgf23* expression, it remains inconclusive what role *fgf23* has in *trpm7* mutants.

While a detectable difference in *fgf23* expression is present in 48hpf *trpm7* mutants, it is possible that it is only a transient secondary response to increased *stc1* expression and has no lasting effect on *trpm7* mutant phenotypes or phosphate levels. To

better assess these phosphate levels in *trpm7* mutants it appears that alternative approaches are necessary, possibly through the use of radioactive P32 uptake assays. Interestingly, the localized expression of *fgf23* in the CS does however suggest the corpuscles may have a larger role in regulating ion homeostasis than previously considered, and it may be worthwhile to examine whether other regulatory factors exhibit localized expression in this domain. Finally, the transgenic *HS:fgf23* line should also facilitate any future studies of phosphate metabolism or *fgf23* function in zebrafish.

Appendix V: Other Potential Effects of *stc1* Overexpression

While I characterized the early larval defects associated with transgenic *stc1* overexpression, other phenotypes were observable at later stages in heat-shocked fish. These phenotypes were present only in fish carrying multiple copies of the transgene and likely are a result of higher levels of overexpression.

In addition to the known anti-hypercalcemic effects of stanniocalcins in fish (Lafeber, Flik et al. 1988; Sundell, Bjornsson et al. 1992; Filvaroff, Guillet et al. 2002; Varghese, Gagliardi et al. 2002), mammalian studies have also shown that overexpressing stanniocalcin leads to growth defects (Filvaroff, Guillet et al. 2002; Varghese, Gagliardi et al. 2002). The possibility therefore exists that the increased *stc1* expression in *trpm7* mutants contributes to growth defects in these mutants. When rearing transgenic fish carrying multiple copies of the *stc1* transgene following heat shock at early embryonic stages, (24-48hpf), I identified a growth defect that begins to manifest at larval stages (Figure A.8).

Interestingly, this growth defect persists in larval stages even if no further heat-shock cycles are administered during larval stages. A possible explanation for this would be an early overload of transgenic *stc1* production results in an irreversible shutdown of endogenous *stc1* production. It remains to be determined whether this growth defect is analogous to growth defects observed in mammalian systems following *stc* overexpression, or whether this growth defect is similar to that observed in *trpm7* mutants. Finally, cursory observation also suggests an increase in larval melanophore size

or number in these heat-shocked individuals (Figure A.8). This may reflect a responsiveness of melanophores to calcium levels in these transgenic individuals and be related to an established link between detection of extracellular calcium levels and pigment aggregation in melanophores of freshwater teleosts (Yamada and Fujii 2002).

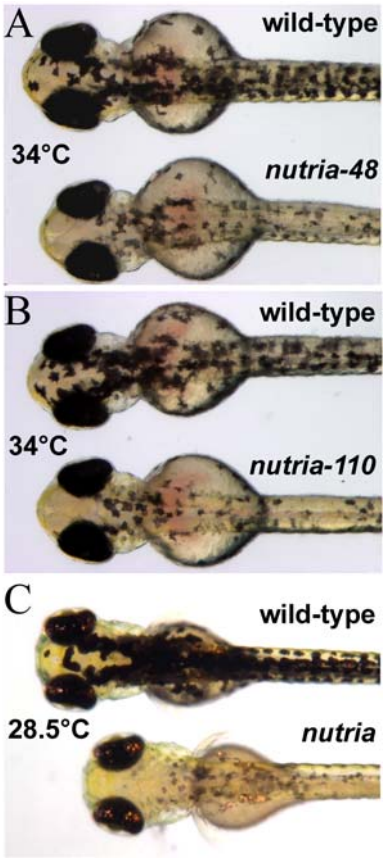

Figure A.1. A non-complementation screen for temperature-sensitive *trpm7* mutant alleles. The severity of the *trpm7* mutant melanophore defect at 2 dpf can be viewed for TS alleles *nutria-48* (A) and *nutria-110* (B) when reared at a restrictive temperature of 34˚C and can be compared with the severity of the original *nutria* allele (C).

	Strength of *trpm7* mutant alleles								
Phenotype	***n19***	***n26***	***n41***	***n48***	***n110***	***n127***	***n154***	***n155***	***n156***
Temperature sensitivity	-	-	-	+	+	+/-	+	-	+
Melanophore defect	+	+	++	++	+++	+++	+	+	+
Growth defect	-	+	+	-	+/-	+/-	-	-	-

Table A.1. Summary of alleles recovered from the non-complementation screen and their phenotypes. Table lists strength of temperature sensitivity, melanophore and growth defects for new *trpm7* alleles. *nutria-48, -110, -154, -156* exhibit temperature sensitivity in the range of 24˚C-34˚C with respect to the melanophore defect, while *nutria-19, -26, -41, -155* are weak alleles with no temperature sensitivity. *nutria-127* exhibits marginal temperature sensitivity with a slightly permissive temperature of 24˚C, and a restrictive temperature of only 28-30˚C.

	Original, Independently Isolated Alleles			
Phenotype	*j124e1 (touchtone)*	*b508 (touchtone)*	*b722 (dalmation)*	*j124e2 (nutria)*
Temperature sensitivity	-	-	-	-
Melanophore defect	++++	++++	+++	++++
Growth defect	lethal	lethal	+/-	++
Touch Insensitivity	+++	+++	++	++

Table A.2. Summary of independently isolated *trpm7* mutant alleles. Table summarizes nomenclature and observed phenotypic severity for previously described *trpm7* mutant alleles.

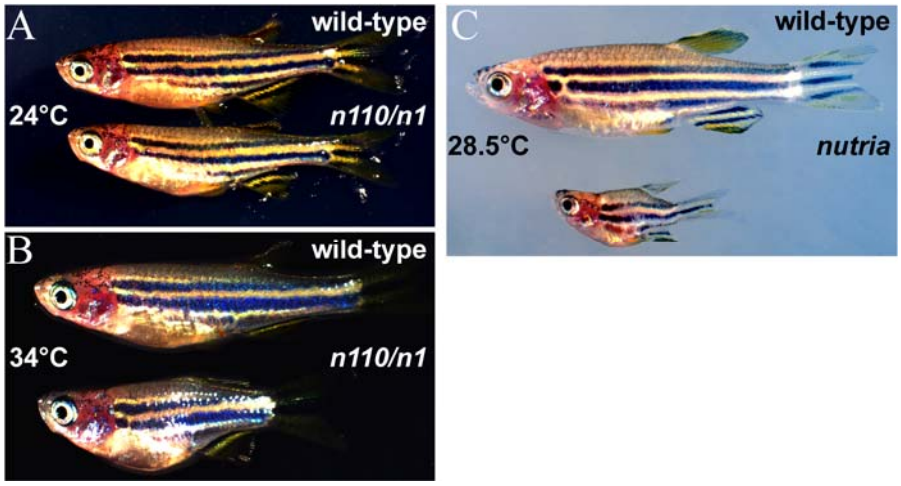

Figure A.2. Temperature sensitive growth defect with *nutria-110* TS allele. *nutria-110 / nutria* mutants and wild-type siblings reared at (A) permissive temperature (24˚C) and (B) restrictive temperature (34˚C). A growth defect is evident at restrictive temperature (B), but is not as severe as that found in the original *nutria* allele (C).

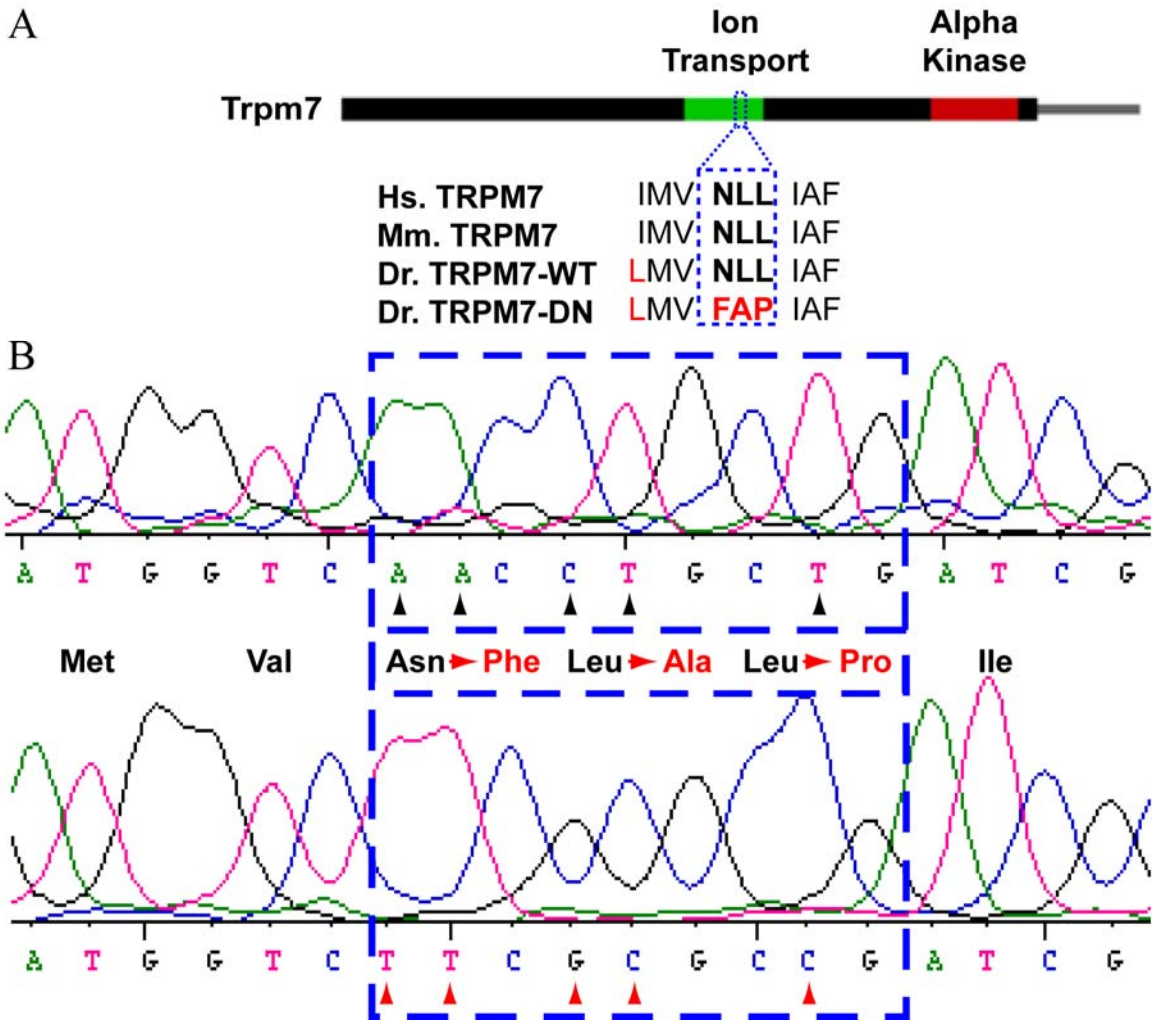

Figure A.3. Construction of a zebrafish DN-*trpm7*. Three amino acids in the channel pore domain of the trpm7 protein highly conserved between mammals and fish were targeted for site directed mutagenesis (A). Sequencing confirms site-directed changes in DNA sequence leading to amino acid changes from NLL to FAP (B).

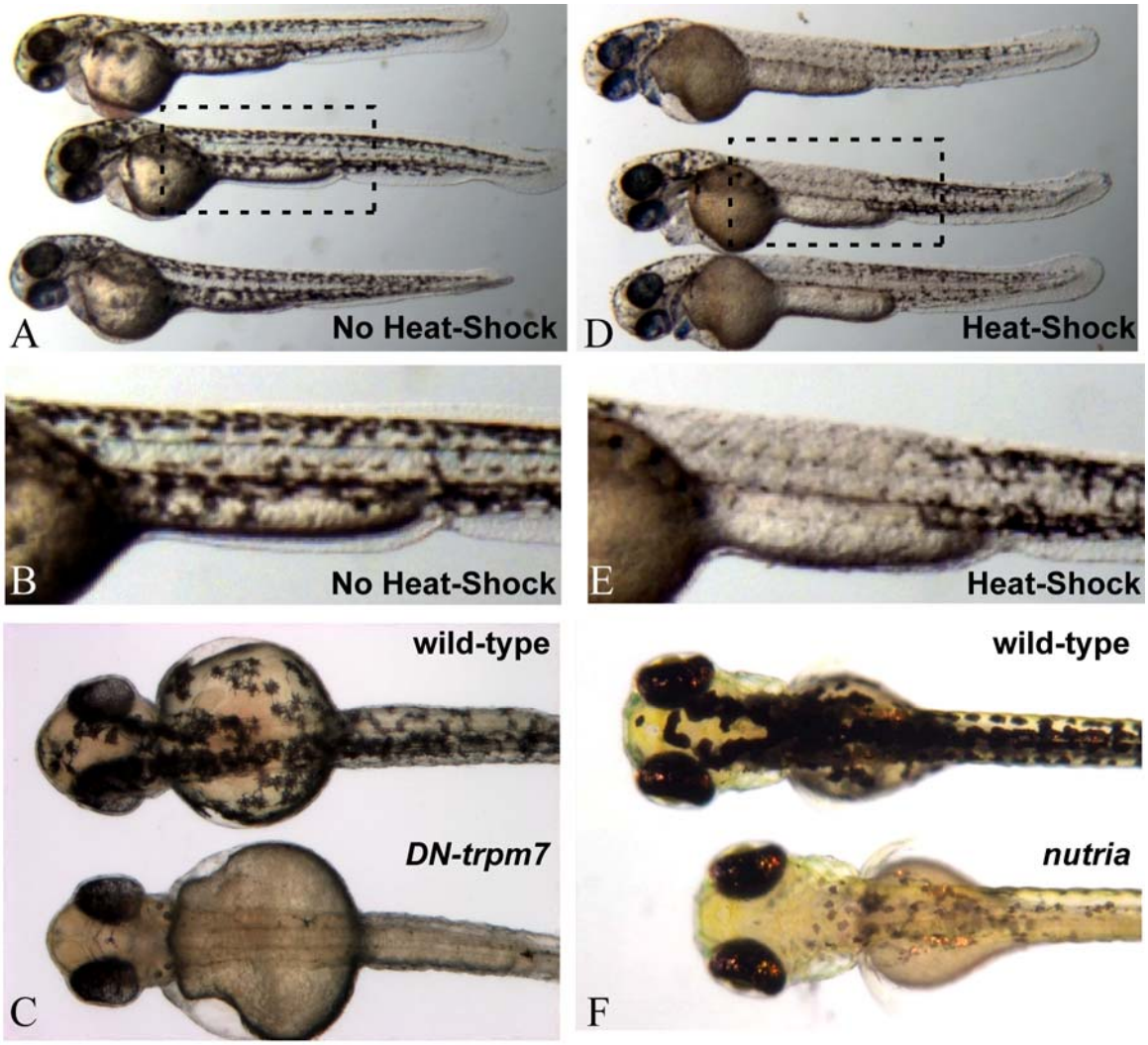

Figure A.4. Mosaic and germline melanophore defects following heat-shock of transgenic *DN-trpm7* embryos. Embryos injected with the Hsp70::*DN-trpm7* construct exhibit a mosaic melanophore defect following heat-shock (B,D) when compared with injected, non heat-shocked embryos (A,C). The severe melanophore defect in F1 progeny of a germline carrier for Hsp70::*DN-trpm7* construct following heat-shock (E) is comparable to the melanophore defect evident in 60 hpf *trpm7*^{nutria} mutants (F).

Water Ion Composition

Minerals	Washington	Iowa	Texas	Detection Limit*
Calcium	8.2	18	12	0.05
Potassium	8.2	5.1	3.6	0.1
Magnesium	27	8.5	17	0.05
Sodium	250	96	24	0.05

ICP Metals	Washington	Iowa	Texas	Detection Limit
Silver	nd**	nd	nd	0.01
Aluminum	nd	nd	nd	0.01
Arsenic	nd	nd	nd	0.01
Boron	0.12	0.06	0.06	0.05
Barium	0.0006	0.0086	0.0086	0.0005
Beryllium	nd	nd	nd	0.0005
Cadmium	nd	nd	nd	0.0005
Cobalt	nd	nd	nd	0.001
Chromium	nd	nd	nd	0.001
Copper	0.001	0.002	0.002	0.001
Iron	nd	nd	0.025	0.005
Mercury	nd	nd	nd	0.01
Lithium	0.007	0.056	0.006	0.005
Manganese	nd	nd	nd	0.0005
Molybdenum	nd	nd	nd	0.005
Nickel	nd	nd	nd	0.005
Phosphorous	0.29	2.63	0.34	0.01
Lead	nd	nd	nd	0.01
Sulfur	19	10	13	0.05
Antimony	nd	nd	nd	0.01
Selenium	nd	nd	nd	0.01
Silicon	0.24	0.17	2.8	0.05
Tin	nd	nd	nd	0.005
Strontium	0.242	0.0922	0.145	0.0005
Titanium	nd	nd	nd	0.001
Thalium	nd	nd	nd	0.01
Vanadium	nd	0.005	0.005	0.005
Yttrium	nd	nd	nd	0.0005
Zinc	0.005	0.01	0.008	0.001

*in mg/L

**not detected

Table A.3. Water mineral composition of different fish facilities. Table summarizes ion content of water from fish facilities at the University of Washington, Iowa, and Texas. Values are listed as mg/L. Notable differences in levels are observable in calcium, magnesium, potassium, and sodium.

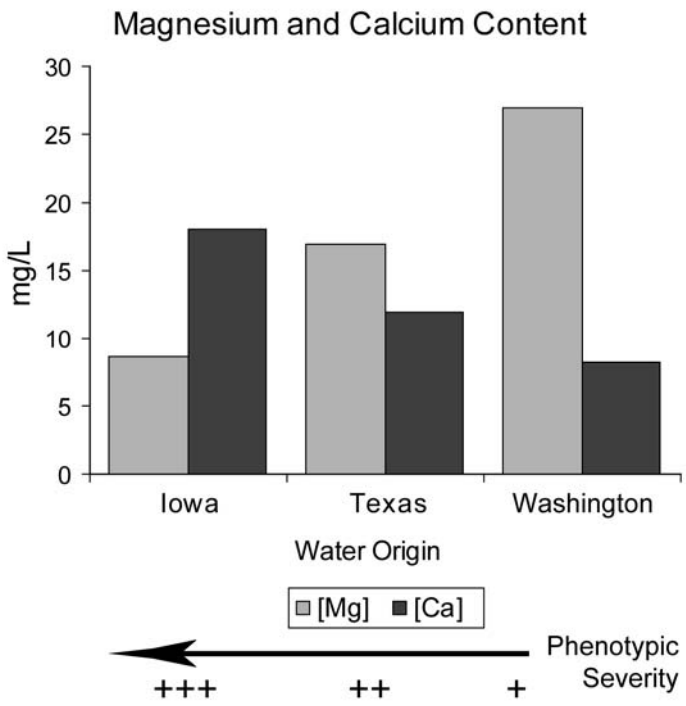

Figure A.5. Association of magnesium and calcium content with *trpm7* phenotypic severity. In water which manifests more severe *trpm7* mutant defects increasing calcium and decreasing magnesium levels are detected.

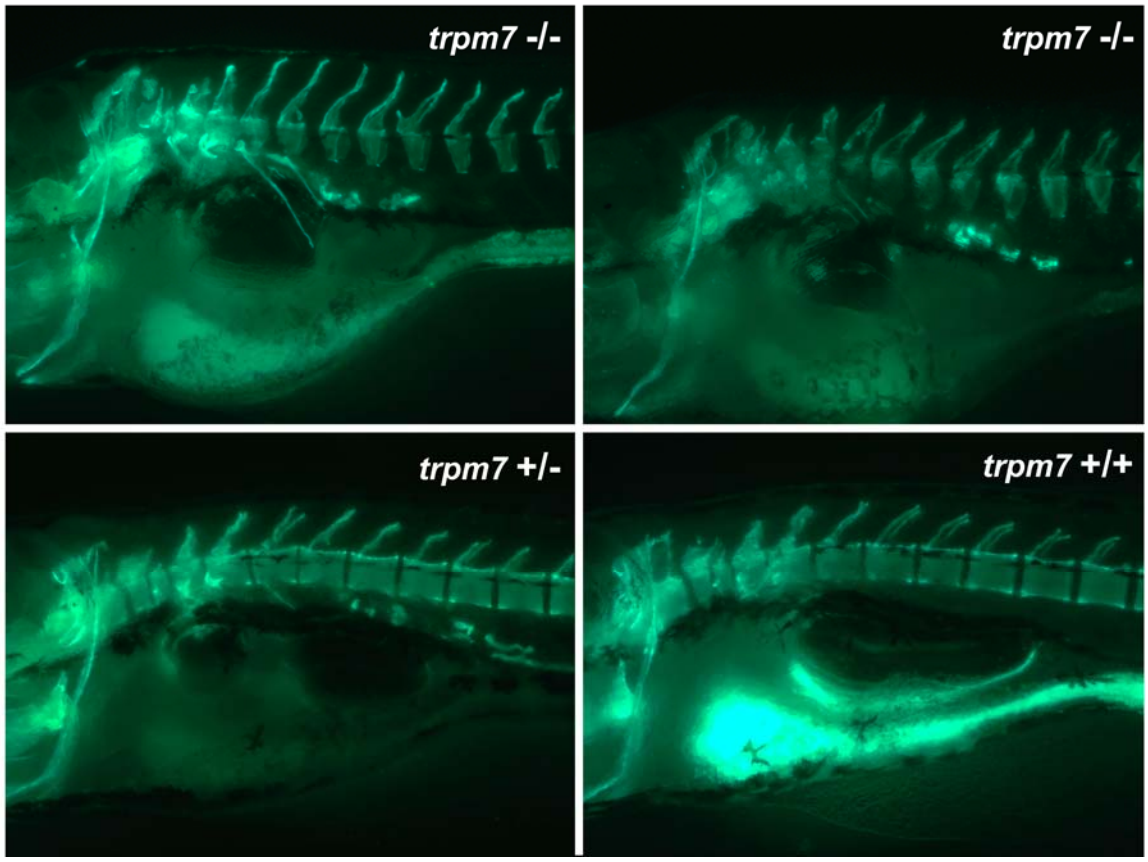

Figure A.6. Kidney stone formation in mutant and heterozygous *trpm7* larvae. After extended staining with calcein, kidney stones are observable in *trpm7* mutant and heterozygous larvae, while wild-type larvae show no kidney stone formation.

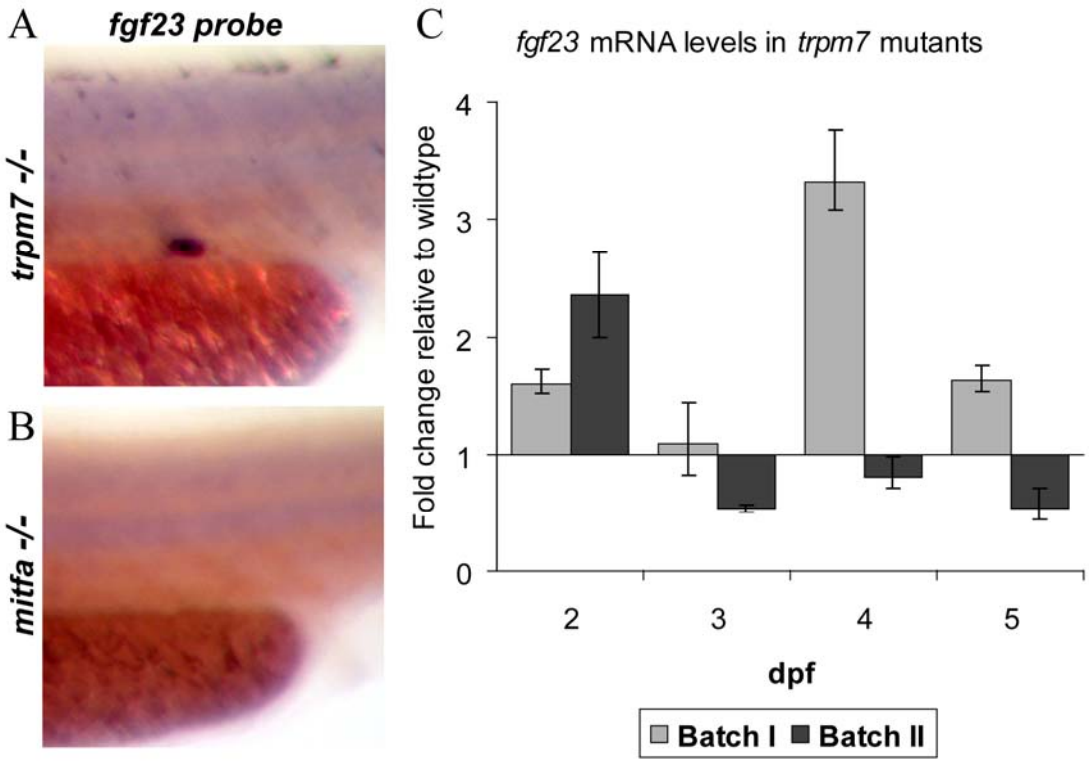

Figure A.7. *fgf23* expression by *in situ* hybridization and qPCR. *In situ* hybridization reveals strong *fgf23* expression in the CS in *trpm7* mutants (A), while *mitfa* mutants, (which lack melanophores but are otherwise wild-type), have no expression over the same exposure time (B). qPCR shows upregulation of *fgf23* in *trpm7* mutants at 2 dpf, however at other stages results are inconclusive as different biologic replicates show divergent results (C).

Figure A.8. Later stage phenotypes with transgenic Hsp70::*stc1* overexpression. Early overexpression, beginning at ~24 hpf, of *stc1* in homozygous transgenic fish leads a growth defect (A). Additionally, superficial observations suggest an increase in melanophore size or number in fish over-expressing *stc1* (B,C).

References

Aarts, M., K. Iihara, et al. (2003). "A key role for TRPM7 channels in anoxic neuronal death." Cell **115**(7): 863-877.

Akerstrom, G., P. Hellman, et al. (2005). "Parathyroid glands in calcium regulation and human disease." Ann N Y Acad Sci **1040**: 53-58.

Alexander, R. T., J. G. Hoenderop, et al. (2008). "Molecular determinants of magnesium homeostasis: insights from human disease." J Am Soc Nephrol **19**(8): 1451-1458.

Altarescu, G., M. Sun, et al. (2002). "The neurogenetics of mucolipidosis type IV." Neurology **59**(3): 306-313.

Amizuka, N., D. Davidson, et al. (2004). "Signalling by fibroblast growth factor receptor 3 and parathyroid hormone-related peptide coordinate cartilage and bone development." Bone **34**(1): 13-25.

Arduini, B. L. and P. D. Henion (2004). "Melanophore sublineage-specific requirement for zebrafish touchtone during neural crest development." Mech Dev **121**(11): 1353-1364.

Bach, G. (2001). "Mucolipidosis type IV." Mol Genet Metab **73**(3): 197-203.

Baek, W. Y., M. A. Lee, et al. (2009). "Positive regulation of adult bone formation by osteoblast-specific transcription factor osterix." J Bone Miner Res **24**(6): 1055-1065.

Bajaj, S. and K. G. Saag (2003). "Osteoporosis: evaluation and treatment." Curr Womens Health Rep **3**(5): 418-424.

Bankir, L., N. Bouby, et al. (1989). "The role of the kidney in the maintenance of water balance." Baillieres Clin Endocrinol Metab **3**(2): 249-311.

Bell, D. M., K. K. Leung, et al. (1997). "SOX9 directly regulates the type-II collagen gene." Nat Genet **16**(2): 174-178.

Bi, W., J. M. Deng, et al. (1999). "Sox9 is required for cartilage formation." Nat Genet **22**(1): 85-89.

Biber, J., N. Hernando, et al. (2009). "Regulation of phosphate transport in proximal tubules." Pflugers Arch **458**(1): 39-52.

Bird, N. C. and P. M. Mabee (2003). "Developmental morphology of the axial skeleton of the zebrafish, Danio rerio (Ostariophysi: Cyprinidae)." Dev Dyn **228**(3): 337-357.

Bischoff-Ferrari, H. A. and H. B. Staehelin (2008). "Importance of vitamin D and calcium at older age." Int J Vitam Nutr Res **78**(6): 286-292.

Blair, H. C., P. H. Schlesinger, et al. (2007). "Calcium signalling and calcium transport in bone disease." Subcell Biochem **45**: 539-562.

Boros, S., R. J. Bindels, et al. (2009). "Active Ca(2+) reabsorption in the connecting tubule." Pflugers Arch **458**(1): 99-109.

Boyce, B. F. and L. Xing (2008). "Functions of RANKL/RANK/OPG in bone modeling and remodeling." Arch Biochem Biophys **473**(2): 139-146.

Brown, E. M. (2007). "The calcium-sensing receptor: physiology, pathophysiology and CaR-based therapeutics." Subcell Biochem **45**: 139-167.

Brown, E. M. and J. B. Lian (2008). "New insights in bone biology: unmasking skeletal effects of the extracellular calcium-sensing receptor." Sci Signal **1**(35): pe40.
Caterina, M. J., M. A. Schumacher, et al. (1997). "The capsaicin receptor: a heat-activated ion channel in the pain pathway." Nature **389**(6653): 816-824.
Chang, A. C., J. Hook, et al. (2008). "The murine stanniocalcin 2 gene is a negative regulator of postnatal growth." Endocrinology **149**(5): 2403-2410.
Chen, R. A. and W. G. Goodman (2004). "Role of the calcium-sensing receptor in parathyroid gland physiology." Am J Physiol Renal Physiol **286**(6): F1005-1011.
Chubanov, V., M. Mederos y Schnitzler, et al. (2005). "Emerging roles of TRPM6/TRPM7 channel kinase signal transduction complexes." Naunyn Schmiedebergs Arch Pharmacol **371**(4): 334-341.
Chubanov, V., K. P. Schlingmann, et al. (2007). "Hypomagnesemia with secondary hypocalcemia due to a missense mutation in the putative pore-forming region of TRPM6." J Biol Chem **282**(10): 7656-7667.
Chubanov, V., S. Waldegger, et al. (2004). "Disruption of TRPM6/TRPM7 complex formation by a mutation in the TRPM6 gene causes hypomagnesemia with secondary hypocalcemia." Proc Natl Acad Sci U S A **101**(9): 2894-2899.
Chung, U. I., B. Lanske, et al. (1998). "The parathyroid hormone/parathyroid hormone-related peptide receptor coordinates endochondral bone development by directly controlling chondrocyte differentiation." Proc Natl Acad Sci U S A **95**(22): 13030-13035.
Clark, J. Y., I. M. Thompson, et al. (1995). "Economic impact of urolithiasis in the United States." J Urol **154**(6): 2020-2024.
Clark, K., M. Langeslag, et al. (2006). "TRPM7, a novel regulator of actomyosin contractility and cell adhesion." EMBO J **25**(2): 290-301.
Cohen, M. M., Jr. (2006). "The new bone biology: pathologic, molecular, and clinical correlates." Am J Med Genet A **140**(23): 2646-2706.
Corey, D. P., J. Garcia-Anoveros, et al. (2004). "TRPA1 is a candidate for the mechanosensitive transduction channel of vertebrate hair cells." Nature **432**(7018): 723-730.
Cornell, R. A., E. Yemm, et al. (2004). "Touchtone promotes survival of embryonic melanophores in zebrafish." Mech Dev **121**(11): 1365-1376.
Cosman, F. (2005). "The prevention and treatment of osteoporosis: a review." MedGenMed **7**(2): 73.
Cubbage, C. C., and Mabee, P.M. (1996). "Development of the cranium and paired fins in the zebrafish *Danio rerio* (ostariophysi, Cyprinidae)." J. Morphol. **229**: 121-160.
D'Souza-Li, L. (2006). "The calcium-sensing receptor and related diseases." Arq Bras Endocrinol Metabol **50**(4): 628-639.
Datta, N. S. and A. B. Abou-Samra (2009). "PTH and PTHrP signaling in osteoblasts." Cell Signal **21**(8): 1245-1254.
de Crombrugghe, B., V. Lefebvre, et al. (2001). "Regulatory mechanisms in the pathways of cartilage and bone formation." Curr Opin Cell Biol **13**(6): 721-727.

Delaisse, J. M., T. L. Andersen, et al. (2003). "Matrix metalloproteinases (MMP) and cathepsin K contribute differently to osteoclastic activities." Microsc Res Tech **61**(6): 504-513.
Demeuse, P., R. Penner, et al. (2006). "TRPM7 channel is regulated by magnesium nucleotides via its kinase domain." J Gen Physiol **127**(4): 421-434.
Deng, Z. L., K. A. Sharff, et al. (2008). "Regulation of osteogenic differentiation during skeletal development." Front Biosci **13**: 2001-2021.
Di Sole, F. (2008). "Adenosine and renal tubular function." Curr Opin Nephrol Hypertens **17**(4): 399-407.
Domowicz, M. S., M. Cortes, et al. (2009). "Aggrecan modulation of growth plate morphogenesis." Dev Biol **329**(2): 242-257.
Dorovkov, M. V. and A. G. Ryazanov (2004). "Phosphorylation of annexin I by TRPM7 channel-kinase." J Biol Chem **279**(49): 50643-50646.
Doumouchtsis, K. K., D. N. Perrea, et al. (2009). "The impact of sex hormone changes on bone mineral deficit in chronic renal failure." Endocr Res **34**(3): 90-99.
Doyle, M. E. and S. M. Jan de Beur (2008). "The skeleton: endocrine regulator of phosphate homeostasis." Curr Osteoporos Rep **6**(4): 134-141.
Draper, B. W., P. A. Morcos, et al. (2001). "Inhibition of zebrafish fgf8 pre-mRNA splicing with morpholino oligos: a quantifiable method for gene knockdown." Genesis **30**(3): 154-156.
Drummond, I. A. (2004). "Zebrafish kidney development." Methods Cell Biol **76**: 501-530.
Drummond, I. A. (2005). "Kidney development and disease in the zebrafish." J Am Soc Nephrol **16**(2): 299-304.
Duncan, L. M., J. Deeds, et al. (2001). "Melastatin expression and prognosis in cutaneous malignant melanoma." J Clin Oncol **19**(2): 568-576.
Duncan, L. M., J. Deeds, et al. (1998). "Down-regulation of the novel gene melastatin correlates with potential for melanoma metastasis." Cancer Res **58**(7): 1515-1520.
Dutton, K. A., A. Pauliny, et al. (2001). "Zebrafish colourless encodes sox10 and specifies non-ectomesenchymal neural crest fates." Development **128**(21): 4113-4125.
Dvorak, M. M. and D. Riccardi (2004). "Ca2+ as an extracellular signal in bone." Cell Calcium **35**(3): 249-255.
Egbuna, O. I. and E. M. Brown (2008). "Hypercalcaemic and hypocalcaemic conditions due to calcium-sensing receptor mutations." Best Pract Res Clin Rheumatol **22**(1): 129-148.
Elizondo, M. R., B. L. Arduini, et al. (2005). "Defective skeletogenesis with kidney stone formation in dwarf zebrafish mutant for trpm7." Curr Biol **15**(7): 667-671.
Feng, X. (2005). "RANKing intracellular signaling in osteoclasts." IUBMB Life **57**(6): 389-395.
Filvaroff, E. H., S. Guillet, et al. (2002). "Stanniocalcin 1 alters muscle and bone structure and function in transgenic mice." Endocrinology **143**(9): 3681-3690.
Fisher, S., P. Jagadeeswaran, et al. (2003). "Radiographic analysis of zebrafish skeletal defects." Dev Biol **264**(1): 64-76.

Fleming, A., R. Keynes, et al. (2004). "A central role for the notochord in vertebral patterning." Development **131**(4): 873-880.
Fonfria, E., P. R. Murdock, et al. (2006). "Tissue distribution profiles of the human TRPM cation channel family." J Recept Signal Transduct Res **26**(3): 159-178.
Franceschi, R. T. and G. Xiao (2003). "Regulation of the osteoblast-specific transcription factor, Runx2: responsiveness to multiple signal transduction pathways." J Cell Biochem **88**(3): 446-454.
Fujita, T. (2000). "Calcium paradox: consequences of calcium deficiency manifested by a wide variety of diseases." J Bone Miner Metab **18**(4): 234-236.
Fujiwara, Y. and D. L. Minor, Jr. (2008). "X-ray crystal structure of a TRPM assembly domain reveals an antiparallel four-stranded coiled-coil." J Mol Biol **383**(4): 854-870.
Gagliardi, A. D., E. Y. Kuo, et al. (2005). "Human stanniocalcin-2 exhibits potent growth-suppressive properties in transgenic mice independently of growth hormone and IGFs." Am J Physiol Endocrinol Metab **288**(1): E92-105.
Gal-Moscovici, A. and S. M. Sprague (2007). "Role of vitamin D deficiency in chronic kidney disease." J Bone Miner Res **22 Suppl 2**: V91-94.
Gattineni, J., C. Bates, et al. (2009). "FGF23 decreases renal NaPi-2a and NaPi-2c expression and induces hypophosphatemia in vivo predominantly via FGF receptor 1." Am J Physiol Renal Physiol **297**(2): F282-291.
Gentili, C. and R. Cancedda (2009). "Cartilage and bone extracellular matrix." Curr Pharm Des **15**(12): 1334-1348.
Gomes, D. A., M. F. Leite, et al. (2006). "Calcium signaling in the nucleus." Can J Physiol Pharmacol **84**(3-4): 325-332.
Gonzalez, E. A. and K. J. Martin (2001). "Renal osteodystrophy." Rev Endocr Metab Disord **2**(2): 187-193.
Goodman, W. G. (2006). "Renal osteodystrophy for nonnephrologists." J Bone Miner Metab **24**(2): 161-163.
Greenwood, M. P., G. Flik, et al. (2009). "The corpuscles of Stannius, calcium-sensing receptor, and stanniocalcin: responses to calcimimetics and physiological challenges." Endocrinology **150**(7): 3002-3010.
Grimm, C., R. Kraft, et al. (2003). "Molecular and functional characterization of the melastatin-related cation channel TRPM3." J Biol Chem **278**(24): 21493-21501.
Groenestege, W. M., J. G. Hoenderop, et al. (2006). "The epithelial Mg2+ channel transient receptor potential melastatin 6 is regulated by dietary Mg2+ content and estrogens." J Am Soc Nephrol **17**(4): 1035-1043.
Grubbs, R. D. and M. E. Maguire (1987). "Magnesium as a regulatory cation: criteria and evaluation." Magnesium **6**(3): 113-127.
Guo, J., U. I. Chung, et al. (2006). "PTH/PTHrP receptor delays chondrocyte hypertrophy via both Runx2-dependent and -independent pathways." Dev Biol **292**(1): 116-128.
Hall, C. M. (2002). "International nosology and classification of constitutional disorders of bone (2001)." Am J Med Genet **113**(1): 65-77.

Hanano, T., Y. Hara, et al. (2004). "Involvement of TRPM7 in cell growth as a spontaneously activated Ca2+ entry pathway in human retinoblastoma cells." J Pharmacol Sci **95**(4): 403-419.
Haraldsson, B. and M. Jeansson (2009). "Glomerular filtration barrier." Curr Opin Nephrol Hypertens **18**(4): 331-335.
Hoenderop, J. G., J. P. van Leeuwen, et al. (2003). "Renal Ca2+ wasting, hyperabsorption, and reduced bone thickness in mice lacking TRPV5." J Clin Invest **112**(12): 1906-1914.
Hofmann, T., V. Chubanov, et al. (2003). "TRPM5 is a voltage-modulated and Ca(2+)-activated monovalent selective cation channel." Curr Biol **13**(13): 1153-1158.
Hou, P., T. Troen, et al. (2004). "Matrix metalloproteinase-12 (MMP-12) in osteoclasts: new lesson on the involvement of MMPs in bone resorption." Bone **34**(1): 37-47.
Huang, C. C., N. D. Lawson, et al. (2003). "reg6 is required for branching morphogenesis during blood vessel regeneration in zebrafish caudal fins." Dev Biol **264**(1): 263-274.
Iwasaki, Y., M. Asai, et al. (2007). "Impaired parathyroid hormone response to hypocalcemic stimuli in a patient with hypomagnesemic hypocalcemia." J Endocrinol Invest **30**(6): 513-516.
Jabbour, S. A. and B. J. Goldstein (2008). "Sodium glucose co-transporter 2 inhibitors: blocking renal tubular reabsorption of glucose to improve glycaemic control in patients with diabetes." Int J Clin Pract **62**(8): 1279-1284.
Jin, J., B. N. Desai, et al. (2008). "Deletion of Trpm7 disrupts embryonic development and thymopoiesis without altering Mg2+ homeostasis." Science **322**(5902): 756-760.
Johnson, S. L. and J. A. Weston (1995). "Temperature-sensitive mutations that cause stage-specific defects in Zebrafish fin regeneration." Genetics **141**(4): 1583-1595.
Kamel, K. S., S. Cheema-Dhadli, et al. (2004). "Dogmas and controversies in the handling of nitrogenous wastes: excretion of nitrogenous wastes in human subjects." J Exp Biol **207**(Pt 12): 1985-1991.
Karaplis, A. C., B. He, et al. (1998). "Inactivating mutation in the human parathyroid hormone receptor type 1 gene in Blomstrand chondrodysplasia." Endocrinology **139**(12): 5255-5258.
Karsenty, G. and E. F. Wagner (2002). "Reaching a genetic and molecular understanding of skeletal development." Dev Cell **2**(4): 389-406.
Kausalya, P. J., S. Amasheh, et al. (2006). "Disease-associated mutations affect intracellular traffic and paracellular Mg2+ transport function of Claudin-16." J Clin Invest **116**(4): 878-891.
Koga, T., Y. Matsui, et al. (2005). "NFAT and Osterix cooperatively regulate bone formation." Nat Med **11**(8): 880-885.
Kollmar, R., S. K. Nakamura, et al. (2001). "Expression and phylogeny of claudins in vertebrate primordia." Proc Natl Acad Sci U S A **98**(18): 10196-10201.
Kraft, R. and C. Harteneck (2005). "The mammalian melastatin-related transient receptor potential cation channels: an overview." Pflugers Arch **451**(1): 204-211.

Krapivinsky, G., S. Mochida, et al. (2006). "The TRPM7 ion channel functions in cholinergic synaptic vesicles and affects transmitter release." Neuron **52**(3): 485-496.
Krishnamurthy, V. G. (1976). "Cytophysiology of corpuscles of Stannius." Int Rev Cytol **46**: 177-249.
Kronenberg, H. M. (2003). "Developmental regulation of the growth plate." Nature **423**(6937): 332-336.
Kronenberg, H. M. (2006). "PTHrP and skeletal development." Ann N Y Acad Sci **1068**: 1-13.
Kuizon, B. D. and I. B. Salusky (1999). "Growth retardation in children with chronic renal failure." J Bone Miner Res **14**(10): 1680-1690.
Kuizon, B. D. and I. B. Salusky (2002). "Cell biology of renal osteodystrophy." Pediatr Nephrol **17**(10): 777-789.
Kunert-Keil, C., F. Bisping, et al. (2006). "Tissue-specific expression of TRP channel genes in the mouse and its variation in three different mouse strains." BMC Genomics **7**: 159.
Kuure, S., R. Vuolteenaho, et al. (2000). "Kidney morphogenesis: cellular and molecular regulation." Mech Dev **92**(1): 31-45.
Kwan, K. M., E. Fujimoto, et al. (2007). "The Tol2kit: a multisite gateway-based construction kit for Tol2 transposon transgenesis constructs." Dev Dyn **236**(11): 3088-3099.
Lafeber, F. P., G. Flik, et al. (1988). "Hypocalcin from Stannius corpuscles inhibits gill calcium uptake in trout." Am J Physiol **254**(6 Pt 2): R891-896.
LaPlante, J. M., J. Falardeau, et al. (2002). "Identification and characterization of the single channel function of human mucolipin-1 implicated in mucolipidosis type IV, a disorder affecting the lysosomal pathway." FEBS Lett **532**(1-2): 183-187.
LaPlante, J. M., C. P. Ye, et al. (2004). "Functional links between mucolipin-1 and Ca2+-dependent membrane trafficking in mucolipidosis IV." Biochem Biophys Res Commun **322**(4): 1384-1391.
Larsson, T., R. Marsell, et al. (2004). "Transgenic mice expressing fibroblast growth factor 23 under the control of the alpha1(I) collagen promoter exhibit growth retardation, osteomalacia, and disturbed phosphate homeostasis." Endocrinology **145**(7): 3087-3094.
Laude, A. J. and A. W. Simpson (2009). "Compartmentalized signalling: Ca2+ compartments, microdomains and the many facets of Ca2+ signalling." FEBS J **276**(7): 1800-1816.
Launay, P., A. Fleig, et al. (2002). "TRPM4 is a Ca2+-activated nonselective cation channel mediating cell membrane depolarization." Cell **109**(3): 397-407.
Layton, A. T., H. E. Layton, et al. (2009). "The mammalian urine concentrating mechanism: hypotheses and uncertainties." Physiology (Bethesda) **24**: 250-256.
Lee, N., J. Chen, et al. (2003). "Expression and characterization of human transient receptor potential melastatin 3 (hTRPM3)." J Biol Chem **278**(23): 20890-20897.
Leypold, B. G., C. R. Yu, et al. (2002). "Altered sexual and social behaviors in trp2 mutant mice." Proc Natl Acad Sci U S A **99**(9): 6376-6381.

Li, M., J. Jiang, et al. (2006). "Functional characterization of homo- and heteromeric channel kinases TRPM6 and TRPM7." J Gen Physiol **127**(5): 525-537.
Li, T. F., Y. Dong, et al. (2004). "Parathyroid hormone-related peptide (PTHrP) inhibits Runx2 expression through the PKA signaling pathway." Exp Cell Res **299**(1): 128-136.
Liedtke, W. and J. M. Friedman (2003). "Abnormal osmotic regulation in trpv4-/- mice." Proc Natl Acad Sci U S A **100**(23): 13698-13703.
Liman, E. R., D. P. Corey, et al. (1999). "TRP2: a candidate transduction channel for mammalian pheromone sensory signaling." Proc Natl Acad Sci U S A **96**(10): 5791-5796.
Liu, X., B. C. Bandyopadhyay, et al. (2006). "A role for AQP5 in activation of TRPV4 by hypotonicity: concerted involvement of AQP5 and TRPV4 in regulation of cell volume recovery." J Biol Chem **281**(22): 15485-15495.
Logar, D. B., R. Komadina, et al. (2007). "Expression of bone resorption genes in osteoarthritis and in osteoporosis." J Bone Miner Metab **25**(4): 219-225.
Loh, Y. H., A. Christoffels, et al. (2004). "Extensive expansion of the claudin gene family in the teleost fish, Fugu rubripes." Genome Res **14**(7): 1248-1257.
Mabee, P. M., K. L. Olmstead, et al. (2000). "An experimental study of intraspecific variation, developmental timing, and heterochrony in fishes." Evolution **54**(6): 2091-2106.
Macpherson, L. J., B. H. Geierstanger, et al. (2005). "The pungency of garlic: activation of TRPA1 and TRPV1 in response to allicin." Curr Biol **15**(10): 929-934.
Maeda, S. S., E. M. Fortes, et al. (2006). "Hypoparathyroidism and pseudohypoparathyroidism." Arq Bras Endocrinol Metabol **50**(4): 664-673.
Marie, P. J. (2003). "Fibroblast growth factor signaling controlling osteoblast differentiation." Gene **316**: 23-32.
Marsell, R., T. Krajisnik, et al. (2008). "Gene expression analysis of kidneys from transgenic mice expressing fibroblast growth factor-23." Nephrol Dial Transplant **23**(3): 827-833.
McCarthy, T. L. and M. Centrella (2001). "Local IGF-I expression and bone formation." Growth Horm IGF Res **11**(4): 213-219.
McGrath, J., S. Somlo, et al. (2003). "Two populations of node monocilia initiate left-right asymmetry in the mouse." Cell **114**(1): 61-73.
McNamara, F. N., A. Randall, et al. (2005). "Effects of piperine, the pungent component of black pepper, at the human vanilloid receptor (TRPV1)." Br J Pharmacol **144**(6): 781-790.
McNeill, M. S., J. Paulsen, et al. (2007). "Cell death of melanophores in zebrafish trpm7 mutant embryos depends on melanin synthesis." J Invest Dermatol **127**(8): 2020-2030.
Miller, A. J., J. Du, et al. (2004). "Transcriptional regulation of the melanoma prognostic marker melastatin (TRPM1) by MITF in melanocytes and melanoma." Cancer Res **64**(2): 509-516.
Mochizuki, T., G. Wu, et al. (1996). "PKD2, a gene for polycystic kidney disease that encodes an integral membrane protein." Science **272**(5266): 1339-1342.

Monteilh-Zoller, M. K., M. C. Hermosura, et al. (2003). "TRPM7 provides an ion channel mechanism for cellular entry of trace metal ions." J Gen Physiol **121**(1): 49-60.
Moochhala, S. H., J. A. Sayer, et al. (2008). "Renal calcium stones: insights from the control of bone mineralization." Exp Physiol **93**(1): 43-49.
Mori, Y., M. Wakamori, et al. (2002). "Transient receptor potential 1 regulates capacitative Ca(2+) entry and Ca(2+) release from endoplasmic reticulum in B lymphocytes." J Exp Med **195**(6): 673-681.
Muraki, K., Y. Iwata, et al. (2003). "TRPV2 is a component of osmotically sensitive cation channels in murine aortic myocytes." Circ Res **93**(9): 829-838.
Nadler, M. J., M. C. Hermosura, et al. (2001). "LTRPC7 is a Mg.ATP-regulated divalent cation channel required for cell viability." Nature **411**(6837): 590-595.
Nasevicius, A. and S. C. Ekker (2000). "Effective targeted gene 'knockdown' in zebrafish." Nat Genet **26**(2): 216-220.
National Kidney Foundation (2002). "K/DOQI clinical practice guidelines for chronic kidney disease: evaluation, classification, and stratification." Am J Kidney Dis **39**(2 Suppl 1): S1-266.
Nauli, S. M., F. J. Alenghat, et al. (2003). "Polycystins 1 and 2 mediate mechanosensation in the primary cilium of kidney cells." Nat Genet **33**(2): 129-137.
Neher, E. and T. Sakaba (2008). "Multiple roles of calcium ions in the regulation of neurotransmitter release." Neuron **59**(6): 861-872.
Nilius, B. (2003). "From TRPs to SOCs, CCEs, and CRACs: consensus and controversies." Cell Calcium **33**(5-6): 293-298.
Nilius, B., J. Prenen, et al. (2003). "Voltage dependence of the Ca2+-activated cation channel TRPM4." J Biol Chem **278**(33): 30813-30820.
Nilius, B., J. Vriens, et al. (2004). "TRPV4 calcium entry channel: a paradigm for gating diversity." Am J Physiol Cell Physiol **286**(2): C195-205.
Nilius, B., H. Watanabe, et al. (2003). "The TRPV4 channel: structure-function relationship and promiscuous gating behaviour." Pflugers Arch **446**(3): 298-303.
Olney, R. C. (2003). "Regulation of bone mass by growth hormone." Med Pediatr Oncol **41**(3): 228-234.
Pandey, A. C. (1994). "Evidence for general hypocalcemic hormone from the stannius corpuscles of the freshwater catfish Ompok bimaculatus (Bl)." Gen Comp Endocrinol **94**(2): 182-185.
Parichy, D. M., J. F. Rawls, et al. (1999). "Zebrafish sparse corresponds to an orthologue of c-kit and is required for the morphogenesis of a subpopulation of melanocytes, but is not essential for hematopoiesis or primordial germ cell development." Development **126**(15): 3425-3436.
Parichy, D. M. and J. M. Turner (2003). "Temporal and cellular requirements for Fms signaling during zebrafish adult pigment pattern development." Development **130**(5): 817-833.

Parichy, D. M., J. M. Turner, et al. (2003). "Essential role for puma in development of postembryonic neural crest-derived cell lineages in zebrafish." Dev Biol **256**(2): 221-241.
Parmar, M. S. (2004). "Kidney stones." BMJ **328**(7453): 1420-1424.
Pedersen, S. F., G. Owsianik, et al. (2005). "TRP channels: an overview." Cell Calcium **38**(3-4): 233-252.
Pennekamp, P., C. Karcher, et al. (2002). "The ion channel polycystin-2 is required for left-right axis determination in mice." Curr Biol **12**(11): 938-943.
Peral, B., J. L. San Millan, et al. (1996). "Screening the 3' region of the polycystic kidney disease 1 (PKD1) gene reveals six novel mutations." Am J Hum Genet **58**(1): 86-96.
Perez, C. A., L. Huang, et al. (2002). "A transient receptor potential channel expressed in taste receptor cells." Nat Neurosci **5**(11): 1169-1176.
Perraud, A. L., A. Fleig, et al. (2001). "ADP-ribose gating of the calcium-permeable LTRPC2 channel revealed by Nudix motif homology." Nature **411**(6837): 595-599.
Pfaffl, M. W., G. W. Horgan, et al. (2002). "Relative expression software tool (REST) for group-wise comparison and statistical analysis of relative expression results in real-time PCR." Nucleic Acids Res **30**(9): e36.
Pi, M., S. C. Garner, et al. (2000). "Sensing of extracellular cations in CasR-deficient osteoblasts. Evidence for a novel cation-sensing mechanism." J Biol Chem **275**(5): 3256-3263.
Pi, M. and L. D. Quarles (2005). "Osteoblast calcium-sensing receptor has characteristics of ANF/7TM receptors." J Cell Biochem **95**(6): 1081-1092.
Potthoff, T., Ed. (1984). Clearing and staining techniques. Ontogeny and systematics of fishes. Lawrence, KS, American Society of Ichthyologists and Herpetologists, Allen Press.
Prawitt, D., M. K. Monteilh-Zoller, et al. (2003). "TRPM5 is a transient Ca2+-activated cation channel responding to rapid changes in [Ca2+]i." Proc Natl Acad Sci U S A **100**(25): 15166-15171.
Provot, S. and E. Schipani (2005). "Molecular mechanisms of endochondral bone development." Biochem Biophys Res Commun **328**(3): 658-665.
Quarles, L. D. (2008). "Endocrine functions of bone in mineral metabolism regulation." J Clin Invest **118**(12): 3820-3828.
Quigley, I. K., J. M. Turner, et al. (2004). "Pigment pattern evolution by differential deployment of neural crest and post-embryonic melanophore lineages in Danio fishes." Development **131**(24): 6053-6069.
Radman, D. P., C. McCudden, et al. (2002). "Evidence for calcium-sensing receptor mediated stanniocalcin secretion in fish." Mol Cell Endocrinol **186**(1): 111-119.
Rankin, W., V. Grill, et al. (1997). "Parathyroid hormone-related protein and hypercalcemia." Cancer **80**(8 Suppl): 1564-1571.
Rawls, J. F. and S. L. Johnson (2001). "Requirements for the kit receptor tyrosine kinase during regeneration of zebrafish fin melanocytes." Development **128**(11): 1943-1949.

Reilly, R. F. and D. H. Ellison (2000). "Mammalian distal tubule: physiology, pathophysiology, and molecular anatomy." Physiol Rev **80**(1): 277-313.
Reiser, J., K. R. Polu, et al. (2005). "TRPC6 is a glomerular slit diaphragm-associated channel required for normal renal function." Nat Genet **37**(7): 739-744.
Rendina, D., G. Mossetti, et al. (2006). "Fibroblast growth factor 23 is increased in calcium nephrolithiasis with hypophosphatemia and renal phosphate leak." J Clin Endocrinol Metab **91**(3): 959-963.
Riminucci, M., M. T. Collins, et al. (2003). "FGF-23 in fibrous dysplasia of bone and its relationship to renal phosphate wasting." J Clin Invest **112**(5): 683-692.
Rodriguez, M., S. Canadillas, et al. (2006). "Regulation of parathyroid function in chronic renal failure." J Bone Miner Metab **24**(2): 164-168.
Runnels, L. W., L. Yue, et al. (2001). "TRP-PLIK, a bifunctional protein with kinase and ion channel activities." Science **291**(5506): 1043-1047.
Ryazanova, L. V., M. V. Dorovkov, et al. (2004). "Characterization of the protein kinase activity of TRPM7/ChaK1, a protein kinase fused to the transient receptor potential ion channel." J Biol Chem **279**(5): 3708-3716.
Samadfam, R., C. Richard, et al. (2009). "Bone formation regulates circulating concentrations of fibroblast growth factor 23." Endocrinology **150**(11): 4835-4845.
Sano, Y., K. Inamura, et al. (2001). "Immunocyte Ca2+ influx system mediated by LTRPC2." Science **293**(5533): 1327-1330.
Schipani, E., K. Kruse, et al. (1995). "A constitutively active mutant PTH-PTHrP receptor in Jansen-type metaphyseal chondrodysplasia." Science **268**(5207): 98-100.
Schipani, E. and S. Provot (2003). "PTHrP, PTH, and the PTH/PTHrP receptor in endochondral bone development." Birth Defects Res C Embryo Today **69**(4): 352-362.
Schlingmann, K. P., S. Waldegger, et al. (2007). "TRPM6 and TRPM7--Gatekeepers of human magnesium metabolism." Biochim Biophys Acta **1772**(8): 813-821.
Schlingmann, K. P., S. Weber, et al. (2002). "Hypomagnesemia with secondary hypocalcemia is caused by mutations in TRPM6, a new member of the TRPM gene family." Nat Genet **31**(2): 166-170.
Schmitz, C., F. Deason, et al. (2007). "Molecular components of vertebrate Mg2+-homeostasis regulation." Magnes Res **20**(1): 6-18.
Schmitz, C., M. V. Dorovkov, et al. (2005). "The channel kinases TRPM6 and TRPM7 are functionally nonredundant." J Biol Chem **280**(45): 37763-37771.
Schmitz, C., A. L. Perraud, et al. (2003). "Regulation of vertebrate cellular Mg2+ homeostasis by TRPM7." Cell **114**(2): 191-200.
Segawa, H., E. Kawakami, et al. (2003). "Effect of hydrolysis-resistant FGF23-R179Q on dietary phosphate regulation of the renal type-II Na/Pi transporter." Pflugers Arch **446**(5): 585-592.
Shimada, T., H. Hasegawa, et al. (2004). "FGF-23 is a potent regulator of vitamin D metabolism and phosphate homeostasis." J Bone Miner Res **19**(3): 429-435.

Sidi, S., R. W. Friedrich, et al. (2003). "NompC TRP channel required for vertebrate sensory hair cell mechanotransduction." Science **301**(5629): 96-99.
Simon, P. (2003). "Q-Gene: processing quantitative real-time RT-PCR data." Bioinformatics **19**(11): 1439-1440.
Sipos, W., P. Pietschmann, et al. (2009). "Pathophysiology of osteoporosis." Wien Med Wochenschr **159**(9-10): 230-234.
Sitara, D., M. S. Razzaque, et al. (2004). "Homozygous ablation of fibroblast growth factor-23 results in hyperphosphatemia and impaired skeletogenesis, and reverses hypophosphatemia in Phex-deficient mice." Matrix Biol **23**(7): 421-432.
Stark, Z. and R. Savarirayan (2009). "Osteopetrosis." Orphanet J Rare Dis **4**: 5.
Stechman, M. J., N. Y. Loh, et al. (2007). "Genetics of hypercalciuric nephrolithiasis: renal stone disease." Ann N Y Acad Sci **1116**: 461-484.
Storey, J. D. and R. Tibshirani (2003). "Statistical significance for genomewide studies." Proc Natl Acad Sci U S A **100**(16): 9440-9445.
Stowers, L., T. E. Holy, et al. (2002). "Loss of sex discrimination and male-male aggression in mice deficient for TRP2." Science **295**(5559): 1493-1500.
Su, L. T., M. A. Agapito, et al. (2006). "TRPM7 regulates cell adhesion by controlling the calcium-dependent protease calpain." J Biol Chem **281**(16): 11260-11270.
Sun, M., E. Goldin, et al. (2000). "Mucolipidosis type IV is caused by mutations in a gene encoding a novel transient receptor potential channel." Hum Mol Genet **9**(17): 2471-2478.
Sundell, K., B. T. Bjornsson, et al. (1992). "Chum salmon (Oncorhynchus keta) stanniocalcin inhibits in vitro intestinal calcium uptake in Atlantic cod (Gadus morhua)." J Comp Physiol B **162**(6): 489-495.
Sutters, M. and G. G. Germino (2003). "Autosomal dominant polycystic kidney disease: molecular genetics and pathophysiology." J Lab Clin Med **141**(2): 91-101.
Takeda, S., J. P. Bonnamy, et al. (2001). "Continuous expression of Cbfa1 in nonhypertrophic chondrocytes uncovers its ability to induce hypertrophic chondrocyte differentiation and partially rescues Cbfa1-deficient mice." Genes Dev **15**(4): 467-481.
Takezawa, R., C. Schmitz, et al. (2004). "Receptor-mediated regulation of the TRPM7 channel through its endogenous protein kinase domain." Proc Natl Acad Sci U S A **101**(16): 6009-6014.
Talmage, R. V. and H. T. Mobley (2008). "Calcium homeostasis: reassessment of the actions of parathyroid hormone." Gen Comp Endocrinol **156**(1): 1-8.
The Zebrafish Information Network. (2005). from http://zfin.org.
Thebault, S., G. Cao, et al. (2008). "Role of the alpha-kinase domain in transient receptor potential melastatin 6 channel and regulation by intracellular ATP." J Biol Chem **283**(29): 19999-20007.
Theman, T. A. and M. T. Collins (2009). "The role of the calcium-sensing receptor in bone biology and pathophysiology." Curr Pharm Biotechnol **10**(3): 289-301.
Thisse, B., Thisse, C (2004). Fast release clones: a high throughput expression analysis.
Thomson, S. C. and R. C. Blantz (2008). "Glomerulotubular balance, tubuloglomerular feedback, and salt homeostasis." J Am Soc Nephrol **19**(12): 2272-2275.

Tian, J., C. Yam, et al. (2003). "A temperature-sensitive mutation in the nodal-related gene cyclops reveals that the floor plate is induced during gastrulation in zebrafish." Development **130**(14): 3331-3342.
Topala, C. N., W. T. Groenestege, et al. (2007). "Molecular determinants of permeation through the cation channel TRPM6." Cell Calcium **41**(6): 513-523.
Tsagalis, G., E. Psimenou, et al. (2009). "Fibroblast growth factor 23 (FGF23) and the kidney." Int J Artif Organs **32**(4): 232-239.
Tseng, D. Y., M. Y. Chou, et al. (2009). "Effects of stanniocalcin 1 on calcium uptake in zebrafish (Danio rerio) embryo." Am J Physiol Regul Integr Comp Physiol **296**(3): R549-557.
Ueta, C., M. Iwamoto, et al. (2001). "Skeletal malformations caused by overexpression of Cbfa1 or its dominant negative form in chondrocytes." J Cell Biol **153**(1): 87-100.
United States Renal Data System. (2003). "USRDS 2003 Annual Data Report. ." from Available at www.usrds.org.
Varghese, R., A. D. Gagliardi, et al. (2002). "Overexpression of human stanniocalcin affects growth and reproduction in transgenic mice." Endocrinology **143**(3): 868-876.
Venkatachalam, K. and C. Montell (2007). "TRP channels." Annu Rev Biochem **76**: 387-417.
Vetter, T. and M. J. Lohse (2002). "Magnesium and the parathyroid." Curr Opin Nephrol Hypertens **11**(4): 403-410.
Vezzoli, G., L. Soldati, et al. (2009). "Roles of calcium-sensing receptor (CaSR) in renal mineral ion transport." Curr Pharm Biotechnol **10**(3): 302-310.
Voets, T., B. Nilius, et al. (2004). "TRPM6 forms the Mg2+ influx channel involved in intestinal and renal Mg2+ absorption." J Biol Chem **279**(1): 19-25.
Voets, T., J. Prenen, et al. (2001). "CaT1 and the calcium release-activated calcium channel manifest distinct pore properties." J Biol Chem **276**(51): 47767-47770.
Wagner, C. A., O. Devuyst, et al. (2009). "Regulated acid-base transport in the collecting duct." Pflugers Arch **458**(1): 137-156.
Walder, R. Y., D. Landau, et al. (2002). "Mutation of TRPM6 causes familial hypomagnesemia with secondary hypocalcemia." Nat Genet **31**(2): 171-174.
Walker, M. B. and C. B. Kimmel (2007). "A two-color acid-free cartilage and bone stain for zebrafish larvae." Biotech Histochem **82**(1): 23-28.
Walker, R. G., A. T. Willingham, et al. (2000). "A Drosophila mechanosensory transduction channel." Science **287**(5461): 2229-2234.
Wang, X., I. Armando, et al. (2009). "The regulation of proximal tubular salt transport in hypertension: an update." Curr Opin Nephrol Hypertens **18**(5): 412-420.
Wei, W. L., H. S. Sun, et al. (2007). "TRPM7 channels in hippocampal neurons detect levels of extracellular divalent cations." Proc Natl Acad Sci U S A **104**(41): 16323-16328.
Westerfield, M., Ed. (2000). The Zebrafish Book: A Guide for the Laboratory Use of Zebrafish (*Danio rerio*). Eugene, Oregon, University of Oregon Press.
Williams, M. E. (2009). "Chronic kidney disease/bone and mineral metabolism: the imperfect storm." Semin Nephrol **29**(2): 97-104.

Wingert, R. A. and A. J. Davidson (2008). "The zebrafish pronephros: a model to study nephron segmentation." Kidney Int **73**(10): 1120-1127.
Wingert, R. A., R. Selleck, et al. (2007). "The cdx genes and retinoic acid control the positioning and segmentation of the zebrafish pronephros." PLoS Genet **3**(10): 1922-1938.
Winn, M. P., P. J. Conlon, et al. (2005). "A mutation in the TRPC6 cation channel causes familial focal segmental glomerulosclerosis." Science **308**(5729): 1801-1804.
Wolf, F. I. (2004). "TRPM7: channeling the future of cellular magnesium homeostasis?" Sci STKE **2004**(233): pe23.
Wolf, F. I. and A. Cittadini (1999). "Magnesium in cell proliferation and differentiation." Front Biosci **4**: D607-617.
Wolff, A. E., A. N. Jones, et al. (2008). "Vitamin D and musculoskeletal health." Nat Clin Pract Rheumatol **4**(11): 580-588.
Worcester, E. M. and F. L. Coe (2008). "New insights into the pathogenesis of idiopathic hypercalciuria." Semin Nephrol **28**(2): 120-132.
Wu, S., Y. Yoshiko, et al. (2006). "Stanniocalcin 1 acts as a paracrine regulator of growth plate chondrogenesis." J Biol Chem **281**(8): 5120-5127.
Yamada, T. and R. Fujii (2002). "An increase in extracellular Ca(2+) concentration induces pigment aggregation in teleostean melanophores." Zoolog Sci **19**(8): 829-839.
Yue, L., J. B. Peng, et al. (2001). "CaT1 manifests the pore properties of the calcium-release-activated calcium channel." Nature **410**(6829): 705-709.
Zajac, J. D. and J. A. Danks (2008). "The development of the parathyroid gland: from fish to human." Curr Opin Nephrol Hypertens **17**(4): 353-356.
Zhang, M., S. Xuan, et al. (2002). "Osteoblast-specific knockout of the insulin-like growth factor (IGF) receptor gene reveals an essential role of IGF signaling in bone matrix mineralization." J Biol Chem **277**(46): 44005-44012.
Zhang, Y., M. A. Hoon, et al. (2003). "Coding of sweet, bitter, and umami tastes: different receptor cells sharing similar signaling pathways." Cell **112**(3): 293-301.
Zhou, X. and P. D. Vize (2004). "Proximo-distal specialization of epithelial transport processes within the Xenopus pronephric kidney tubules." Dev Biol **271**(2): 322-338.

Vita

Michael Reuben Elizondo was born in Austin, Texas and raised as a native Texan to very loving and supportive parents, Homer and Belinda Elizondo. He has 1 younger sister, Suzanne. After graduating from the Science Academy at LBJ High School in 1997, he went on to attend the University of Texas. Here, after briefly double majoring in English and Microbiology, he shifted his focus to laboratory research. He worked as an undergraduate researcher in the lab of Dr. Ian J. Molineux where he received an Undergraduate Research Fellowship to pursue research related to the evolution of T3 and T7 bacteriophages. After graduating with a Bachelor of Science in Microbiology from the University of Texas in 2001, he entered graduate school at the Institute for Cell and Molecular Biology at the University of Texas. Here he joined Dr. David M. Parichy's zebrafish lab. When the lab moved to the University of Washington in 2005, he followed them to Seattle to complete the research for his dissertation. As a graduate student he was awarded 2nd Prize in the Graduate Student Poster Competition at the 6th International Zebrafish Conference on Development and Genetics in 2004 and was granted an F31 Ruth L. Kirschstein NRSA Minority Predoctoral Fellowship from the NIH and NIDDK in 2005.

Permanent Address: 4406 Bouvet Court, Austin, Texas 78727

This dissertation was typed by the author.